The Dissertation Committee for Teresa E Sorvillo Certifies that this is the approved version of the following dissertation:

A Recombinant Vesicular Stomatitis Virus Expressing the Junin Virus Glycoprotein for Arenavirus Countermeasure Development

Committee:

Thomas W. Geisbert

John H. Connor

Thomas Ksiazek

Chad E. Mire

Chien-Te Tseng

A Recombinant Vesicular Stomatitis Virus Expressing the Junin Virus Glycoprotein for Arenavirus Countermeasure Development

by

Teresa Eirena Sorvillo, B.S.

Dissertation

Presented to the Faculty of the Graduate School of

The University of Texas Medical Branch

in Partial Fulfillment

of the Requirements

for the Degree of

Doctor of Philosophy, Microbiology and Immunology

The University of Texas Medical Branch

October 2019

Dedication

This dissertation is dedicated to my family: my dad Frank, mom Jeanne, and brother Bryan, all of whom have supported me tremendously on this journey. I will always be grateful to both of my parents for their example as life-long learners. To my dad, who has always inspired and fostered my love for learning, particularly science, and who paved the way for this career path with hours of childhood science experiments and reading me *The Hot Zone* when I was 10 years old. To my mom, who has always encouraged me to ponder and pursue answers to the big questions; and who has given me the gift of seeing a woman tenaciously pursue her education and aspirations. To my brother, who never lets me take life too seriously and has kept me laughing for 30 years.

This dissertation is also dedicated to my "East Coast parents", Camille and Roland Lamothe…in loving memory of Roland Lamothe…for always believing I was capable of this accomplishment and for always standing by me without question, during both the difficult and joyous times.

Last, but certainly not least, to my dear friend, confidant, and teacher, Steve Roman, without whom this path would never have been possible. I am eternally grateful to you.

Acknowledgements

I would like to thank the many people who have contributed directly or indirectly to this work and who have supported me on this PhD journey. First, I would like to thank my PI and mentor, Thomas (Tom) Geisbert, PhD for taking a chance on me 6 years ago and for supporting me in all of my academic pursuits, both inside of the BSL-4 and outside doing the field work that I love. I would also like to sincerely thank Chad Mire, PhD for all his mentorship, guidance, and support. Your excitement for science and "Friday data", no matter how insignificant, were a huge source of motivation to me. In addition, I would like to thank Robert (Bob) Cross, PhD for his mentorship and scientific guidance.

The work in this dissertation would not have been possible without the assistance of many members of the Geisbert lab. Thank you to Joan Geisbert, Daniel Deer, Robert Cross, and Karla Fenton for their contributions to the animal work described in Chapter 2. Additional thank you to Karla Fenton and Natalie Dobias for contributions via histology and immunohistochemistry.

To James (Jim) LeDuc, PhD, for his mentorship as well as his support in my travel to the Institute of Human Viral Diseases (INEVH) in Argentina which served as the foundation for Chapter 2 of this dissertation.

I would also like to thank current and former members of the Geisbert lab not previously mentioned who have shown both emotional and academic support: Sergio Rodriguez, Courtney Woolsey, Krista Versteeg, Ben Satterfield, Corri Levine, Krystle

Agans, Vika Borisevich, Stephanie Foster, Kevin Melody, Abhi Prasad, and Kira Zapalac.

A sincere thank you to my doctoral committee members for their guidance, mentorship, and scientific discussions: Thomas Geisbert PhD, Chad Mire PhD, Thomas Ksiazek DVM, PhD, Kent Tseng PhD, and John Connor PhD.

Finally, to my dear friends who have become my Texas family, in particular, Terence, Ela, Sammy, Geraldine, Krista, and Karla.

A Recombinant Vesicular Stomatitis Virus Expressing the Junin Virus Glycoprotein for Arenavirus Countermeasure Development.

Publication No._____

Teresa Eirena Sorvillo, Ph.D.

The University of Texas Medical Branch, 2019

Supervisor: Thomas W. Geisbert

TABLE OF CONTENTS

List of Tables

List of Figures

List of Abbreviations

ADCC	Antibody-dependent cell-mediated cytotoxicity
ADCP	Antibody-dependent cell-mediated phagocytosis
AHF	Argentine hemorrhagic fever
AST	Aspartate transaminase
BHK	Baby hamster kidney cells
BSL	Biosafety level
CHAPV	Chapare virus
CNS	Central nervous system
CPE	Cytopathic effect
DIC	Disseminated intravascular coagulation
ELISA	Enzyme-linked immunosorbent assay
FDA	United States Food and Drug Administration
FRhL	Fetal Rhesus lung cells
GTOV	Guanarito virus
GP	Glycoprotein
GPC	Glycoprotein precursor gene
H&E	Hematoxylin and eosin
HHS	United States Department of Health and Human Services
HUVEC	Human umbilical vein endothelial cells
ICAM	Intracellular adhesion molecule
IFA	Immunofluorescence assay

IHC	Immunohistochemistry
IL-6	Interleukin-6
i.c.	Intracranial
i.m.	Intramuscular
i.p.	Intraperitoneal
INEVH	Maiztegui Institute of Human Viral Diseases
ISG	Interferon stimulated gene
JUNV	Junin virus
LASV	Lassa virus
LCMV	Lymphocytic choriomeningitis virus
LUJV	Lujo virus
MACV	Machupo virus
MCP-1	Monocyte chemoattractant protein-1
MRC	Medical Research Council cells
NASEM	National Academies of Sciences, Engineering, and Medicine
NHP	Nonhuman primate
NIAID	National Institute of Allergy and Infectious Diseases
PAHO	Pan American Health Organization
PBMC	Peripheral blood mononuclear cells
PCR	Polymerase chain reaction
PFU	Plaque forming units
PRNT	Plaque reduction neutralization test
SBAV	Sabia virus

TCRV	Tacaribe virus
TNF	Tumor necrosis factor
UTMB	University of Texas Medical Branch
VCAM	Vascular cell adhesion molecule
VHF	Viral hemorrhagic fever

Chapter 1: Introduction[1]

A quarter century ago a landmark publication by the United States National Academies of Sciences, Engineering, and Medicine (NASEM) entitled "Emerging Infections: Microbial Threats to Health in the United States" resulted in the christening of a new term, "emerging infectious diseases" which continues to be relevant even now, twenty-seven years later [2]. This watershed report captured the societal changes underway in our rapidly evolving world: the growth of the world's population; changes in economic development and land use; dramatic increase in the speed and frequency of international travel and commerce; the adaptation of microbes and the appearance of never before seen pathogens; and the breakdown of traditional public health measures. This societal evolution has only increased with time and the growing frequency of outbreaks predicted in the report has come to pass with the emergence and re-emergence of countless pathogens.

The NASEM report was a call-to-action, drawing attention to numerous pathogens which were emerging at the time. One particular group of emerging pathogens which were a focus of the NASEM report were arenaviruses, a group of viruses capable of causing severe hemorrhagic disease in humans. These rodent-borne viruses were cited in order to highlight the ever-increasing threat of zoonotic pathogens on human health as populations continue to encroach upon previously uninhabited areas of the globe. Junin virus (JUNV), an arenavirus endemic to Argentina, was a pointed example of the threat that expanding agricultural practices have on facilitating human contact with reservoir rodent hosts, leading to yearly outbreaks of the hemorrhagic fever disease [2]. Even as the NASEM report was being written, another novel highly virulent arenavirus was emerging in Venezuela for the first time and would later become known as Guanarito virus (GTOV) [2-

[1] Sections of Chapter 1 are adapted from: 1. Le Duc JW, Sorvillo TE. A Quarter Century of Emerging Infectious Diseases - Where Have We Been and Where Are We Going? Acta Med Acad **2018**; 47:117-30. (https://creativecommons.org/licenses/by-nc/4.0/)

4]. And these warnings regarding arenaviruses are even more relevant today. On July 18, 2019 the Pan American Health Organization (PAHO) released an epidemiological alert regarding an outbreak of fatal hemorrhagic fever disease in Bolivia with sequence specificity showing high identity to Chapare virus (CHAPV), a new and emerging arenavirus, which has been traced to agricultural exposure during the harvest of rice [5].

In addition to highlighting the importance of expanding zoonotic transmission of disease, the NASEM report highlighted the significance of global connectivity via airline travel and international commerce in the emergence and spread of infectious diseases. In the 27 years since the report was released, the spread of emerging diseases has been facilitated by our modern international travel network that allows anyone to reach almost any place in the world in less that the incubation period of virtually all infectious diseases. This was dramatically demonstrated when a traveler from West Africa entered into the United States while asymptomatically incubating Ebola virus [6]. The event resulted in the transmission of Ebola virus to two nurses in Dallas, Texas and the subsequent monitoring of 177 potentially exposed individuals [6]. The importance of increasing global connectedness was further demonstrated in a recent literature review of Lassa fever, a highly virulent arenaviral disease, which identified 33 imported cases of the virus to non-endemic areas between 1969 and 2017, including 8 cases imported to the United States [7-10]. These events collectively reinforce the idea that highly pathogenic viral hemorrhagic fevers (VHF) like filoviruses and arenaviruses that were once considered relegated to remote parts of the globe can be on our doorsteps rapidly.

Over the past quarter century since the report's publication a much greater awareness has also evolved regarding the importance of biosafety and biosecurity surrounding pathogens. As a result, the Select Agent program was developed in the United States, designed to limit the distribution of dangerous pathogens to known entities and appropriately trained and screened individuals [11]. VHFs such as pathogenic arenaviruses have been added to the list of select agents by the United States Department of Health and

Human Services (HHS) including: Lassa (LASV), JUNV, Machupo (MACV), CHAPV, GTOV, and Sabia viruses (SABV) [11]. Additionally, select arenaviruses have been categorized by the National Institute of Allergy and Infectious Diseases (NIAID) as Category A priority pathogens due to their virulence and potential for aerosol transmission, making them a prominent biodefense concern.

With the many circumstances of our changing world, more frequent exposure to zoonotic disease, human encroachment into previously uninhabited areas of the world, biodefense and biosecurity concerns, and our rapidly connected global world, preparation for emerging infectious diseases like arenaviruses via the development of countermeasures and effective diagnostic tools is an incredibly important research goal. Arenaviruses are pathogens of significant public health and biodefense importance due to the severity of the disease they can cause, their propensity to be transmitted via aerosol, and the lack of effective countermeasures, particularly ones with Food and Drug Administration (FDA) approval. Two of the most prominent arenaviruses from a public health standpoint are LASV and JUNV which cause significant morbidity and mortality on an annual basis in their respective endemic areas [9, 12, 13]. While extensive research has been conducted in order to advance LASV vaccine and therapeutic development, less research attention has been focused on the development of countermeasures against JUNV. The focus of this dissertation will therefore be to address the limitations of currently available JUNV countermeasures through the development of novel strategies for JUNV detection and prevention.

ARENAVIRUS PHYLOGENY

Arenaviruses are classified within the family *Arenaviridae*. *Arenaviridae* contains three genera: *Hartmanivirus* and *Reptarenavirus* which contain viruses known to infect reptiles, and *Mammarenavirus* which contains viruses known to be human pathogens [14].

The genus *Mammarenavirus* contains approximately 41 viral species which are further divided into two serologically and geographically distinct groupings: Old World (Lassa-LCMV complex) and New World (Tacaribe complex) viruses [14, 15]. The Old World grouping consists of three major species of human pathogens, *Lassa mammarenavirus* (LASV) which causes significant disease burden in western Africa, *Lujo mammarenavirus* (Lujo virus- LUJV) which has caused a single outbreak of fatal disease in South Africa, and *Lymphocytic choriomeningitis mammarenavirus* (Lymphocytic choriomengingitis virus- LCMV) the first arenavirus to be described and considered to be the prototype virus with worldwide distribution [14, 16, 17]. The New World group is divided into four clades (A through D) with Clade B encompassing several South American hemorrhagic fever viruses including *Argentinian mammarenavirus* (JUNV), *Machupo mammarenavirus* (MACV), *Guanarito mammarenavirus* (GTOV), *Brazilian mammarenavirus* (SABV), and *Chapare mammarenavirus* (CHAPV) [14].

ARENAVIRUS VIRION AND LIFE CYCLE

Arenaviruses fall within Group V of the Baltimore classification system. They are negative stranded, enveloped viruses with a bi-segmented, single stranded RNA genome. The viruses' four genes are contained in one small (S) and one large (L) genomic segment which encode a total of four viral proteins. The L segment encodes an RNA-dependent RNA polymerase (L) and a RING domain matrix-like protein (Z), while the S segment encodes a nucleoprotein (NP) and the glycoprotein precursor (GPC) [18-20]. The arenaviral genome utilizes an ambisense coding strategy where the two open reading frames on each genomic segment are encoded in opposite orientations, one negative stranded and one positive stranded, and divided by a hairpin intergenic region which signals transcriptional termination [18, 21].

In order to enter cells, all arenaviruses must undergo receptor-mediated endocytosis utilizing their integral membrane glycoprotein (GP) [22]. The arenavirus GP is tripartite and consists of the following components: G1, G2, and stable signal peptide (SSP). In the mature viral glycoprotein G1 contains the receptor binding domain, G2 plays an essential role in membrane fusion and contains the transmembrane domain, and SSP is thought to play a role in intracellular translocation of the GPC and pH-dependent membrane fusion [23, 24]. Host cell surface receptors utilized for arenavirus entry differ between phylogenetically distinct virus groupings. LASV, LCMV, and Clade C New World viruses have been shown to utilize α-dystroglycan, a receptor which plays a role in anchoring skeletal muscle to extracellular matrices but which is expressed on cells in both muscle and non-muscle tissue [25]. Clade B New World viruses are known to utilize the ubiquitous iron transporter transferrin receptor 1 (TfR1) [26]. Following cellular entry, a pH-dependent conformational change occurs in the viral GP's G2 subunit (class 1 fusion protein), initiating endosomal membrane fusion and release of L, NP and the viral genome into the cytoplasm [23]. Early stage transcription begins with the NP and L genes as the L polymerase transcribes each gene into its mRNA counterpart [27]. Accumulation of the NP protein is believed to signal a switch in the L polymerase enabling it to read through the intergenic hairpin structures of each gene segment in order to create full-length complementary genomic copies [28]. From these complementary strands, late stage transcription occurs with the production of Z and GPC mRNA. The JUNV GPC is then post-translationally modified within the endoplasmic reticulum/Golgi where it undergoes N-linked glycosylation and is cleaved into its three major components by cellular the protease SKI-1/S1P [29]. Evidence suggests the JUNV GP subsequently localizes with lipid raft microdomains at the plasma membrane prior to virus assembly [30]. Signaling from the Z protein in conjunction with host ESCRT proteins is believed to be crucial for arenavirus protein translocation to the plasma membrane where viral assembly and budding occurs [31].

JUNIN VIRUS

Epidemiology

JUNV, the causative agent of Argentine hemorrhagic fever (AHF), is a particularly significant arenavirus and human pathogen. JUNV is endemic to the Pampas farming region of Argentina where an estimated 5 million persons are at-risk of infection [32]. Evidence suggests the endemic area has continued to expand northward during the last 50 years due to the broadening range of the reservoir host, the Drylands Vesper Mouse (*Calomys musculinus*) [33, 34]. AHF was first described in 1953 and JUNV, the etiologic agent, was confirmed in 1958 [35, 36]. After the first documented outbreaks, the incidence of AHF averaged between 500 and 3500 cases per year until 1991 when administration of a live-attenuated JUNV vaccine to high risk populations in the endemic area was initiated. Despite ongoing administration of the vaccine, there are still between 300 and 1000 cases of AHF reported annually [32]. Prior to widespread administration of the vaccine, a 1983 study found that the seroprevalence of JUNV in humans within the endemic area was 11-12%, of which approximately 2-5% were inapparent or asymptomatic infections [37]. Male agricultural workers involved in the harvest of grain have historically been the primary population afflicted with AHF because infection typically occurs via inhalational exposure to the excrement or fluids of infected rodents, or occasionally, through cuts in the skin acquired during harvest [38]. A 1994 serosurvey of rodents in the endemic area concluded that the overall prevalence of JUNV infection in the reservoir host species was approximately 10.9% [39, 40]. Documented human-to-human transmission of JUNV is rare; however, nosocomial infections have been documented. In recent years increasing evidence of JUNV transmission from rodents to humans in urban areas has been reported (unpublished data, A. Sinchi, INEVH 2018). While urban transmission in the endemic area had historically been minimal, a 2003 survey of rodent species in one Argentine city,

Rio Cuarto, discovered a high capture number (5%) of *C. musculinis,* supporting the idea that urban transmission of JUNV is probable [41].

JUNV Clinical Disease

AHF begins with a flu-like illness, 4-21 days after JUNV exposure, which is characterized by fever, malaise, headache, and myalgia [33]. Other symptoms of the prodromal phase include hemorrhage and lesions of the soft palate, gingival bleeding, photophobia, retro-orbital pain, and conjunctival congestion [33]. Approximately 30% of symptomatic persons develop a severe, late-stage disease which is characterized by neurologic and/or hemorrhagic symptoms and begins 8-12 days after the onset of initial symptoms. Neurologic involvement presents with mental confusion, ataxia, tremors, seizure and coma, while hemorrhagic involvement presents with blood in vomit, stool, urine, and lungs, as well as hematoma and shock [33]. Symptoms that manifest during the late stage of disease are believed to be strain dependent, a hypothesis supported by *in vivo* studies comparing the hemorrhagic (Espindola) and neurologic (Ledesma) prototype strains [42, 43]. The clinical disease course is characterized by thrombocytopenia and leukopenia which begin during the prodromal phase and progress throughout the duration of disease. Overall, mortality rates for persons with symptomatic AHF are as high as 30% [33].

JUNV Pathogenesis

In terms of viral pathogenesis, alveolar macrophages are hypothesized to be the major target of early infection during inhalational exposure to the virus [44]. Additionally, there is evidence to suggest that monocytes and dendritic cells are early targets for JUNV infection, in turn, spreading the virus to draining lymph nodes and then parenchymal tissues

[44]. JUNV infection in humans is often characterized by the involvement of lymphoid tissues and liver; however, the virus has a broad tropism, affecting a number of different organs including the kidneys, lungs, vascular endothelium, and central nervous system (CNS) [45, 46]. The pathogenesis of JUNV in fatal human cases has been well-documented through autopsy [46]. Typical findings within lymphoid tissues include reticulum cell hyperplasia and frequent macrophage erythrophagocytosis (indicating bone marrow depletion) as well as splenic hemorrhage (red pulp) [46]. Liver involvement is characterized by elevated aspartate transaminase (AST) levels and focal hepatocyte necrosis with the presence of acidophilic bodies, indicating cell apoptosis [46]. Lungs are typically found to have hemorrhagic foci localized to the alveoli which is believed to be a direct byproduct of aerosol transmission [46]. Kidneys are frequently enlarged with observable renal pelvic hemorrhage [46]. Capillary dilation without observable vascular lesions or damage is often observed in most major organs. In addition, perivascular hemorrhage and fibrin thrombi are often present in various major arteries [46]. Finally, CNS pathology is characterized by focal hemorrhage in the brain perivascular space and meningeal congestion [46].

Vascular dysregulation is a hallmark of AHF and is characterized by increased vascular permeability, thrombocytopenia, and disfunction of the fibrinolytic system. Despite the well-documented presence of coagulopathy in fatal cases of AHF, only a select few fatalities have been attributed to true disseminated intravascular coagulopathy (DIC), the primary syndrome associated with many highly pathogenic VHFs [47-49]. DIC is characterized by systemic dysfunction of both coagulation and fibrinolysis leading to widespread deposition of fibrin clots, hemorrhage, and leading to shock and death. DIC is typically diagnosed using a scoring system which takes into account several parameters including: platelet count, D-dimer (product of fibrin breakdown) and fibrinogen levels, and prothrombin time [50]. The role for DIC in JUNV pathogenesis is unclear but most evidence indicates it occurs infrequently [46, 51]. Instead, low but consistent levels of

systemic coagulation/fibrinolysis dysfunction are believed to contribute to fatality, and the markers described above are generally not elevated enough to meet the threshold for true DIC [52, 53]. As previously described, overt hemorrhagic manifestations from human JUNV infection are often described. Though JUNV infects and can replicate in the vascular endothelium, cellular damage is not believed to be the cause of hemorrhagic manifestations, rather vascular integrity is believed to be affected by changes in endothelial cell homeostasis. This is evidenced by the absence of overt cellular damage in human umbilical vein endothelial cells (HUVEC) infected with JUNV *in vitro* [54, 55]. Gomez *et al.* (2003) showed that HUVEC cells infected with JUNV, instead, induced upregulation of the adhesion molecules ICAM-1 (intracellular adhesion molecule-1) and VCAM-1 (vascular cellular adhesion molecule 1), a phenomenon known to cause vascular leak through cytoskeletal rearrangement. Upregulation of nitric oxide (NO) production was also detected which is known to increase vascular permeability [56, 57]. Lander *et al.* (2014) also showed that HUVEC cell monolayers derived from lung tissue (HUVEC-L) and infected with JUNV showed no overt signs of cytopathic effect (CPE) but did develop increased vascular permeability which they attribute to alterations in adherens junctions (AJ) as well as increased levels of IL-6 (interleukin-6) and MCP-1 (monocyte chemoattractant protein-1) which are cytokines/chemokines known to affect vascular permeability through cytoskeletal rearrangement (IL-6) and reduction of tight junctions (MCP-1) [58-60]. Importantly, elevated levels of IL-6 and MCP-1 are well documented in fatal or severe cases of other VHFs including Andes, Dengue, Ebola viruses [60-62]

Overall, AHF can often present with a severe hemorrhagic or neurologic disease course, infecting a wide array of human cells and tissues, and result in significant mortality if left untreated, all of which emphasizes the importance of this pathogen as a prominent public health and biodefense concern.

Immune Responses to JUNV Infection

In order to proceed with the development of countermeasures to combat a highly virulent virus like JUNV, it is essential to understand the protective mechanisms of natural human immunity. Uncertainty exists regarding the contribution of innate immune responses to protection from fatal JUNV disease. Interferon (IFN) antagonism via JUNV NP and Z proteins has been well documented. The Z protein of pathogenic arenaviruses has been shown to inhibit RIG-I, although this has not been demonstrated for nonpathogenic arenaviruses [63]. NP has also been documented to bind and inhibit RIG-I and MDA5 preventing IRF3 nuclear translocation [64]. Despite the IFN antagonism of these proteins, JUNV infection in humans is characterized by highly elevated interferon alpha (IFN-α) cytokine levels (2,000 – 64,000 IU/ml) which have been correlated with fatal disease [65, 66]. Elevated (tumor necrosis factor alpha) TNF-α, IL-6, and IL-10 are also associated with fatal AHF [67].

There has been much speculation regarding the cellular source of inflammatory cytokines during JUNV infection. Interestingly, experiments have demonstrated that although the primary initial cell targets of JUNV infection are monocytes and macrophages, these cell types are not a source of inflammatory cytokine production [68]. It has been demonstrated, however, that type I IFN responses can be activated in human monocyte derived dendritic cells infected with JUNV and that this does trigger interferon stimulated gene (ISG) upregulation [69]. It has also been shown that human plasmacytoid dendritic cells infected with JUNV produce high levels of type I IFNs, indicating this may be, in part, the source of elevated inflammatory cytokines [70]. Evidence for parenchymal cell contribution to innate inflammatory responses also exists from experiments done in A549 cells [71].

An understanding of the interplay between JUNV infection, innate inflammatory responses, and survival is still tenuous. As mentioned, higher levels of inflammatory

cytokines are associated with fatal disease and the cytokines themselves have no direct inhibitory effect on JUNV replication as demonstrated by Groseth *et al.* (2011) and Huang *et al.* (2012) [68, 71]. On the other hand, mice, which are ordinarily resistant to AHF, become susceptible to JUNV infection and develop lethal disease when they are IFN (α or b) receptor deficient, suggesting the development of type 1 IFN responses do play an important role in survival, if not directly, perhaps via initiation of effective adaptive immune responses. It is also important to note that nonpathogenic New World arenaviruses, both the attenuated JUNV vaccine strain Candid #1 and Tacaribe virus, induce even greater type 1 IFN responses than virulent strains of JUNV, also implying these responses may play some protective role in JUNV infection [71, 72]. Further studies are needed to tease apart the role that innate inflammatory responses ultimately play in JUNV disease outcomes.

Adaptive immune responses are believed to be critical in the resolution of JUNV infection in humans. Old World arenaviruses such as LASV rely heavily on T-cell (CD8) responses for protection and survivors are often found to have undetectable IgG antibody titers after the resolution of disease [73]. Alternatively, survival from New world arenavirus infections, including JUNV, is believed to be due primarily to IgG antibody responses which begin 2-3 weeks after symptom onset and correspond with an improvement of clinical symptoms [74].

The clearest evidence of antibody-mediated protection in the case of JUNV comes from the therapeutic use of convalescent immune plasma from JUNV survivors which has been shown to reduce mortality to less than 1% in AHF patients [74, 75]. Importantly, neutralizing antibody titer in convalescent plasma has been shown to correlate with protection [76]. IgG antibody responses generated during human JUNV infection are typically directed toward the JUNV GP and NP viral proteins; however, protective neutralizing antibodies are known to target the JUNV GP [77]. In fact, studies have shown that antibodies directed exclusively against the JUNV GP produce robust neutralization

titers and are sufficient to fully protect guinea pigs from lethal JUNV challenge [78]. More specifically, JUNV neutralizing monoclonal antibodies known to target the GP's G1 subunit and receptor binding domain have been demonstrated to fully protect guinea pigs from lethal JUNV infection [77, 79-82]. Recently, neutralizing antibodies specific for the viral NP protein have also been identified indicating NP may be accessible on the virion surface and is another potential target for virus neutralization, although there is no *in vivo* data evaluating the protective efficacy of such antibodies [83].

Although neutralizing antibodies have been implicated extensively in JUNV protection, the effect of Fc-mediated immune responses on protection cannot be overlooked. An important study from Kenyon *et al.* (1990) addressed this idea by evaluating the protective efficacy of the F(ab) portions of JUNV neutralizing antibodies alone, in the absence of Fc effector function [84]. Whole neutralizing antibody preparations and F(ab)-only fractions could effectively neutralize virus *in vitro*. Interestingly, whole neutralizing antibody preparations could also protect guinea pigs from lethal JUNV infection while F(ab)-only fractions could not, indicating that virus neutralization alone was not sufficient for protection and that other mechanisms such as antibody-dependent cell-mediated cytotoxicity (ADCC), antibody-dependent cell-mediated phagocytosis (ADCP), or classical complement pathway activation may play an important role in protection via the clearance of JUNV infected cells [84]. A study looking at human IgG subclasses in JUNV survivors supports this notion. Ambrosio *et al.* (2003) reported that individuals who recovered from both mild and severe forms of AHF had a predominance of IgG1 antibodies [85]. IgG3 antibodies were found at low levels and only in severe cases while IgG2 and IgG4 were not detected at any time [85]. Importantly, Fc receptors from both IgG1 and IgG3 antibodies are known to have the most effective complement binding/activation as well as induction of ADCC activity.

Overall, currently available knowledge regarding JUNV immune responses and their role in protection is critical for informing the development of countermeasures against

the virus. Further research will need to be conducted to understand innate inflammatory responses and their role in protection. Importantly, we do know that adaptive immune responses are essential for JUNV survival, specifically antibody responses directed against the viral GP which can both neutralize the virus and facilitate effector functions. Ultimately, to further elucidate JUNV immunity and to screen for the efficacy of next-generation vaccines and therapeutics, *in vivo* studies using animal models of JUNV infection will be necessary.

Animal Models of JUNV Infection

Small animal models which recapitulate the JUNV disease course in humans are extremely important for initial, early screening of candidate vaccines and therapeutics. Adult mice are typically resistant to JUNV infection [86]. Newborn or adult TLR-4 knockout mice inoculated intracranially (i.c.) are susceptible to JUNV infection but present with an encephalitic disease inconsistent with AHF. Additionally, mouse models that are susceptible to JUNV infection exhibit different immune responses than those observed in human JUNV infection, *e.g.,* type 1 IFN and TNF-α production from macrophages as well as T-cell mediated pathogenesis [87, 88]. Overall, mice do not adequately recapitulate AHF disease. Guinea pigs are overwhelmingly the most accurate small animal model of JUNV infection. Both inbred strain 13 and outbred Hartley guinea pigs are susceptible to virulent JUNV strains Romero and Espindola via i.p. (intraperitoneal) infection and a uniformly lethal dose can be typically achieved using 100-5000 plaque forming units (PFU) of virus [42, 89-92]. Importantly, guinea pig models of AHF present with clinical signs that mirror many human symptoms including fever, tremor, and ocular or oral hemorrhage [42, 89, 90]. Guinea pigs also develop thrombocytopenia and elevated AST levels consistent with human infection. Additionally, virus can be detected in the liver, spleen, CNS, lymph nodes, and serum/plasma of infected animals [42, 89, 90].

Higher order animal models, *e.g.* nonhuman primates (NHPs), are essential for evaluating the safety and efficacy of vaccines and therapeutics before the initiation of clinical trials in human populations. Two specific NHP species have been well-characterized as models that recapitulate many of the major components of human JUNV disease: the common marmoset (*Callithrix jacchus*) and rhesus macaques (*Macaca mulatta*). The marmoset has been demonstrated to develop uniformly fatal disease when infected (i.m.) with JUNV strain XJ, developing both hemorrhagic and neurologic clinical signs and succumbing to disease within an average of 21 days [93-95]. Systemic JUNV infection has been shown to occur and virus can be detected in a variety of tissues at the time of death including brain, spleen, lymph nodes, and liver [96]. Marmosets have historically been used to evaluate both immune plasma and ribavirin for the treatment of JUNV disease [93]. They have also been used in studies to evaluate the protective efficacy of TCRV immunity against JUNV challenge [96]. While the JUNV marmoset model has been utilized effectively for JUNV countermeasure screening, it does not recapitulate the CNS-specific lesions or tissue damage that are reported often in fatal human cases of AHF [97]. Data are also limited regarding the pathogenesis of JUNV strains other than XJ in the marmoset model and rhesus macaques are therefore the preferred high order animal species for use in JUNV countermeasure studies.

Rhesus macaques develop a disease that closely mimics human AHF after (i.m.) JUNV inoculation [44, 98, 99]. Interestingly, it has been shown that the JUNV strain-specific phenotypic differences observed in human patients can also be observed/replicated in rhesus macaques [44, 98, 99]. Strain Espindola, which was isolated from a fatal human case of JUNV, is uniformly lethal and causes a disease that is predominated by a hemorrhagic phenotype including oral bleeding and petechial rashes [44, 98, 99]. Strain Ledesma, also isolated from a fatal human case, is dominated by neurologic clinical signs including tremor and balance /limb weakness [44, 98, 99]. Strain Romero, isolated from a nonfatal case, is similarly nonlethal in the rhesus macaque model, causing a “mixed” but

mild disease [44, 98, 99]. All of the above-mentioned strains cause thrombocytopenia, leukopenia, and elevated liver enzymes/hepatocyte necrosis in the rhesus macaque model [44, 98, 99]. An aerosol model of JUNV infection has also been developed in rhesus macaques which is important for mimicking the primary route of transmission/infection to humans [100]. Aerosol and i.m. routes of inoculation with JUNV strain Espindola have been shown to result in virtually identical clinical disease courses where the virus is uniformly lethal after an average of 21 days [100]. Notably, rhesus macaques were the NHP model utilized for much of the preclinical testing of Candid #1 safety and immunogenicity [101, 102].

Overall, animal models which recapitulate the hallmark clinical features of human JUNV infection are essential for verifying the safety and efficacy of new vaccine or therapeutic candidates. Initial screening of JUNV countermeasures can be effectively performed in a guinea pig model with subsequent evaluation in the rhesus macaque NHP model which has been shown to reliably represent human responses during AHF.

Human AHF	Neonatal Mouse	Type I IFN receptor KO Mouse	Guinea pig	Common Marmoset	Rhesus macaque
Clinical features					
Fever	n	n	Y	Y	Y
Petichial rash	n	n	Y	n	Y
Oral hemorage	n	n	Y	Y	Y
Tremor/neurologic signs	Y	Y	Y	Y	Y
Death	Y	Y	Y	Y	Y
Hematologic features					
Thrombocytopenia	unknown	unknown	Y	Y	Y
Leukopenia	unknown	unknown	Y	Y	Y
Pathologic features					
Hepatocyte necrosis	n	n	Y	Y	Y
CNS lesions	Y	Y	Y	n	Y
Route of administration	i.c.	i.p.	i.p./i.m.	i.m.	i.m./aerosol
JUNV strain suceptibility	XJ13	Romero	Romero, Espindola, XJ, Ledesma	XJ	Espindola, Ledesma

Table 1-1. Animal models of JUNV infection. Major clinical, hematologic, and pathologic features commonly present during human AHF are compared in five animal models of JUNV infection.

Therapeutics

Therapeutic countermeasures available for the treatment of AHF are limited. The antiviral ribavirin, though not licensed to treat JUNV, has been shown to delay time-to-death in nonhuman primates (NHP) but provides minimal protection unless administered prophylactically [74, 103]. Clinical trials of ribavirin indicate a similar lack of efficacy in human patients, likely due to the absence of symptom specificity during the first week of infection resulting in delayed diagnosis and treatment [104, 105]. As mentioned previously, convalescent plasma from JUNV survivors has been shown to be effective as a therapeutic. A double-blind placebo-controlled study determined that administration of immune plasma reduced overall case-fatality from 16.5% to 1.1% [33, 74, 75]. Despite the effectiveness of convalescent plasma, there are several limitations with regard to its use, including inherent difficulties with maintaining and ensuring the safety of plasma stocks, the need for administration within 8 days of symptom onset, and the occurrence of a delayed neurologic syndrome in approximately 10% of treated patients [75]. Importantly, virus neutralization has been identified as a correlate of antibody protection prompting research to focus on the development of monoclonal antibody-based therapies [76].

In 1989, a panel of monoclonal antibodies was generated by Sanchez *et al.* and, due to advances in the large scale production of humanized monoclonal antibodies, some of the more promising candidates were recently developed further for testing *in vivo* [77, 90]. Three antibodies, known as J199, J200, and J202 were all found to provide 100% protection to guinea pigs when administered as a single dose, 2 days after JUNV challenge. J199 was also found to be 100% protective when administered 7- and 11-days post-challenge, making it the most promising JUNV monoclonal antibody candidate to-date [90]. Additional therapeutic candidates have been studied *in vitro*, including siRNAs and small molecule inhibitors, but none have demonstrated the efficacy of monoclonal antibodies and none are yet licensed for use in humans [106, 107].

Currently, there are no FDA licensed therapeutic countermeasures for the treatment of AHF. JUNV monoclonal antibodies are the most promising therapeutic candidates in development but need further evaluation for efficacy in higher-order animal models (NHPs). Considering the promise of monoclonal antibody-based therapies, the development of tools for *in vitro* biosafety level 2 (BSL-2) screening purposes may be important, particularly for expanding JUNV research outside of the typical BSL-4 containment requirements. In addition, although a live-attenuated JUNV vaccine is currently in-use in the endemic area, its significant limitations are well-documented (outlined below) and emphasize further the need for JUNV therapeutic development.

Vaccine – Candid #1

A live-attenuated JUNV strain named Candid #1 is the only available vaccine for the prevention of AHF in Argentina [32]. Candid #1 was developed as a collaboration of the global community including PAHO, the Argentine government, the United States Army Medical Research Institute of Infectious Diseases (USAMRIID), and the United Nations. The vaccine strain was generated from virulent JUNV strain XJ passaged 44 times through mouse brain with subsequent passaging in FRhL cells (x19) [32].

Widespread administration of the vaccine in Argentina began in 1991 and studies have demonstrated that the vaccine is both immunogenic and effective [32]. An average of 91.1% of vaccinated persons seroconvert within 5 months of a single vaccination and over a 9-year period the vaccine effectiveness was determined to be 98.1 % [32]. Although effective in Argentina, Candid #1 has several significant limitations which preclude it from receiving FDA approval in the United States. Specifically, Candid #1 retains a low level of neurotropism. A study in rhesus macaques vaccinated intramuscularly with Candid #1 resulted in neuronal lesions that were consistent with wild type JUNV infection in 4 out of 24 animals [32]. Candid #1 also has an unstable attenuated

phenotype, with a single *in vivo* passage yielding isolates up to 100-fold more neurovirulent than the parental attenuated virus [32]. Further, the attenuated phenotype is believed to rely heavily on a single amino acid substitution (F427I) in the glycoprotein's transmembrane domain [108]. Adverse events associated with Candid #1 have been reported to be as high as 29-35% and include low platelet count, vomiting, and fever [32]. An unpublished study from Dr. Mauricio Mariani (INEVH 2018) examined potential Candid #1 virus reversion, specifically neurovirulence, by collecting isolates from vaccinated individuals who developed febrile illness post-vaccination. He injected the isolated virus into a guinea pig model where Candid #1 infection typically does not show evidence of virus replication in the brain or bone marrow; however, he found that virus isolated from two Candid #1 vaccinees could be detected and isolated from guinea pig brain and bone marrow. These data reinforce concerns of neurotropism and attenuation instability after Candid #1 passage *in vivo*.

I propose that an alternative JUNV vaccine that can overcome hurdles for FDA licensure should be explored. One such alternative could be the use of the recombinant vesicular stomatitis virus (rVSV) vaccine vector system. rVSV-based vaccines are promising because they have demonstrated protective efficacy against hemorrhagic fever viruses in guinea pigs, hamsters, NHPs, and humans [109-112].

Recombinant Vesicular Stomatitis Virus Vaccine Platform

Recombinant vesicular stomatitis virus (rVSV)- based vaccines have been effective in providing protection against hemorrhagic fever viruses in humans. Notably, a Phase III clinical trial of a rVSV *Zaire ebolavirus* vaccine in Guinea demonstrated 100% vaccine efficacy and has since been administered to nearly 200,000 people in the Democratic Republic of the Congo to combat an ongoing outbreak of *Zaire ebolavirus* (EBOV) [111]. Further, a rVSV expressing the GPC of Lassa virus (LASV), a prominent Old World

Arenavirus, has been shown to be fully protective against lethal LASV challenge in guinea pigs and NHPs, indicating the same strategy may be promising for the development of a JUNV vaccine [113, 114].

VSV infection is typically asymptomatic or causes mild disease in humans and has low seroprevalence in human populations, circumventing issues of preexisting immunity [115-117]. VSV also grows to high titers in nearly all mammalian cell lines and has been shown to elicit strong cellular and humoral immune responses in vivo making it an ideal vaccine platform [116]. Additionally, a number of rVSV-based vaccines have shown post-exposure protective efficacy in NHP models, including 100% protection against *Sudan ebolavirus* and *Marburg marburgvirus* (MARV) when administered 30 min after challenge [101, 118, 119]. rVSV vaccines have also been demonstrated to be safe for use in immunocompromised, Simian immunodeficiency virus (SIV) infected, NHPs [120]. Supporting the idea that rVSV vaccines may be safe for immunocompromised persons, the rVSV EBOV vaccine was inadvertently administered to 25 HIV-infected persons during the PREVAIL-I clinical trial without adverse effect, although more data is needed on safety in these populations [121]. rVSV vaccines have also been shown to induce long-term protective responses in animal models including guinea pigs and NHPs [114, 122, 123]. A rVSV MARV vaccine was 100% protective in NHP's 14 months post-vaccination and a rVSV EBOV vaccine was 100% protective in guinea pigs 18 months post-vaccination. There is also evidence about the durability of the antibody response generated from rVSV EBOV vaccinated humans showing strong IgG antibody persistence at least 2 years post-vaccination [124, 125].

In conclusion and based on the above summarized data, my dissertation will move forward with addressing the following hypotheses:

A recombinant vesicular stomatitis virus expressing the Junin virus glycoprotein (rVSVΔG-JUNVGP) can be utilized as:

1. **A vaccine against lethal JUNV challenge.**

   I will investigate this hypothesis by evaluating the protective efficacy of rVSVΔG-JUNVGP in a guinea pig model of lethal JUNV infection. In addition to assessing survival outcomes, I will quantify JUNV tissue and plasma load after challenge to determine whether the vaccine protects against systemic viral dissemination. I will also evaluate IgG antibody responses to vaccination, including titer, quality, and neutralization ability to begin to elucidate correlates of vaccine protection.

2. **An accurate and rapid method for quantification/detection of JUNV neutralizing antibodies.**

   I plan to test this hypothesis in two parts. First, by showing that rVSVΔG-JUNVGP can detect neutralizing monoclonal antibodies with the same accuracy as wild type and attenuated JUNV strains via PRNT assay. I will also show that rVSVΔG-JUNVGP can detect neutralizing antibodies in guinea pig plasma as well as human serum with the same accuracy as wild type JUNV, demonstrating its potential for use as a tool for JUNV serologic detection in the endemic area.

3. **A platform for the development of chimeric arenavirus glycoprotein antigens.**

   After successfully demonstrating that a rVSV expressing the JUNV GP is protective in a guinea pig model (AIM 1), I will show that other immunogenic arenavirus epitopes can be inserted/swapped into the JUNV GPC gene to generate chimeric arenavirus GPs. I will show that these chimeric proteins may be immunogenic (via immunofluorescence assay) and are functional (via a rVSV

pseudotype assay), and thus have the potential for use in a cross-protective arenavirus vaccine.

Chapter 2: rVSVΔG-JUNVGP Vaccine[2]

JUNV is categorized as NIAID Category A priority pathogen due to its virulence in humans. In many cases JUNV causes severe hemorrhagic or neurologic disease. It has a potential for aerosol transmission, making it a prominent biodefense concern. Mortality rates for persons with symptomatic AHF are as high as 30% [33].

As reviewed in Chapter 1, therapeutic countermeasures available for the treatment of AHF are limited. The antiviral ribavirin, though not licensed to treat JUNV, has been shown to delay time-to-death in nonhuman primates (NHP) but provides minimal protection unless administered prophylactically [103]. Clinical trials of ribavirin indicate a similar lack of efficacy in human patients, likely due to the lack of symptom specificity during the first week of infection causing difficultly in adequately diagnosing and initiating rapid treatment for JUNV [105]. Convalescent plasma from JUNV survivors has been shown to be effective as a therapeutic, reducing overall case-fatality to 1%, however there are inherent difficulties with maintaining and ensuring the safety of plasma stocks [33, 74-76].

A live-attenuated JUNV strain named Candid #1 is the only available vaccine for the prevention of AHF in Argentina. Although used in Argentina, Candid #1 has several limitations which preclude it from receiving Food and Drug Administration (FDA) approval in the United States. Specifically, Candid #1 retains a low level of neurotropism. A study in rhesus macaques vaccinated intramuscularly with Candid #1 resulted in neuronal lesions that were consistent with wild type JUNV infection in 4 out of 24 animals [32]. Candid #1 has an unstable attenuated phenotype, with a single *in vivo* passage yielding isolates up to 100-fold more neurovirulent than the parental attenuated virus [32]. Further, the attenuated phenotype is believed to rely heavily on a single amino acid

[2] Selections of Chapter 2 have been submitted for publication: Sorvillo TE, Cross RW, Fenton KA, Mire CE, Geisbert TW. Single Dose rVSVΔG-JUNVGP Vaccine Protects Guinea Pigs Against Lethal Junin Virus Challenge. Submitted to NPJ Vaccines, Oct 2019.

substitution (F427I) in the glycoprotein's transmembrane domain [108]. Adverse events associated with Candid #1 have been reported to be as high as 29-35% and include low platelet count, vomiting, and fever [32]. Due to these Candid #1 limitations, an alternative JUNV vaccine that can overcome these hurdles for FDA licensure should be explored.

One such alternative could be the use of the recombinant vesicular stomatitis virus (rVSV) vaccine vector system. Inserting foreign glycoprotein sequences into the VSV reverse genetics system and recovering rVSVs has been procedurally well-established with a significant history of success [109, 110, 112, 113, 126]. rVSV-based vaccines have also been effective in providing protection against hemorrhagic fever viruses in humans. Notably, a Phase III clinical trial of a rVSV *Zaire ebolavirus* vaccine in Guinea demonstrated 100% vaccine efficacy and has since been administered to nearly 200,000 people in the Democratic Republic of the Congo to combat an ongoing outbreak of *Zaire ebolavirus* [111]. Further, a rVSV expressing the GPC of Lassa virus (LASV), a prominent Old World arenavirus, has been shown to be fully protective against lethal LASV challenge in NHPs [113], indicating the same strategy may be promising for the development of a JUNV vaccine. Importantly, the JUNV GP has been demonstrated to be a potent immunogen which elicits protective neutralizing antibody responses. Studies have shown that antibodies directed exclusively against the JUNV GP produce robust neutralization titers and are sufficient to fully protect guinea pigs from lethal JUNV challenge, suggesting that the GP would be a prudent antigen choice for JUNV vaccine development [78].

In this chapter I present data on the recovery of a rVSV expressing the JUNV GP (rVSVΔG-JUNVGP) and characterization of this vaccine vector. Additionally, I assessed rVSVΔG-JUNVGP as a vaccine in a lethal JUNV guinea pig challenge model.

METHODS

Viruses and Cell lines

Vero 76 cells (American Type Culture Collection-ATCC) were maintained in Eagle's Minimum Essential Medium (EMEM) supplemented with 10% fetal bovine serum (FBS), 1% penicillin/streptomycin (P/S), and 1% GlutaMAX. Baby hamster kidney cells (BHK) cells (Michael Whitt, University of Tennessee Health Science Center) were maintained in Dulbecco's Modified Eagle's Medium (DMEM) supplemented with 5% FBS, 1% P/S, and 1% GlutaMAX. JUNV Espindola and Romero stocks were obtained from Thomas Ksiazek, University of Texas Medical Branch (UTMB). JUNV strain Espindola (P3790) was passaged twice in Vero E6 cells and once in Vero 76 cells with prior passage history in mice (2x). JUNV strain Romero (P3235) was passaged three times in Vero E6 cells with prior passage history in mice (2x) and medical research council (MRC) cells (x2). JUNV vaccine strain Candid #1 was acquired from the UTMB Arbovirus Reference Collection with prior passage history in Vero (2x) and FRhL cells. All experiments conducted with JUNV were performed in biosafety level 4 (BSL-4) containment at the Galveston National Laboratory, UTMB.

rVSVΔG-JUNVGP Cloning, Recovery, and Characterization

A reverse genetics system for the development of rVSVs expressing non-homologous glycoproteins has been described previously [126, 127]. Briefly, the native VSV glycoprotein (G) gene was removed via Mlu1/Nhe1 restriction digest (New England Biolabs, Inc.) from a Bluescript plasmid containing the full length VSV genome. A codon-optimized cDNA sequence (generated by GenScript) encoding the JUNV Espindola GPC was ligated in its place using a Fast-Link DNA ligation kit (Epicentre). The following strains of *Escherichia coli* (*E. coli*) were utilized to transform and propagate the plasmid:

C600 (Zymo Research), NEB 10-beta (New England BioLabs Inc.), JM109 (Zymo Research), and HI-Control 10G (Lucien) competent cells. Bacterial colonies were screened for the presence of rVSVΔG-JUNVGPC plasmid via polymerase chain reaction (PCR) using a GoTaq polymerase (Promega), VSV M forward, VSV L reverse, and JUNV GPC-specific primers. Plasmid isolation and purification was performed using the ZymoPURE Plasmid Maxiprep kit (Zymo Research). The resulting plasmid was transfected into BHK cells and recovered as described by Lawson *et al.* (1995) [127]. Recovered virus was plaque purified and passaged two times through Vero76 cells. The resulting virus stocks were characterized by generating a growth curve in Vero76 cells inoculated at a multiplicity of infection (MOI) of 0.01. Supernatants were harvested every 12 hours from 0-96 hours post-inoculation (PI). For comparison, a growth curve was generated using rVSV-GFP (wild type rVSV expressing VSV Indiana GP and green fluorescent protein); Vero76 cells were inoculated at a MOI of 0.01 and supernatants were harvested at 0, 6, and 24 hours PI. Immunofluorescence assays (IFA) were conducted with rVSVΔG-JUNVGP to evaluate the expression of both the VSV matrix protein (M) and the JUNV GP. Vero76 cells were inoculated at a MOI of 0.01 and fixed with 4% paraformaldehyde (PFA) 24 hours PI. The fixed monolayers were permeabilized using 0.1% Triton X-100 followed by incubation with a primary VSV-M monoclonal (1^0) antibody (23H12) diluted 1:1000 and anti-mouse IgG Alexa Flour 488 secondary (2^0) antibody diluted 1:1000. Cell nuclei were counterstained with 4′,6-diamidino-2-phenylindole (DAPI). BHK cells were inoculated and fixed as described above but were not permeabilized in order to evaluate the expression of JUNV GP exclusively on the cell surface. Fixed BHK cells were incubated with a primary JUNV GP monoclonal 1^0 antibody (Mapp Biopharmaceutical, Inc.) (1:5000) and anti-human IgG Alexa Flour 488 2^0 antibody (1:5000). Sequencing was performed by the UTMB Molecular Genomics Core using the Applied Biosciences (ABI) Prism 3130XL DNA sequencer and using VSV M forward, VSV L reverse, and JUNV GP-specific primers. All sequence data were analyzed using SnapGene 4.1.9 software.

Guinea Pig Vaccine Studies

In vivo studies were conducted with weight-matched (451-500 gram) outbred female Hartley guinea pigs purchased from Charles River Laboratories. In all studies, clinical scores were assessed daily and documented as: Normal (1), Rough (2), Sick (3), Paralysis and/or Euthanize (4). All animals were necropsied after meeting euthanasia criteria or on day 35. Animal work was conducted in biosafety level 4 (BSL-4) containment at the Galveston National Laboratory under the approved guidelines of the UTMB Institutional Animal Care and Use Committee (IACUC). Animal research was performed in compliance with the Animal Welfare Act and other Federal statutes and regulations relating to animals and experiments involving animals and adheres to the principles stated in the eighth edition of the *Guide for the Care and Use of Laboratory Animals*, National Research Council, 2011. UTMB is fully accredited by the Association for Assessment and Accreditation of Laboratory Animal Care International.

EXPERIMENT 1: STUDY DESIGN

Fifteen animals were divided into prime (1-1 through 1-6), prime-boost (2-1 through 2-6), and control groups (C-1 through C-3). Animals from the prime and prime-boost groups were vaccinated i.p. with 7.5e6 PFU of rVSVΔG-JUNVGP (day -35). Animals in the prime-boost group received an additional 7.5e6 PFU dose on day -14. All animals were challenged i.p. with a lethal dose (1000 PFU) of JUNV strain Romero. Blood was collected from all animals on the following days: -14, 0, 7, 14, and 35 or terminal. Liver and spleen tissue were collected from all animals upon necropsy. Brain tissue was collected from all animals which succumbed after day 12 post-challenge, including all survivors.

EXPERIMENT 2: STUDY DESIGN

Forty-two animals were divided into two groups, each challenged with a different strain of JUNV (Romero or Espindola). Animals were further divided into four vaccine groups per challenge virus: rVSVΔG-JUNVGP prime (n=6), rVSVΔG-JUNVGP prime-boost (n=6), Candid #1 (n=6), and control (n=3). All animals in rVSVΔG-JUNVGP vaccine groups received a single 7.5e6 PFU i.p. vaccine injection 35 days before JUNV challenge while animals in rVSVΔG-JUNVGP prime-boost vaccine groups received an additional 7.5e6 PFU dose on day -21. Animals in Candid #1 groups received a single 1000 PFU i.p. vaccine injection 35 days before challenge. Animals were challenged i.p. on day 0 with either 1000 PFU of JUNV strain Romero or 4000 PFU of JUNV strain Espindola. Six additional historical controls of JUNV Espindola-challenged guinea pigs were included in the overall analysis. Blood was collected from all animals on the following days: -56, -28, 0, 9, 16 and 35 or terminal. Liver, spleen and brain tissue were collected from all animals at necropsy. The following animal designations were used: rVSVΔG-JUNVGP prime-Romero (3-1 through 3-6), rVSVΔG-JUNVGP prime-boost-Romero (5-1 through 5-6), Candid #1-Romero (7-1 through 7-6), rVSVΔG-JUNVGP prime-Espindola (4-1 through 4-6), rVSVΔG-JUNVGP prime-boost-Espindola (6-1 through 6-6), Candid #1-Espindola (8-1 through 8-6), Romero controls (C-R1 through C-R3), and Espindola controls (C-E1 through C-E3).

EXPERIMENT 3: STUDY DESIGN

Twenty-four animals were divided into two groups, each receiving the rVSVΔG-JUNVGP vaccine via a different route: intramuscular (i.m.) or i.p. These groups were further divided into prime and prime-boost vaccinated cohorts. Three total control animals remained unvaccinated. Animals in the study were given the following designations: control (C-1 through C-3), prime i.m. (1-1 through 1-6), prime-boost i.m. (2-1 through 2-6), prime i.p. (3-1 through 3-6), and prime-boost i.p. (4-1 through 4-6). Animals from the

prime and prime-boost groups were vaccinated with 1e7 PFU of rVSVΔG-JUNVGP administered via the indicated route (day -56). Animals in the prime-boost group received an additional 1e7 PFU dose on day -28. All animals were challenged i.p. with a lethal dose (1000 PFU) of JUNV strain Romero on day 0. Weight and temperature measurements were recorded every 3 days between day 0 and 21, day 28, and 35 or terminal for each animal. Temperatures were assessed using Bio Medic Data Systems, Inc. electronic implantable transponders. Blood was collected from all animals on the following days: -56, -28, 0, 9, and 35 or terminal. Liver, spleen and brain tissue were collected from all animals at necropsy.

Plasma and Tissue Virus Load

Virus titers were determined via plaque assay. Plasma was diluted 10-fold and plated on Vero 76 cell monolayers in duplicate wells (200 µl) with 0.8% agarose overlay. Tissues were homogenized into a 10% working dilution and titered as above. All plates were stained with 5% neutral red 5 days PI and plaques were read on day 6. The limit of detection for the assay is 25 PFU.

Antibody Titers

IgG antibody titers were assessed via enzyme-linked immunosorbent assay (ELISA). Purified JUNV strain Romero G1/G2 protein was used to coat 96 well polystyrene ELISA plates at 1µg/ml diluted in 1x PBS. Plasma samples were serially diluted two-fold (starting 1:100 or 1:1000) using 5% BSA/0.05% Tween20 in 1xPBS, plated in triplicate, and incubated overnight at 4^0C. Plates were washed with 0.2% Tween20 in 1xPBS and incubated for 1 hour with goat anti-guinea pig IgG conjugated to horseradish peroxidase (HRP) diluted 1:5000. Plates were washed, incubated with ABTS

(2,2'-azino-bis(3-ethylbenzothiazoline-6-sulphonic acid)) peroxidase substrate (KPL) for 20-30 minutes, and read at 405nm on a Molecular Devices Emax precision microplate reader. Data are reported as IgG reciprocal endpoint dilution titers.

Antibody Avidity

IgG antibody quality was evaluated with an ELISA-based avidity assay that utilizes varying concentrations of urea to disrupt antibody/antigen complex binding. ELISA methodologies listed above were modified such that plasma samples for each animal, or monoclonal antibodies, were diluted to achieve a uniform optical density (0.8 - 1.0). After plasma/antibody incubation, plates were washed, 1M through 11M concentrations of urea (diluted in PBS) were each plated in triplicate, incubated for 15 minutes at room temperature, and washed before proceeding to secondary antibody incubation. Data are calculated as percent antibody/antigen dissociation compared with PBS-only treated controls.

JUNV Monoclonal Antibodies

A panel of six JUNV monoclonal antibodies, originally produced and characterized by Sanchez *et al.* (1989), were obtained from Biodefense and Emerging Infections Research Resources Repository (BEI Resources) [77]. Antibody GB03-BE08, also identified as J199, was also obtained courtesy of Mapp Biopharmaceutical, Inc. [90]. GB03-BE08 was produced from mouse hybridoma while J199 was produced from transgenic *N. benthamiana* and contains a human antibody constant region; all avidity data reported on these antibodies are cumulative and represent repeated testing with both GB03-BE08 and J199. See Table 3-1 for detailed information regarding antibody epitope specificity and protective efficacy *in vivo*.

Neutralization Antibody Titers

Plaque reduction neutralization tests (PRNT) were performed to evaluate neutralizing antibody titers. Plasma was diluted two-fold (1:10 to 1:20480) in EMEM supplemented with 10% guinea pig complement [128]. Plasma dilutions were then incubated 1:1 with 100 PFU of JUNV Espindola for 1 hour at 37ºC. JUNV strain Espindola was utilized specifically in this assay because the GP is homologous to that of rVSVΔG-JUNVGP. Plasma and virus dilutions were plated in duplicate (200µl) on Vero 76 cell monolayers with 0.8% agarose overlay. Plates were stained 5 days PI with 5% neutral red and plaques were counted on day 6 PI to determine the plasma dilution required to achieve 50% plaque reduction ($PRNT_{50}$) compared to baseline (day -56) plasma samples.

Histology and Immunohistochemistry

Embedded tissues were sectioned (4um) and deparaffinized in xylene, graded ethanol and DI water. Antigen retrieval was performed in 10mM pH6 citrate buffer (20 minutes) at 95 degrees C. Sections were quenched in 3% hydrogen peroxide (10 minutes) before being processed for immunohistochemistry (IHC) using the Thermo Scientific Lab Vision Autostainer 360. Avidin D and Biotin (Invitrogen) were applied (15 minutes) and sections were treated with Background Buster (Innovex Biosciences) (30 minutes) to prevent nonspecific signal. Immunoreactivity for *in vivo* Experiment #1 was detected using anti-JUNV mouse ascites (courtesy of Dr. Thomas Ksiazek) at 1:400 dilution (1 hour), and for Experiment #2, anti-JUNV NP mouse polyclonal primary antibody at 1:1000 dilution (1 hour) (LifeSpan BioSciences, Inc.). Following primary antibody incubation, all sections were treated with biotinylated goat anti-mouse IgG 2^0 antibody (Vector Labs) at 1:1600

(30 minutes) and streptavidin-HRP (30 minutes) (Vector Labs). Slides were developed with Dako DAB chromagen and counterstained with Harris Hematoxylin.

Statistical Analyses

GraphPad Prism 7.03 was utilized for Kaplan-Meier survival curves, Log-rank tests, unpaired t-tests (Mann-Whitney), and analysis of variance (ANOVA) statistical analyses of survival, IgG antibody titer, avidity, and neutralization titer. All statistical notations correspond with the following p values: *$p < 0.05$, **$p < 0.01$, ***$p < 0.001$, ****$p<0.0001$.

RESULTS & DISCUSSION

rVSVΔG-JUNVGPC Molecular Cloning

I performed initial attempts to ligate the JUNV Espindola GPC (cDNA sequence derived from viral RNA) into the rVSVΔG vector backbone which were unsuccessful (Figure 2-1). Vector and insert preparations were carefully screened for purity and vector:insert ratios were optimized. Transformation of ligation reactions (using *E. coli* strain C600) yielded significant numbers of bacterial colonies but none were positive via PCR for the desired rVSVΔG-JUNVGPC plasmid.

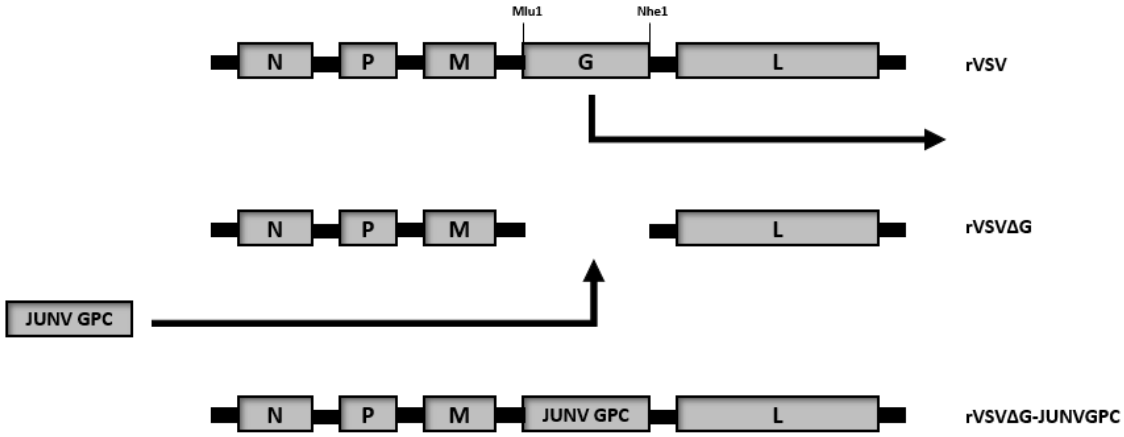

Figure 2-1. rVSVΔG-JUNVGPC plasmid cloning. The VSV reverse genetics system consists of a Bluescript plasmid containing the full-length VSV genome encoding the following viral proteins: nucleoprotein (N), phosphoprotein (P), matrix protein (M), glycoprotein (G), and RNA-dependent RNA polymerase (L). Mlu1 and Nhe1 restriction sites/digests were used to remove the native VSV G gene. A JUNV GPC cDNA fragment was ligated in its place, resulting in the rVSVΔG-JUNVGPC plasmid.

In order to evaluate whether recirculation of the vector backbone due to incomplete restriction digestion was the cause, a control ligation reaction was performed using only the rVSVΔG vector. Vector-only control reactions consistently yielded minimal bacterial colonies indicating that recircularization of the vector sequence was unlikely. Next, I purified and analyzed (via gel electrophoresis) any plasmid DNA recovered from the PCR-negative (vector + insert) bacterial colonies. Interestingly, the results indicated that a truncated plasmid was being propagated and recovered from the majority of bacterial colonies (Appendix A-1).

I analyzed via gel electrophoresis the vector + insert ligation reactions prior to bacterial transformation to evaluate whether they were resulting in an appropriately sized (rVSVΔG-JUNVGPC) plasmid (Figure 2-2). I was able to determine that the ligation reactions were, in fact, successful, indicating that bacterial propagation of the plasmid in

E. coli (strain C600) was possibly resulting in modification or recombination of the plasmid construct. In order to understand the reason behind this occurrence, I conducted *in silico* analysis of the JUNV GPC sequence, searching for the presence of recombination hotspot sequences. Recombination hotspots are DNA sequences that are more likely (hundreds of times) than their surrounding/flanking genetic sequences to undergo recombination during plasmid replication. They are short nucleotide sequences which are known to form hairpin structures during plasmid replication and are hence more likely to result in DNA breaks, leading to recombination events [129].

In silico analysis revealed that the JUNV strain Espindola GPC contained 5 recombination hotspots within its 1.6 kilobase (KB) sequence, or greater than 3 per KB (Table 2-1). In order to determine the relative significance of this finding I also evaluated the rVSVΔG nucleotide sequence which is 14 KB and determined that it contained only 11 recombination hotspots, or less than 1 per KB (Table 2-1). Additionally, I evaluated the GPC sequence from LASV strain Josiah which has been successfully cloned into rVSVΔG using the methodologies listed above. The LASV GPC contained 2 recombination hotspots in its 2 KB DNA sequence which is also only 1 per KB (Table 2-1). This information in conjunction with my experimental results suggested that recombination may be preventing successful rVSVΔG-JUVGPC plasmid recovery.

Several methodologies were attempted in order to prevent rVSVΔG-JUNVGPC plasmid recombination from taking place during bacterial propagation. I utilized several alternative *E. coli* strains including NEB 10-beta, HI-Control 10G, and recombination deficient (rec A-) JM109, among others. I also attempted to grow all bacterial cultures at lower temperatures (23ºC) which can slow plasmid replication, counteracting DNA instability and minimizing recombination events. I utilized rolling circle amplification (RCA) PCR in order to attempt to amplify the rVSVΔG-JUNVGPC plasmid outside of the confines of bacterial growth. Ultimately, the above-mentioned strategies proved unsuccessful or inefficient.

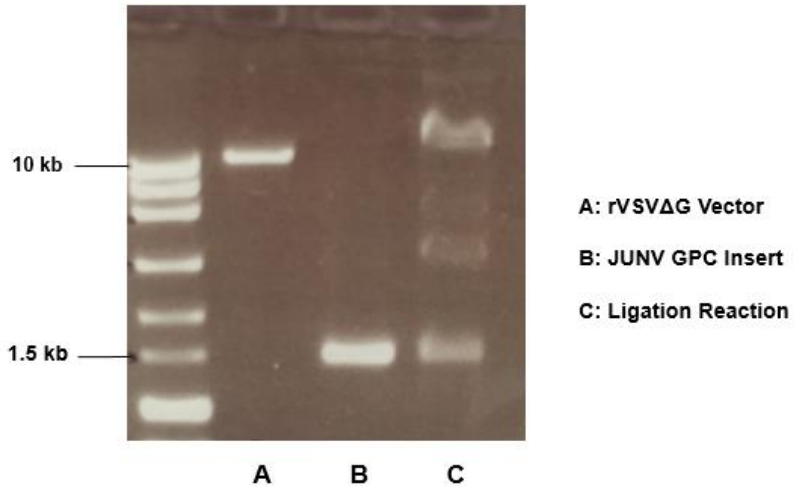

Figure 2-2. Successful ligation of rVSVΔG vector with JUNV GPC insert. Agarose gel (0.8%) stained with ethidium bromide (10mg/ml). Lane A: 100 ng purified rVSVΔG vector DNA (~14 kb). Lane B: 100 ng purified JUNV GPC insert DNA (~1.6 kb). Lane C: 5µl of rVSVΔG + JUNV GPC ligation reaction showing evidence of successful ligation (top band).

Gene	Length (kb)	Total Recombination Hotspots	Recombination Hotspots/kb
JUNV Espindola GPC	1.6	5	3.125
JUNV Romero GPC	1.6	5	3.125
rVSVΔG	14	11	0.786
LASV Josiah GPC	2	2	1.0

Table 2-1. Recombination Hotspot Quantification. *In silico* (SnapGene 4.1.9) quantification of recombination hotspots present in the JUNV GPC, LASV GPC, and rVSVΔG genetic sequences. The following nucleotide sequences were quantified [129]: GCN-NGC, GAA-TTC, GAG-CTG, CGG-CCG, CAG-CTG.

Lastly, I ordered a codon optimized JUNV GPC gene sequence designed to remove any recombination hotspots by making single nucleotide point mutations but maintaining amino acid sequence integrity. Ultimately, this JUNV GPC sequence resulted in successful propagation and isolation of the rVSVΔG-JUNVGPC plasmid when used in conjunction with two specific *E. coli* strains: NEB 10 and HI Control 10G. PCR and restriction digest confirmation were performed as seen in Figure 2-3. VSV-specific primers which flank the GPC gene were utilized to screen for the presence of the JUNV GPC and positive colonies yielded 1.6 kb bands (Figure 2-3A). Restriction digests were performed using purified plasmid from PCR-positive bacterial colonies. Digests using Nhe1 alone resulted in a 15-16 kb band and digests using both Mlu1/Nhe1 resulted in bands at 14 and 1.6 kb, the size of the vector and insert respectively (Figure 2-3B). The parent plasmid from which rVSVΔG was derived (rVSVΔG-ChEBOV3GP) was used as a control (Figure 2-3B).

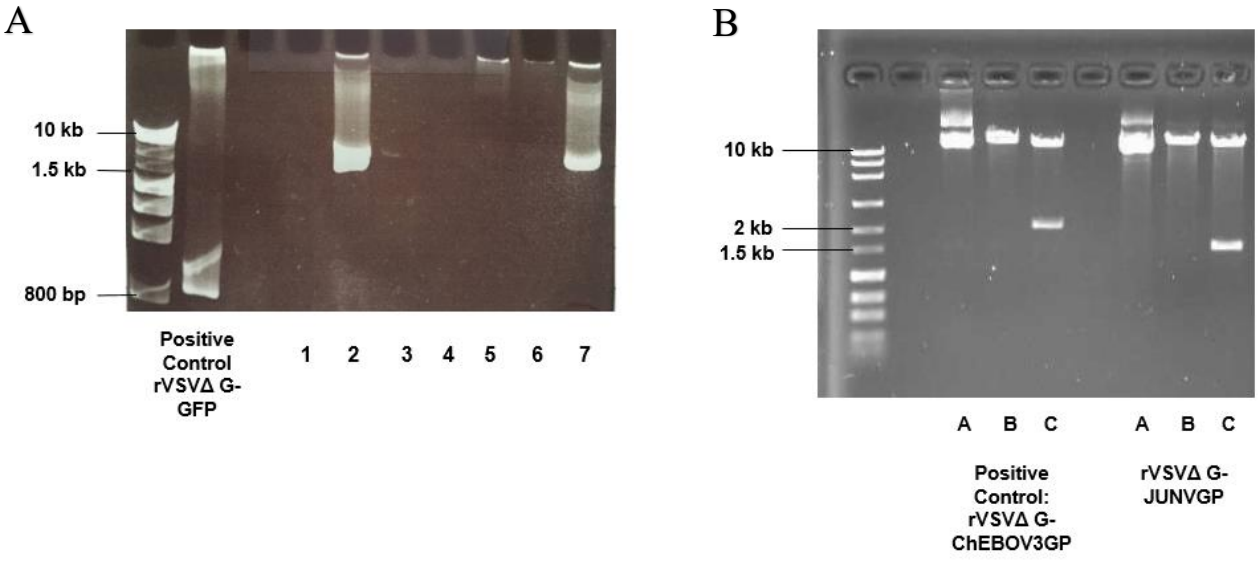

Figure 2-3. rVSVΔG-JUNVGP plasmid confirmation via PCR and restriction digest. A, PCR screening of (n=7) bacterial colonies resulting from transformation of rVSVΔG + JUNV GPC ligation reaction. PCR reaction utilized GoTaq DNA polymerase and VSV M forward/VSV L reverse primers which flank the GPC gene. Bacterial colonies 2 and 7 were positive for a 1.6 kb band corresponding with the size of the JUNV GPC gene. PCR reactions (including PCR control) were run on a 6% polyacrylamide gel. B, Restriction digest of purified, PCR positive plasmid. The parent plasmid from which rVSVΔG was derived (rVSVΔG-ChEBOV3GP) was also digested as a control. Lane A: uncut plasmid. Lane B: Nhe1 only digest. Lane C: Mlu1/Nhe1 double digest. Restriction digests were run on a 0.8% agarose gel. All gels were stained with ethidium bromide (10mg/ml).

rVSVΔG-JUNVGP Virus Recovery and Characterization

I was successful in recovering rVSVΔG-JUNVGP virus and generating a growth curve to demonstrate replication competence in Vero76 cells where peak viral titer occurred 36 hours PI (Figure 2-4B). Immunostaining for VSV M in permeabilized Vero76 cells resulted in observable M protein localized to the cell cytoplasm, nucleus, and plasma membrane, a pattern typical for wild type VSV (Figure 2-4C, Left). JUNV GP immunostaining on non-permeabilized cells resulted in observable GP on the cell surface (Figure 2-4C, Right), indicating the GPC was processed and translocated effectively to the plasma membrane when expressed from the rVSV genome. Sequencing was also performed on plaque purified virus seed stocks to evaluate the integrity of the JUNV GPC gene specifically which revealed a single amino acid substitution (I101F) in G1. Ultimately, we were successful in generating the desired rVSV-based JUNV vaccine construct and were able to effectively proceed with evaluating its protective efficacy in a guinea pig model of JUNV infection.

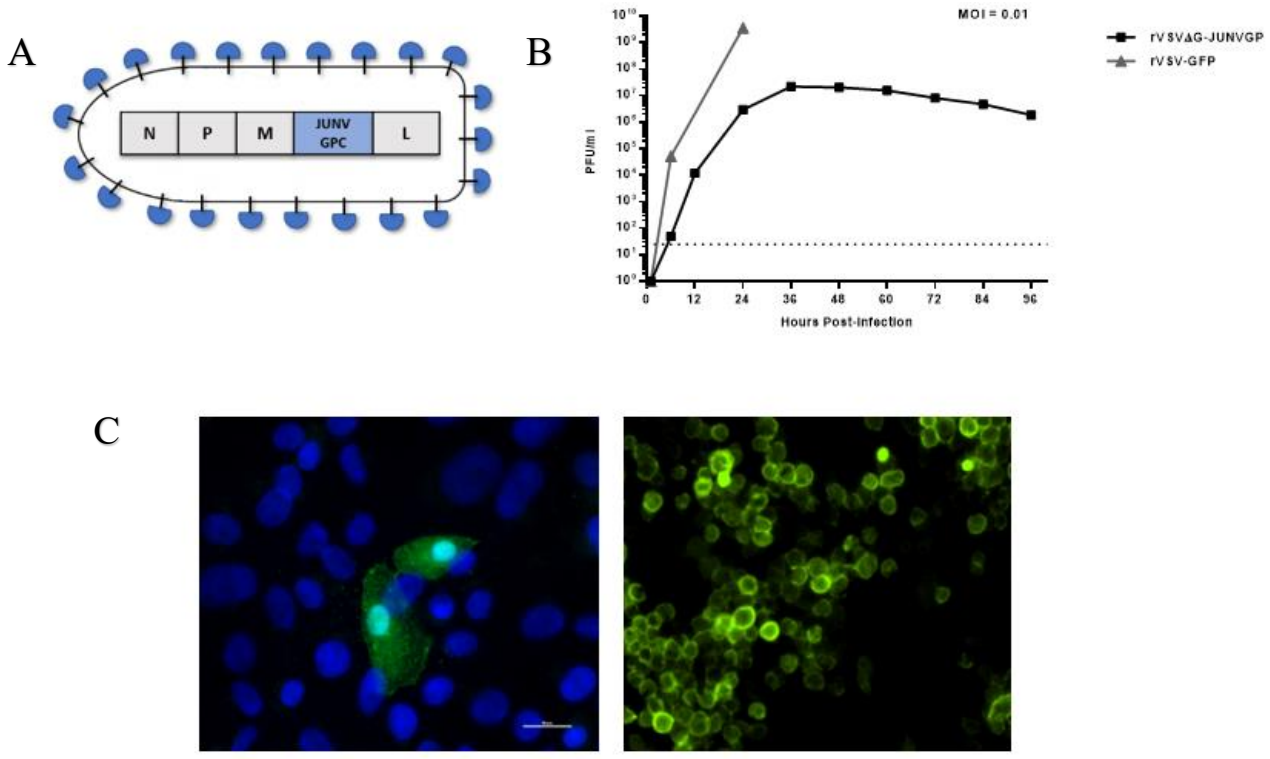

Figure 2-4. Characterization of recovered rVSVΔG-JUNVGP virus. A, Representative image of the rVSVΔG-JUNVGP virion, elongated and bullet-shaped, expressing JUNV GP on the surface. The genome contains: VSV nucleoprotein (N), VSV phosphoprotein (P), VSV matrix protein (M), JUNV GPC, VSV polymerase (L). B, Growth kinetics of rVSVΔG-JUNVGP and rVSV-GFP in Vero76 cells inoculated at a MOI of 0.01. rVSVΔG-JUNVGP supernatants were collected every 12 hours from 0-96 hours with peak viral titer at 36 hours. rVSV-GFP supernatants were collected at 0, 6, and 24 hours with peak viral titer at 24 hours. All supernatants were evaluated via plaque assay (25 PFU limit of detection). C, Immunofluorescence assay (IFA) of rVSVΔG-JUNVGP infected Vero76 and BHK cells respectively. VSV M staining (Alexa Flour 488, green) is observable in the cytoplasm, nucleus, and on the plasma membrane of Vero76 cells permeabilized with 0.1% Triton X-100 (Left). Cell nuclei are visible (blue) via DAPI counterstain. JUNV GP staining (Alexa Flour 488, green) can be seen on the surface of BHK cells (Right); cells were not permeabilized in order to evaluate GP expression exclusively on the plasma membrane.

In Vivo Vaccine Efficacy - Experiment 1

Proof-of-concept: rVSVΔG-JUNVGP Demonstrates protective efficacy in a Lethal JUNV guinea pig model.

I utilized a guinea pig model of JUNV infection to assess the protective efficacy of rVSVΔG-JUNVGP. Two groups of 6 guinea pigs each received a prime dose of rVSVΔG-JUNVGP, administered i.p., thirty-five days before lethal JUNV challenge. One group received a boost dose fourteen days before challenge (Figure 2-5A). Survival for animals receiving the prime versus prime-boost injection was 17% and 83%, respectively whereas the virus was uniformly lethal in all control animals (Figure 2-5B).

A

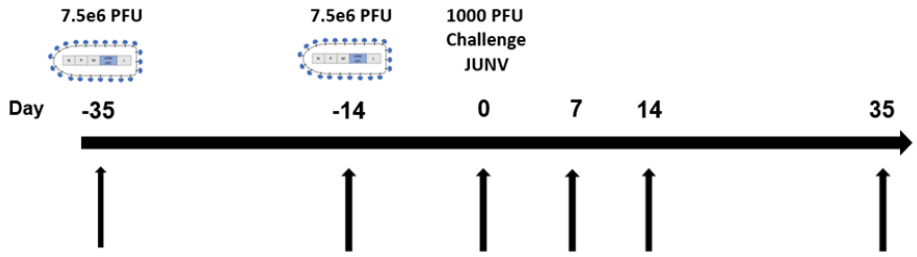

B

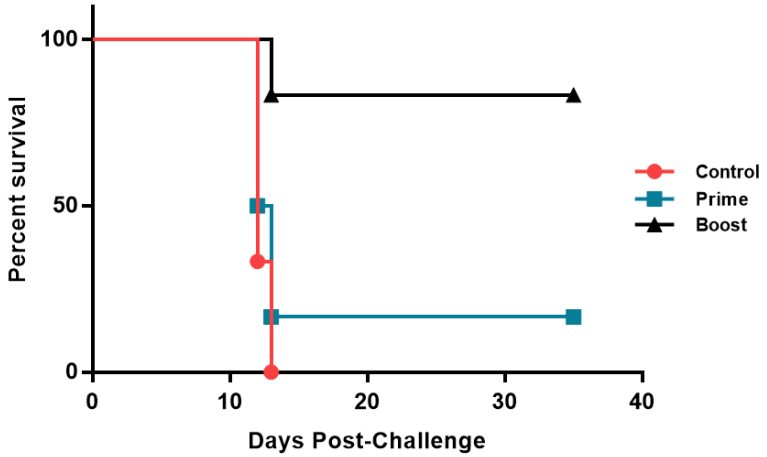

Figure 2-5. Timeline and survival data for rVSVΔG-JUNVGP vaccination study in guinea pigs. A, Prime and prime-boost cohorts were vaccinated on day -35 with 7.5e6 PFU of rVSVΔG-JUNVGP. The prime-boost cohort was vaccinated again on day -14 with 7.5e6 PFU of rVSVΔG-JUNVGP. All animals were challenged with 1000 PFU of JUNV Romero on day 0. Arrows indicate dates of plasma collection: -14, 0, 7, 14, 35 or terminal. B, Kaplan-Meier survival curve for prime, prime-boost, and control guinea pig groups. Control animals are represented in red, prime animals in blue, and prime-boost animals in black.

Assessment of clinical score data indicates there was no difference between groups in the average duration of illness for non-survivors; all animals succumbed to disease within 24 hours of developing clinical signs (Figure 2-6A). Clinical signs of disease were not detected in any surviving animals (Figure 2-6A). Importantly, none of the surviving animals had detectable viremia on days 7, 14, or 35 (Figure 2-6B). All non-survivors, regardless of their vaccination status, had comparable titers of circulating virus on days 7 and 14 (or terminal) (Figure 2-6B). The same pattern was seen for virus titers in tissue. Non-survivors had equivalent titers of virus in the liver, spleen, and brain at terminal time points while no detectable JUNV was found in the tissues of survivors (Figure 2-6C).

Control and vaccinated animals that succumbed to infection had similar observable histopathologic changes including diffuse hepatocellular vacuolar degeneration in the liver and germinal center degeneration, lymphoid depletion, and hemorrhage in the spleen (Figure 2-7A). Lesions were not observed in the liver, spleen, or brain of surviving animals via histology (Figure 2-7A). JUNV-specific antigen labeling was detected in all three tissues of animals that succumbed to infection, including controls and vaccinated non-survivors (Figure 2-7B). Notably, viral antigen was not detected in the tissues of surviving animals (Figure 2-7B), including the brain. No virus, viral antigen, or histopathologic changes were found in the liver, spleen, or brain of surviving animals. These findings regarding the brain are particularly important because rodent models of JUNV occasionally

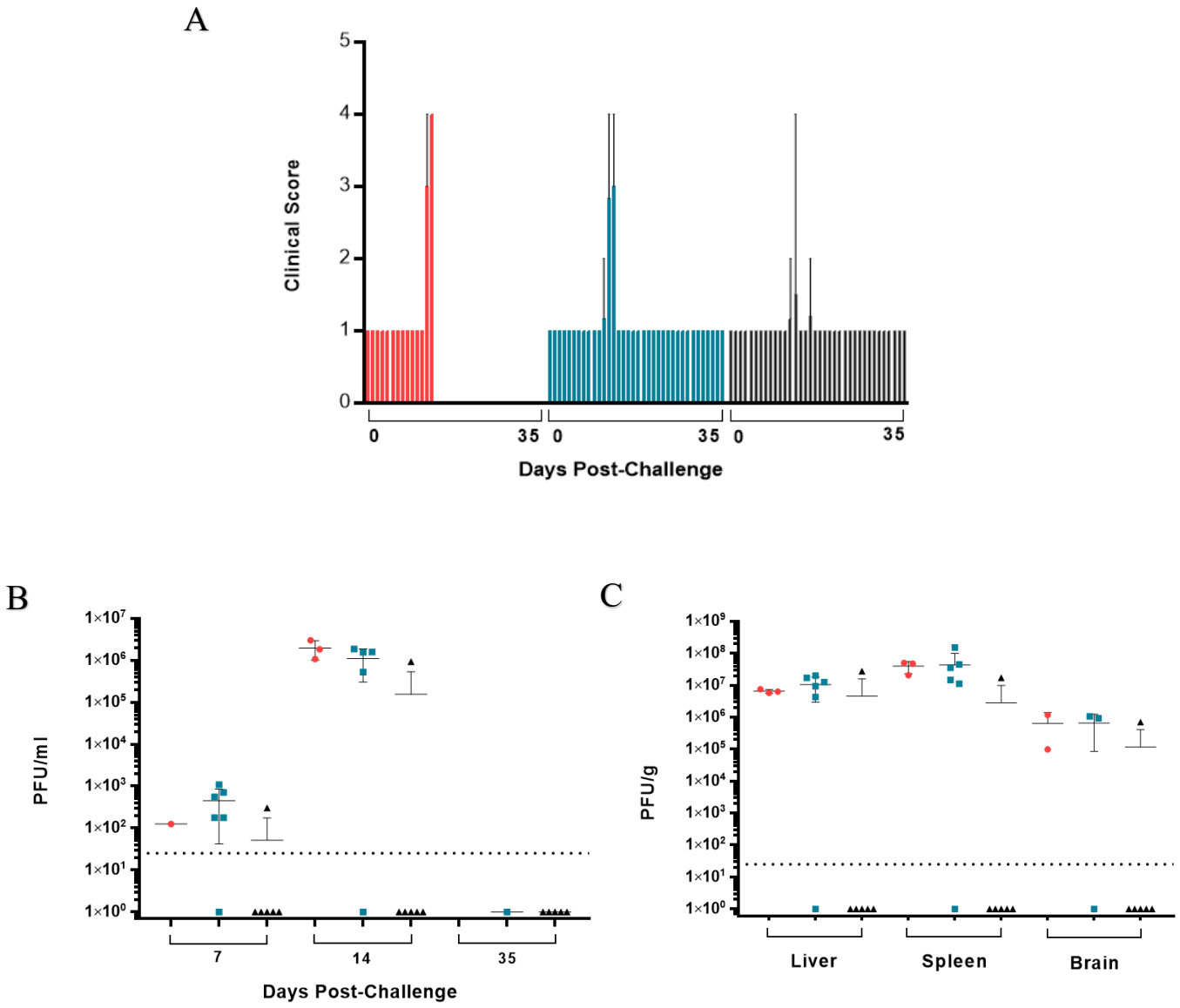

Figure 2-6. Clinical signs of disease and JUNV replication in rVSVΔG-JUNVGP vaccinated guinea pigs. A, Average clinical scores on days 0-35 for prime, prime-boost, and control animals. Scores were characterized as the following: Normal (1), Rough (2), Sick (3), Paralysis and/or Euthanize (4). B, Plasma titers (PFU/ml) for prime, prime-boost, and control groups on days 7, 14, and 35. B, Terminal liver, spleen, and brain titers (PFU/g) for prime, prime-boost, and control groups. All control animals are represented in red, prime animals in blue, and prime-boost animals in black.

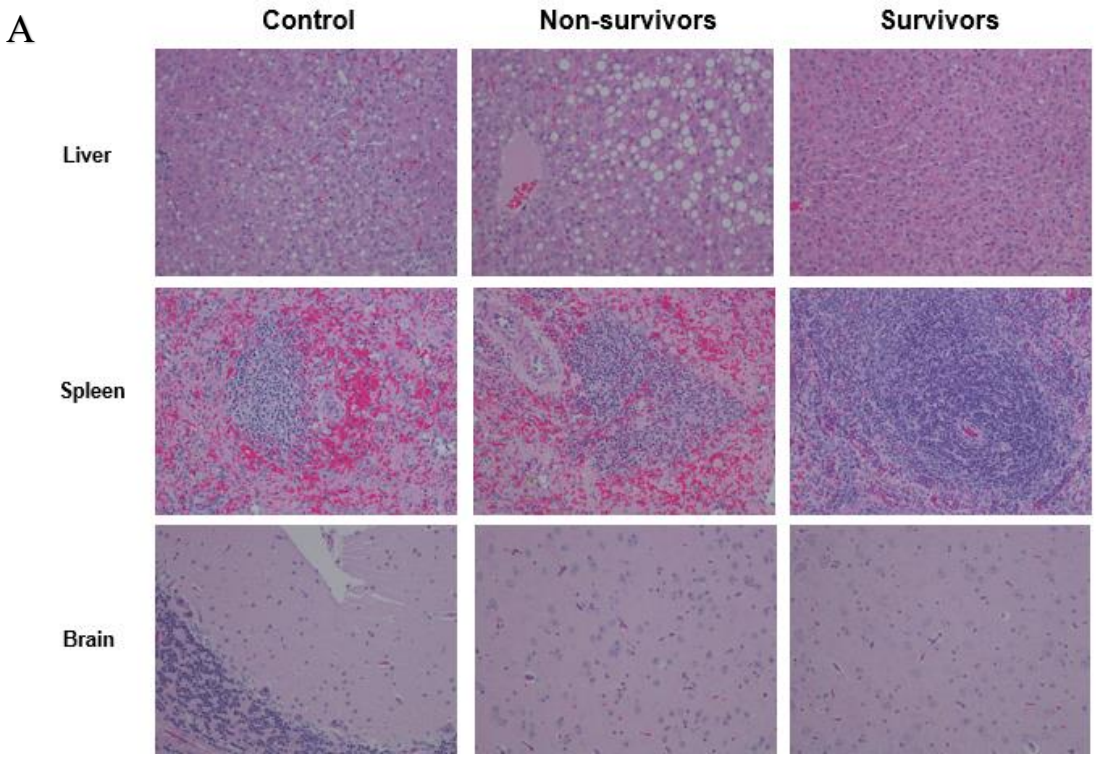
A
Control
Non-survivors
Survivors
Liver
Spleen
Brain

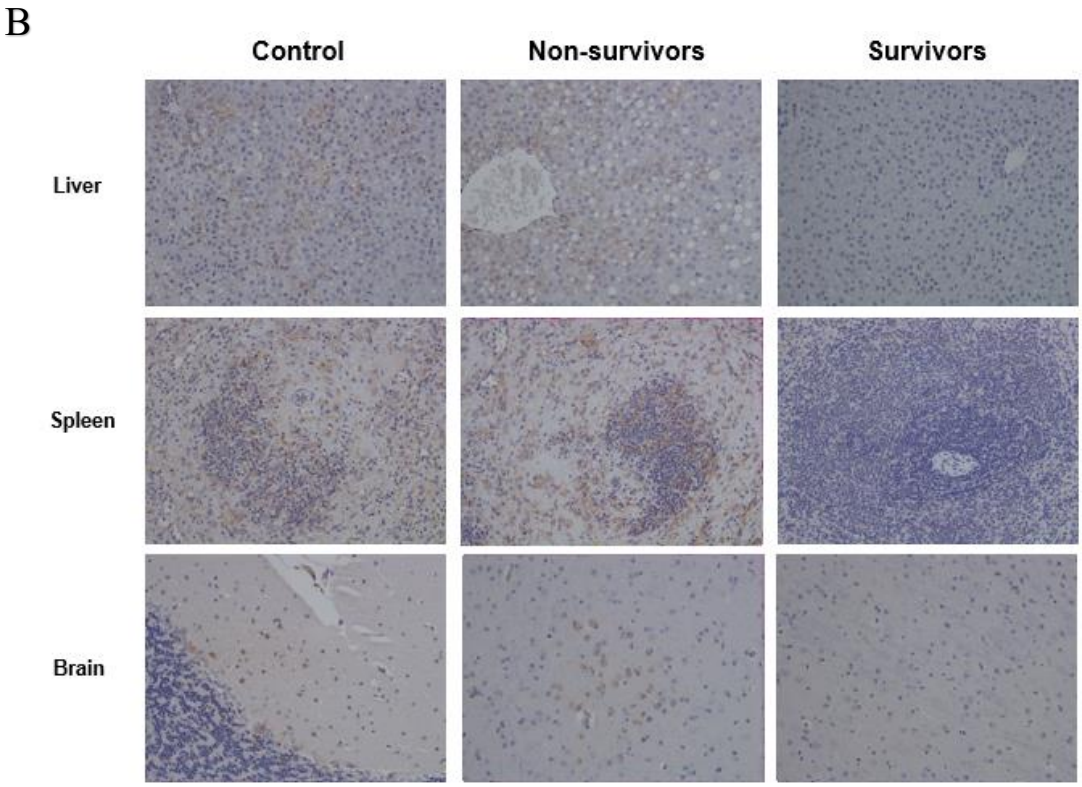
B
Control
Non-survivors
Survivors
Liver
Spleen
Brain

Figure 2-7. Histology and Immunohistochemistry from rVSVΔG-JUNVGP vaccinated animals – Experiment 1. Representative images of liver, spleen, and brain from control, non-surviving, and surviving animals. A, H&E: tissue stained with hematoxylin and eosin. Control and non-surviving animals have observable hepatocyte vacuolation (liver), germinal center degeneration characterized by lymphoid depletion and hemorrhage (spleen), and gliosis (brain). No significant lesions in liver, spleen, or brain of survivors. B, IHC: tissue stained with JUNV-specific polyclonal antibody. Control and non-surviving animals have observable immunolabeling of hepatocytes (liver), germinal centers (spleen), and neurons (brain). No detectable immunolabeling in the liver, spleen, or brain of survivors. Images of the brain for surviving/non-surviving animals are from the brainstem and images for the control animal are from the cerebellum. Brain images are 10x and spleen/liver are 20x magnification

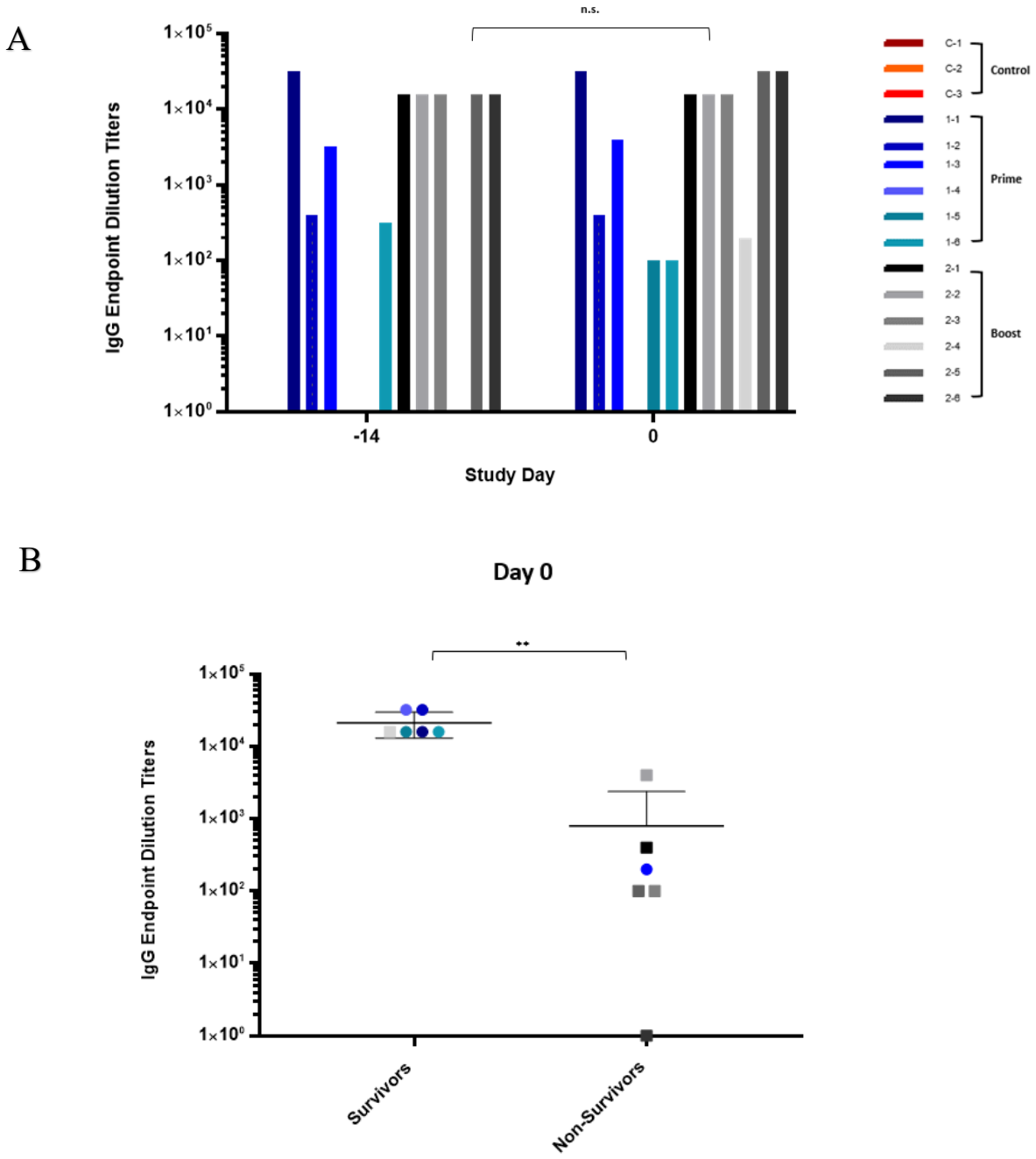

Figure 2-8. IgG antibody response in rVSVΔG-JUNVGP vaccinated animals. A, IgG data reported as reciprocal endpoint dilution titer on days -14 and 0 for each animal from both prime and prime-boost groups. Plasma from control animals was used as a baseline. Control animals are represented in red, prime animals in blue, and prime-boost animals in black/grey. B, Average IgG antibody titer from surviving versus non-surviving animals on day 0. IgG antibody titer was significantly associated with survival. All statistical notations correspond with the following p values: *p < 0.05, **p < 0.01, ***p < 0.001.

present with signs of late neurologic disease which is thought to be the result of viral recrudescence from persistence in the brain [42, 130]. They also indicate that rVSVΔG-JUNVGP may successfully circumvent the issues of neurotropism associated with Candid #1 vaccination.

Studies in NHP models suggest that antibodies may be an important correlate of protection for the rVSV-based EBOV vaccine (rVSVΔG-EBOVGP) [131]. In this study, results from ELISA data suggest a correlation between JUNV GP-specific IgG antibody titer and survival as well. All animals that developed a robust IgG antibody response by the day of challenge (≥16000 endpoint dilution titer) survived JUNV challenge (Figure 2-8A/B). Non-survivors were found to have statistically significantly lower IgG antibody titers (≤4000 endpoint dilution titer) at the time of challenge (Figure 2-8A/B). Interestingly, the single non-survivor in the boost group did not benefit from the second, boost vaccination. After a single vaccination this animal had no detectable IgG response (day -14) and after a second vaccination the animal had an endpoint dilution titer of 200 (day 0) but subsequently succumbed to JUNV infection (Figure 2-8A). Importantly, all surviving animals developed robust IgG titers after the initial prime vaccination and only two animals had a notable increase in IgG titer after boost (Figure 2-8A). These data prompt the question of whether a boost is ultimately necessary for a robust IgG titer and further studies will need to be performed to determine whether or not this is the case. It is important to note however that these data only address antibody titer and do not address antibody neutralization and affinity/quality after vaccination, factors that could be important for vaccine efficacy and will be addressed more thoroughly in Experiment 3.

In this initial proof-of-concept experiment, we reported for the first time, a VSV-based vaccine against JUNV which demonstrated 83% protective efficacy in a lethal JUNV guinea pig model. Further, we demonstrated that surviving animals generated a robust JUNV GP-specific IgG antibody response. In moving forward with additional studies to achieve 100% vaccine protection we considered the fact that rVSVΔG-JUNVGP is

constructed using the JUNV Espindola GPC while our guinea pig model of JUNV infection utilizes JUNV strain Romero. We wondered if challenging with a non-homologous glycoprotein affected overall antibody avidity in relation to the challenge virus. If so, we wondered if lower antibody avidity could, in part, explain why some animals that seroconverted (albeit to low IgG titers) and did not survive. In Experiment 2, we moved on to address this question.

In Vivo Vaccine Efficacy - Experiment 2

EVALUATING JUNV STRAIN-SPECIFIC PROTECTION: HOMOLOGOUS GLYCOPROTEINS DO NOT ENHANCE PROTECTIVE EFFICACY OF RVSVΔG-JUNVGP VACCINE.

We conducted a second vaccine efficacy study of rVSVΔG-JUNVGP in a lethal JUNV guinea pig model in order to test new parameters with the ultimate goal of achieving 100% vaccine efficacy. As previously mentioned, rVSVΔG-JUNVGP expresses and therefore generates an immune response directed toward the JUNV strain Espindola GP. Our lethal guinea pig model of JUNV infection was developed to utilize JUNV strain Romero. GPs from the two virus strains differ in only a single amino acid (residue 116) located in the G1 subunit (Figure 2-9). This particular residue is located near the receptor binding domain which is an important known target of protective JUNV neutralizing antibodies (Figure 2-9) [79-82, 132]. The JUNV Espindola GP contains an alanine at position 116 while JUNV Romero GP contains a glutamic acid at the same position (Figure 2-9). We wondered if generating a high avidity immune response around a neutral amino acid like alanine, and then challenging with an antigen containing glutamic acid (significantly larger and hydrophilic sidechain), would result in lower overall antibody avidity and therefore less than optimal vaccine protection. To address this question, we utilized both JUNV Romero and JUNV Espindola to challenge rVSVΔG-JUNVGP-vaccinated guinea pigs in order to determine whether differences in protective efficacy

exist between the two virus strains. Additionally, we included Candid #1 vaccine cohorts to compare directly to rVSVΔG-JUNVGP in our JUNV guinea pig challenge models.

For each challenge virus, JUNV Romero and Espindola, 2 cohorts of 6 guinea pigs each received a prime dose of rVSVΔG-JUNVGP, administered i.p., thirty-five days before JUNV challenge (Figure 2-10A). One cohort per virus received a boost dose twenty-one days before challenge (Figure 2-10A). One cohort per virus also received a single dose (1000 PFU) of Candid #1, a known protective dose in an outbred Hartley guinea pig JUNV challenge model (Figure 2-10A) [32].

Survival for animals receiving the prime versus prime-boost rVSVΔG-JUNVGP injection and challenged with JUNV Romero was 67% and 50%, respectively, whereas the virus was uniformly lethal in all control animals (Figure 2-10B). Survival for animals receiving the prime versus prime-boost rVSVΔG-JUNVGP injection and challenged with JUNV Espindola was 83% and 67%, respectively, while the virus was lethal in 77% of control animals (including n=6 historic controls) (Figure 2-10C). Additionally, survival for animals receiving the Candid #1 vaccination was 50% when challenged with JUNV Romero versus 100% when challenged with JUNV Espindola (Figure 2-10B/C).

Analyses of survival data showed no statistical difference in survival for the prime or prime-boost rVSVΔG-JUVGP vaccinated animals challenged with JUNV Romero versus Espindola, indicating that glycoprotein homology between vaccine and challenge viruses may not be important for rVSVΔG-JUNVGP protection. Interestingly, there was a significant difference in survival for animals receiving the Candid #1 vaccination and challenged with the two JUNV strains, indicating the vaccine protected more effectively against JUNV Espindola. This particular data contradicts published studies showing Candid #1 as being 100% protective against both virus strains in lethal JUNV guinea pig models [32, 91, 92], suggesting that the JUNV Romero guinea pig model developed and

A

```
JUNV Espindola   1    MGQFISFMQEIPTFLQEALNIALVAVSLIAIIKGIVNLYKSGLFQFFVFLALAGRSCTEEAFKIGLHTEFQTVSFSMVGL  80
JUNV Romero      1    MGQFISFMQEIPTFLQEALNIALVAVSLIAIIKGIVNLYKSGLFQFFVFLALAGRSCTEEAFKIGLHTEFQTVSFSMVGL  80

JUNV Espindola   81   FSNNPHDLPLLCTLNKSHLYIKGGNASFMISFDDIAVLLPQYDVIIQHPADMSWCSKSDDQIWLSQWFMNAVGHDWHLDP  160
JUNV Romero      81   FSNNPHDLPLLCTLNKSHLYIKGGNASFMISFDDIEVLLPQYDVIIQHPADMSWCSKSDDQIWLSQWFMNAVGHDWHLDP  160

JUNV Espindola   161  PFLCRNRTKTEGFIFQVNTSKTGVNENYAKKFKTGMHHLYREYPDSCLNGKLCLMKAQPTSWPLQCPLDHVNTLHFLTRG  240
JUNV Romero      161  PFLCRNRTKTEGFIFQVNTSKTGVNENYAKKFKTGMHHLYREYPDSCLNGKLCLMKAQPTSWPLQCPLDHVNTLHFLTRG  240

JUNV Espindola   241  KNIQLPRRSLKAFFSWSLTDSSGKDTPGGYCLEEWMLVAAKMKCFGNTAVAKCNLNHDSEFCDMLRLFDYNKNAIKTLND  320
JUNV Romero      241  KNIQLPRRSLKAFFSWSLTDSSGKDTPGGYCLEEWMLVAAKMKCFGNTAVAKCNLNHDSEFCDMLRLFDYNKNAIKTLND  320

JUNV Espindola   321  ETKKQVNLMGQTINALISDNLLMKNKIRELMSVPYCNYTKFWYVNHTLSGQHSLPRCWLIKNNSYLNISDFRNDWILESD  400
JUNV Romero      321  ETKKQVNLMGQTINALISDNLLMKNKIRELMSVPYCNYTKFWYVNHTLSGQHSLPRCWLIKNNSYLNISDFRNDWILESD  400

JUNV Espindola   401  FLISEMLSKEYSDRQGKTPLTLVDICFWSTVFFTASLFLHLVGIPTHRHIRGEACPLPHRLNSLGGCRCGKYPNLKKPTV  480
JUNV Romero      401  FLISEMLSKEYSDRQGKTPLTLVDICFWSTVFFTASLFLHLVGIPTHRHIRGEACPLPHRLNSLGGCRCGKYPNLKKPTV  480

JUNV Espindola   481  WRRRH  485
JUNV Romero      481  WRRRH  485
```

B

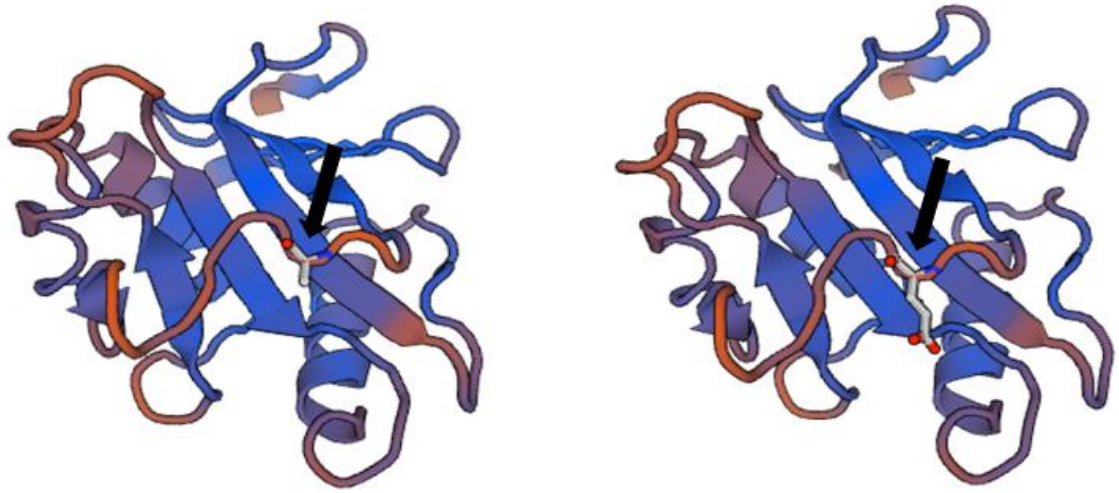

Figure 2-9. Single amino acid difference between JUNV Romero and JUNV Espindola GPC. A, Primary amino acid sequence alignment comparing the GPC gene of JUNV Espindola and Romero strains. Amino acid 116 (black arrow) is the single divergent residue between the virus strains. B, G1 of the JUNV GP modeled via Swiss-Model (https://creativecommons.org/licenses/by-sa/4.0/legalcode). Amino Acid 116 is depicted on the receptor binding domain of G1 for both JUNV Espindola (Left, alanine) and Romero (Right, glutamic acid).

A

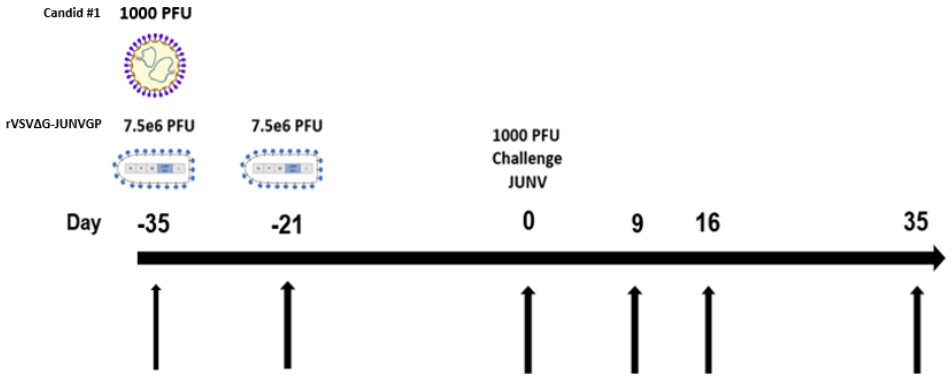
Candid #1
1000 PFU
rVSVΔG-JUNVGP
7.5e6 PFU
7.5e6 PFU
1000 PFU
Challenge
JUNV
Day
-35
-21
0
9
16
35

B

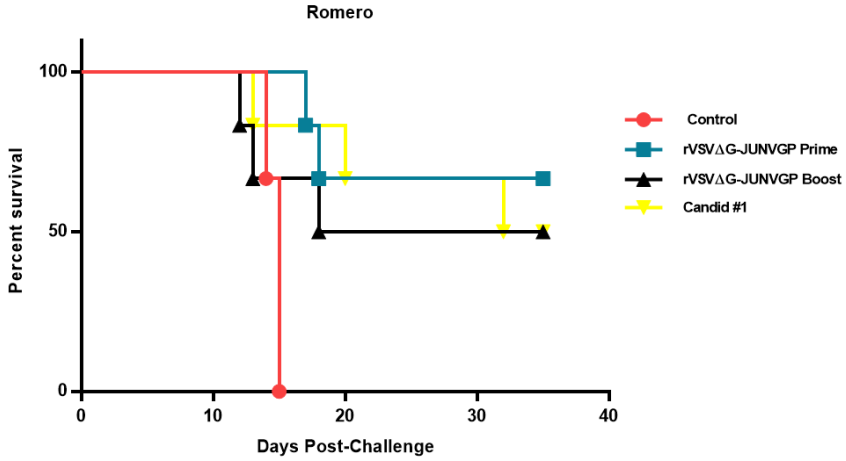
Romero
Percent survival
100
50
0
0
10
20
30
40
Days Post-Challenge
Control
rVSVΔG-JUNVGP Prime
rVSVΔG-JUNVGP Boost
Candid #1

C

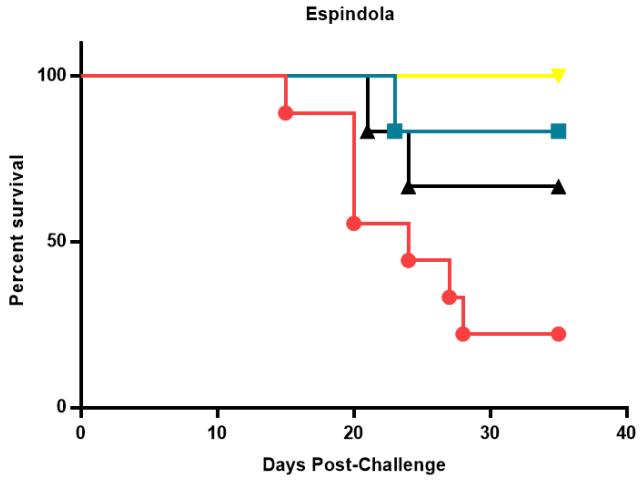
Espindola
Percent survival
100
50
0
0
10
20
30
40
Days Post-Challenge

Figure 2-10. Timeline and survival data for rVSVΔG-JUNVGP vaccination in guinea pigs. A, Prime and prime-boost cohorts were vaccinated i.p. on day -35 with 7.5e6 PFU of rVSVΔG-JUNVGP. The prime-boost cohort was vaccinated again on day -21 with 7.5e6 PFU of rVSVΔG-JUNVGP. The Candid #1 cohort was vaccinated i.p. on day -35 with 1000 PFU of the vaccine. Animals were challenged with 1000 PFU of JUNV Romero or 4000 PFU of JUNV Espindola on day 0. Arrows indicate dates of plasma collection: -35, -21, 0, 9, 16, 35 or terminal. B-C, Kaplan-Meier survival curve for rVSVΔG-JUNVGP prime and prime-boost, Candid #1, and control guinea pig groups challenged with (B) JUNV strain Romero or (C) JUNV strain Espindola. Control animals are represented in red, rVSVΔG-JUNVGP prime animals in blue, rVSVΔG-JUNVGP prime-boost animals in black, and Candid #1 animals in yellow.

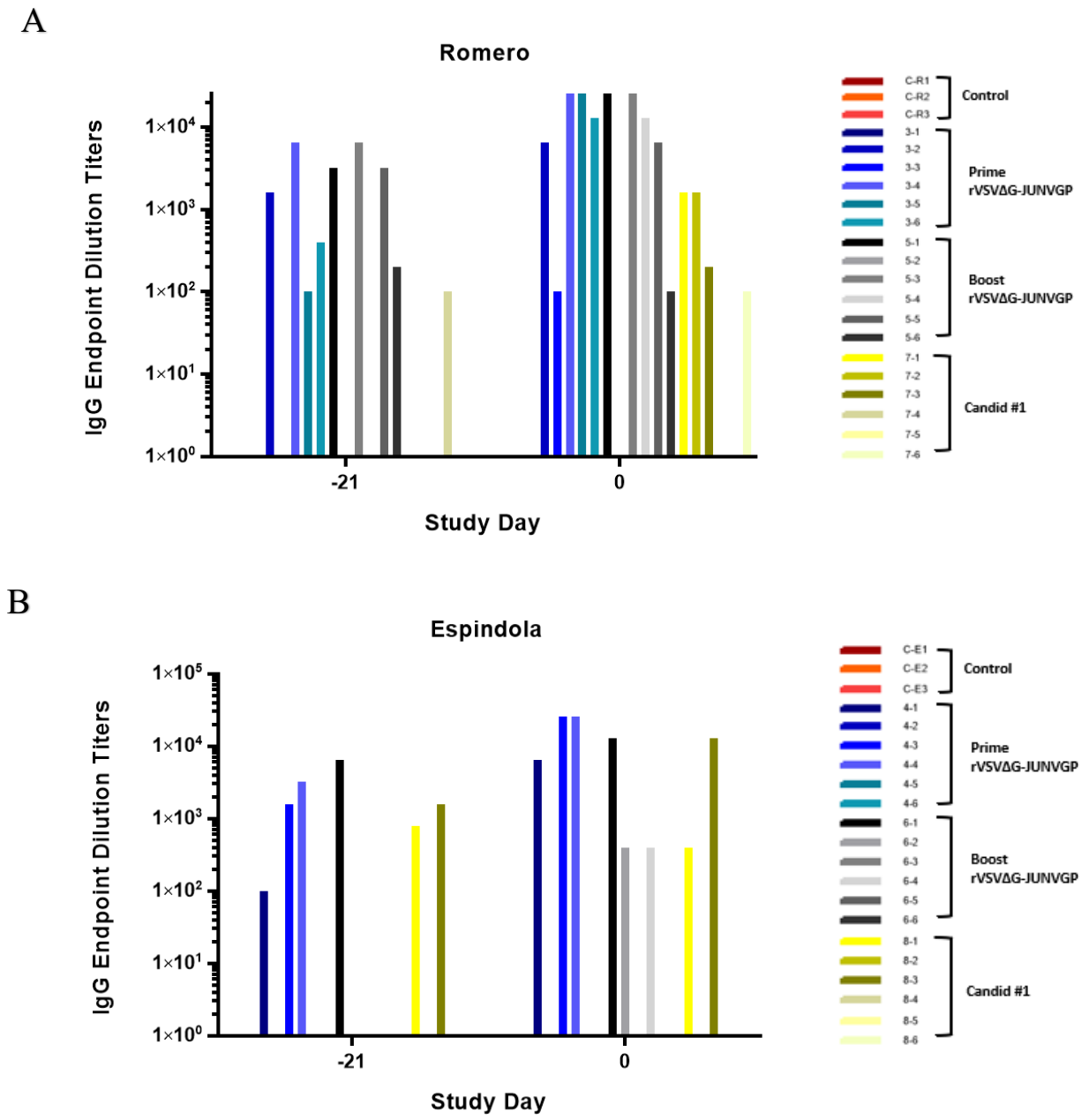

Figure 2-11. IgG antibody response in rVSVΔG-JUNVGP vaccinated animals. A-B, IgG data reported as reciprocal endpoint dilution titers on days -21 and 0 for each animal from rVSVΔG-JUNVGP prime, rVSVΔG-JUNVGP prime-boost, Candid #1 and control groups. Animals in graph A were challenged with JUNV Romero and animals in graph B with JUNV Espindola. Day -35 plasma samples from each animal were used as a baseline. Control animals are represented in red, rVSVΔG-JUNVGP prime animals in blue, rVSVΔG-JUNVGP prime-boost animals in black, and Candid #1 animals in yellow.

utilized by our laboratory is particularly stringent. Along these lines, it appears promising that the rVSVΔG-JUNVGP-vaccinated cohorts performed as well or better than the Candid #1 vaccinated cohort against challenge with JUNV Romero in our model.

ELISA data regarding JUNV-GP specific IgG antibody responses show highly variable titers amongst each vaccine group where IgG titers range from undetectable to 25600 (reciprocal endpoint dilution titer) within the same cohorts (Figure 2-11A/B). It should be noted that ELISA assays were performed with Romero-specific antigen so IgG antibody titer data should be interpreted with some caution. Importantly though, there was no significant difference in IgG titers between rVSVΔG-JUNVGP prime and prime-boost vaccinated cohorts on day 0 and the survival data mentioned above, *i.e.* no significant difference between JUNV Romero and Espindola challenged groups, was reflective of this (Figure 2-11A/B). All (6/6) Candid #1 vaccinated animals survived challenge with JUNV Espindola but ELISA data indicates only 2/6 of these animals developed JUNV-GP specific IgG antibodies (Figure 2-11B). Conversely, only 50% (3/6) of Candid #1 vaccinated animals survived challenge with JUNV Romero, however, 4/6 animals had detectable IgG antibodies (Figure 2-11A). These data indicate that JUNV-GP specific IgG antibody titer did not correspond with Candid #1 vaccine protection in our study. These data are not altogether unexpected; while antibodies are thought be a correlate of Candid #1 vaccine protection, both GP and NP-specific antibodies are known to be generated and potentially play a role in protection and an evaluation of NP-specific responses was not performed here as it was outside of the scope of this particular study [133, 134].

It is important to note that several results from this particular experiment were outside of the normal ranges typically observed for our JUNV Romero guinea pig challenge model. The disease course in control animals infected with JUNV Romero was delayed; animals reliably and consistently succumb to infection before day 12 in our model (see Figure 2-5B and Figure 2-12B). In this experiment, control animals did not succumb until day 15 (Figure 2-10B). Additionally, none of the animals in the study (controls or non-

survivors) developed detectable viremia by day 9 post-challenge (data not shown) which is also unusual for our JUNV Romero guinea pig model (see Figure 2-6B and Figure 2-14A). In addition to the delayed disease course, as previously mentioned, JUNV-GP specific IgG titers were significantly variable within each vaccine cohort. These collective findings, in addition to incomplete rVSVΔG-JUNVGP vaccine protection, suggest that there may have been inconsistencies with the actual physical administration or delivery of the vaccines and challenge viruses. For the sake of efficiency, the vaccine and challenge injections were administered by several different individuals during this experiment and it is feasible that this lack of uniformity is reflected in the variability of animal outcomes.

The inconsistencies in IgG seroconversion post-vaccination also called into question the route of vaccination. We wondered if administering the rVSVΔG-JUNVGP vaccine via the i.m. route would induce a more uniform antibody response. Inoculum administered via the i.m. route is known to undergo rapid uptake into the blood stream, quickly reaching draining lymph nodes. Alternately, inoculum administered via the i.p. route is typically absorbed into the mesenteric vessels and must undergo hepatic metabolism before reaching circulation and draining lymph nodes [135]. For this reason, we hypothesized i.m. vaccination may confer more uniform protective responses and as a result, Experiment 3 was designed to evaluate i.m. versus i.p. vaccine administration of rVSVΔG-JUNVGP.

In Vivo Vaccine Efficacy - Experiment 3

Evaluating Route of rVSVΔG-JUNVGP Administration: Single i.p. Vaccine Injection Provides 100% Protection.

In order to assess additional parameters which may affect vaccine efficacy, and with the ultimate goal of achieving consistent JUNV-GP specific IgG immune responses and 100% vaccine protection, we conducted a third *in vivo* study in a JUNV guinea pig

model. This study was designed to evaluate the performance of rVSVΔG-JUNVGP using two routes of vaccination: i.p. and i.m. Evidence suggests that i.m. vaccination may circumvent the hepatic metabolism that typically occurs after i.p. vaccination, potentially reaching draining lymph nodes more effectively [135]. We therefore hypothesized that i.m. vaccination may induce a more uniform antibody response and therefore generate better protective efficacy. Additionally, in Experiment 3 we ensured that all vaccine and challenge injections were performed by the same individual to rule out user error or variability. We also increased the time between prime, boost, and challenge injections, allowing 4 weeks between each procedure in order to evaluate whether this would allow for additional protective immune responses to develop. Some data suggests that allowing at least 4 weeks between prime and boost vaccine doses prevents competition between primary waves of immune activation [136].

Four groups of 6 guinea pigs each received a prime dose of rVSVΔG-JUNVGP, administered i.m. or i.p., fifty-six days before lethal JUNV challenge. Two groups received a boost dose (i.m. or i.p.) twenty-eight days before challenge (Figure 2-12A). In the i.m. vaccinated prime and prime-boost cohorts the vaccine regimen proved to be 0% and 16% efficacious, respectively (Figure 2-12B). In the i.p. vaccinated prime and prime-boost cohorts the vaccine regimen proved to be 100% for both. Uniform lethality was observed in the control cohort (Figure 2-12B).

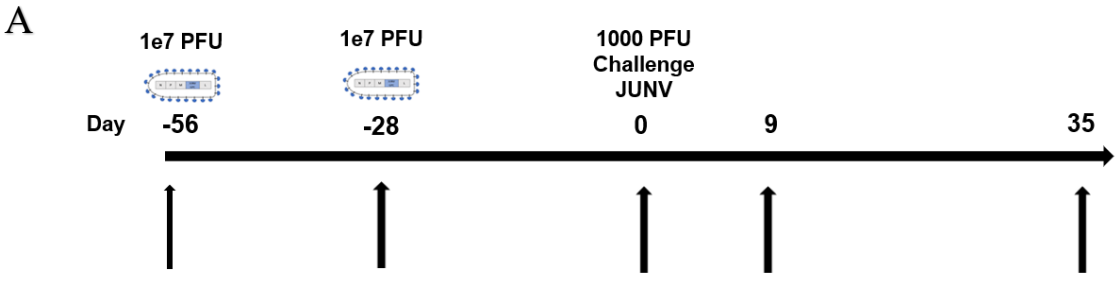

B

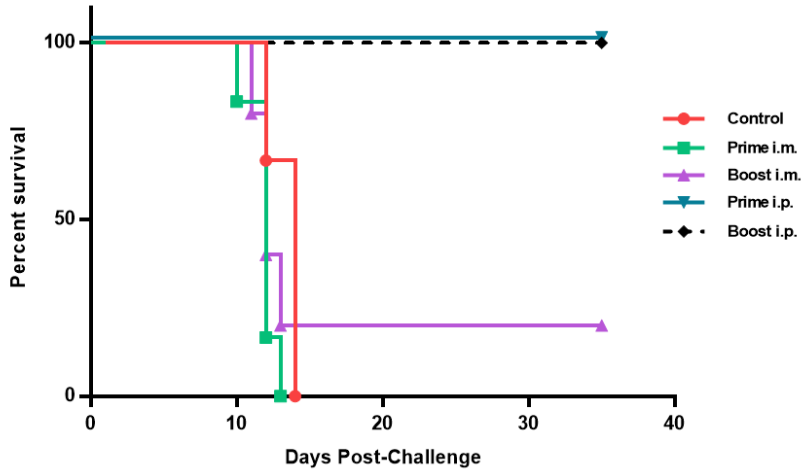
100
50
0
Percent survival
0
10
20
30
40
Days Post-Challenge
Control
Prime i.m.
Boost i.m.
Prime i.p.
Boost i.p.

C

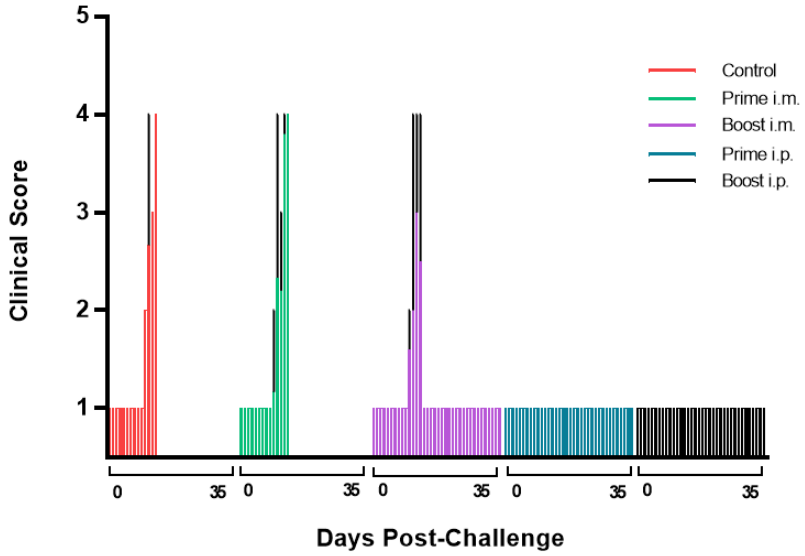
5
4
3
2
1
Clinical Score
0
35
0
35
0
35
0
35
0
35
Days Post-Challenge
Control
Prime i.m.
Boost i.m.
Prime i.p.
Boost i.p.

Figure 2-12. Timeline, survival, and clinical score data for rVSVΔG-JUNVGP vaccination study in guinea pigs. A, Prime and prime-boost cohorts from both i.m. and i.p. groups were vaccinated on day -56 with 1e7 PFU of rVSVΔG-JUNVGP. The prime-boost cohorts (i.m. and i.p.) were vaccinated again on day -28 with 1e7 PFU of rVSVΔG-JUNVGP. All animals were challenged with 1000 PFU of JUNV Romero on day 0. Arrows indicate dates of plasma collection: -56, -28, 0, 9, 35 or terminal. B, Kaplan-Meier survival curve for prime i.p., prime-boost i.p., prime i.m., prime-boost i.m., and control guinea pig groups. C, Average clinical scores on days 0-35 for each guinea pig groups. Scores were characterized as the following: Normal (1), Rough (2), Sick (3), Paralysis and/or Euthanize (4). Control animals are represented in red, prime i.p. animals in blue, prime-boost i.p. animals in black, prime i.m. animals in green, and prime-boost i.m. in purple.

Post JUNV-challenge, all animals were followed for changes in clinical score, weight, and temperature. Temperatures became elevated over baseline beginning on day 7 (+0.7º C to +1.0º C) and peaking on day 9 (+0.9º to +1.5º C) for control and non-surviving animals (Figure 2-13A). Temperatures remained near baseline values in all surviving animals for the duration of the study with the exception of a single animal (3-6). Elevated temperature in this animal began on day 4 (+0.7º C) and peaked on day 9 (+1.3º C) but remained higher than average until day 35 when it returned to baseline (Figure 2-13A). A similar trend was seen with regard to animal weight change over time. Control animals and non-survivors were found to have detectable weight loss starting on day 7 which continued until euthanasia (Figure 2-13B). Conversely, all surviving animals gained weight consistently for the duration of the study post-challenge. A single outlier, again animal 3-6, began to lose weight on day 7 which continued until day 28 (-10%); however, this animal returned to baseline weight by day 35 (Figure 2-13B). The overall assessment of clinical score data indicated that clinical signs of disease were not observed in any of the vaccinated surviving animals, including animal 3-6 (Figure 2-12C).

Notably, none of the surviving vaccinated animals had detectable viremia on days 9 or 35, including animal 3-6, while control and non-surviving animals had comparable

titers of circulating virus on days 9 and at euthanasia (Figure 2-14A). The same pattern was seen for virus load in tissue. Control and non-surviving animals had equivalent infectious virus isolated from the liver, spleen, and brain at terminal time points while no detectable JUNV was found in the tissues of vaccinated surviving animals (Figure 2-14B). The tissues of control and non-surviving animals were observed to have characteristic histopathologic changes from JUNV infection including diffuse hepatocellular vacuolar degeneration in the liver and germinal center degeneration, lymphoid depletion, and hemorrhage in the spleen (Figure 2-15). Lesions were not observed in the liver, spleen, or brain of surviving animals via histology (Figure 2-15). JUNV-specific antigen labeling was detected in all three tissues of control animals and non-survivors, but notably, viral antigen was not detected in the tissues of vaccinated survivors (Figure 2-15), including the brain.

The survival and virus load data revealed that for surviving vaccinated animals, the regimens were 100% efficacious against JUNV challenge. To evaluate if there were any differences between the immune response to either vaccine regimen or route of administration, JUNV GP-specific IgG antibody titers were assessed for all animals on days -56, -28, 0 and day 35 or terminal. Overall, a significant difference in IgG antibody production between i.m. versus i.p. vaccinated animals was detected, and this difference was directly reflective of survival (Figure 2-16). Specifically, all i.p. vaccinated animals (n=12) seroconverted, developing uniformly robust IgG antibody titers by day -28; no statistically significant difference in titer was detected between prime and prime-boost animals (Figure 2-17A). In contrast, only 4 i.m. vaccinated animals seroconverted by day -28, two from the prime and two from the prime-boost groups (no statistical difference) (Figure 2-17B). IgG antibody titers in these animals were significantly lower than those of i.p. vaccinated animals on the same day (Figure 2-17A/B).

On day 0 IgG titers from animals that had received a single i.p. vaccination was significantly lower than on day -28; however, these animals were able to maintain robust

IgG titers for at least 4 weeks before being challenged (Figure 2-17A). IgG titers in animals receiving prime-boost i.p. vaccinations increased overall from day -28 to day 0, however, this increase was not statistically significant (Figure 2-17A). There was a statistically significant difference in IgG titer between the prime and prime-boost i.p. vaccinated animals at JUNV challenge on day 0, however, at the time of challenge all animals had high JUNV GP specific IgG titers in excess of 1e5 (reciprocal dilution) (Figure 2-17A). On day 0 IgG titers from animals that had received i.m. vaccinations remained low or non-detectable (Figure 2-17B). Only three i.m. vaccinated animals had detectable IgG titers on day 0: animal 1-5 (prime cohort), and animals 2-3 and 2-1 (prime-boost cohort) (Figure 2-17B). It is very interesting to note that animals 1-5 and 2-1 had very similar IgG titers on the day of challenge, 6400 and 8000, respectively; however, only animal 2-1 survived challenge (Figure 2-17B). Overall, circulating IgG titers peaked for all surviving animals on day 35 post-challenge (Figure 2-17A/B). Control animals failed to develop detectable IgG antibody at any point during the study including days -28, 0, and terminal time points.

The substantial difference in IgG immune responses and survival between i.m. and i.p. rVSVΔG-JUNVGP vaccinated animals was surprising and notable (Figure 2-16). Further studies would be necessary to attempt to understand the underlying causes for this difference, particularly because evidence in the literature contradicts these findings with regard to arenaviruses. The non-pathogenic New World Clade B arenavirus *Tacaribe mammarenavirus* (TCRV), has been shown to induce robust antibody responses, sufficient to protect against JUNV challenge, when administered i.m. to guinea pigs [137]. Other studies have shown that a recombinant vaccinia virus expressing the TCRV GP generated high titer IgG responses via i.m. vaccination of guinea pigs which were also sufficient to protect against JUNV challenge [138]. Evidence of divergent immune responses between i.m. and i.p. vaccination routes in rodent models have been documented for other viruses including influenza and parainfluenza viruses [139, 140]. While we do not have enough data to understand the reason for this difference in our study, we do know that populations

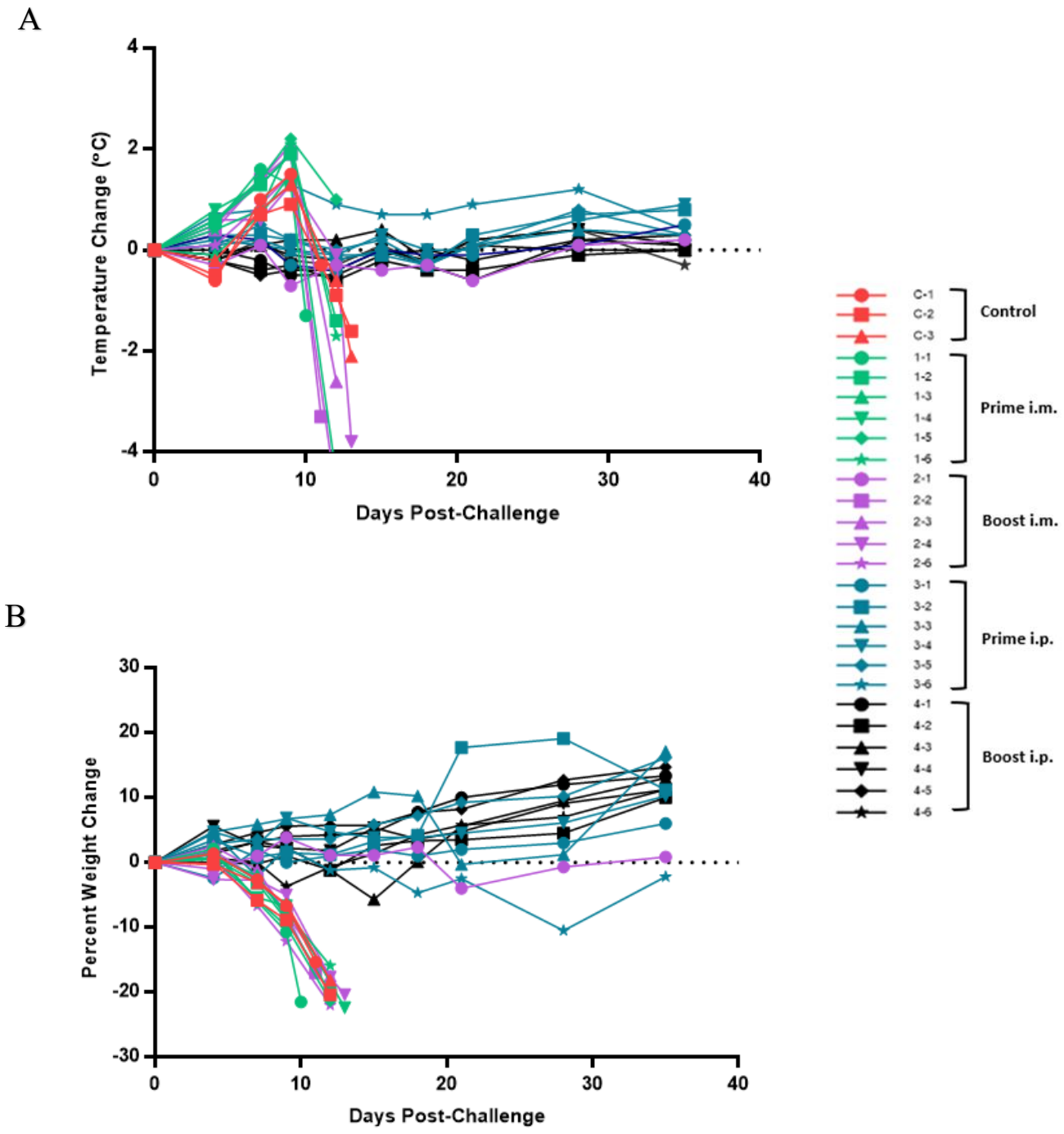

Figure 2-13. Guinea pig temperature and weight changes over time. A-B, Baseline measurements were taken on day 0. Additional measurements were taken and every 3 days through day 21, day 28 and day 35 or terminal. For all graphs, control animals are represented in red, prime i.m. animals in green, prime-boost i.m. animals in purple, prime i.p. animals in blue, and prime-boost i.p. animals in black.

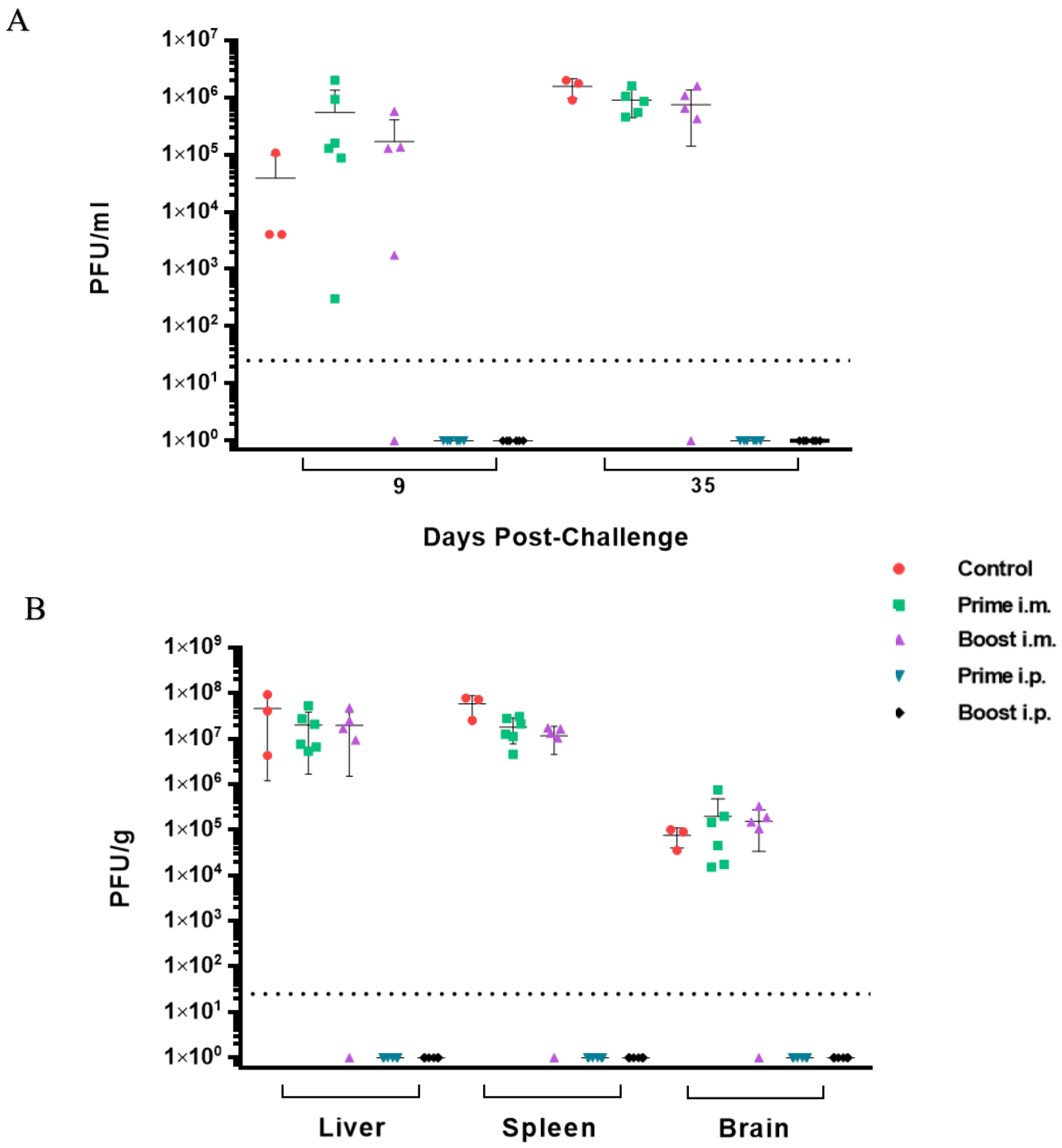

Figure 2-14. JUNV replication in vaccinated guinea pigs. A, Plasma titers (PFU/ml) on day 9 ad 35 and B, Terminal liver, spleen, and brain titers (PFU/g) for prime i.m., prime-boost i.m., prime i.p., prime-boost i.p. and control groups. For all graphs, control animals are represented in red, prime i.m. animals in green, prime-boost i.m. animals in purple, prime i.p. animals in blue, and prime-boost i.p. animals in black.

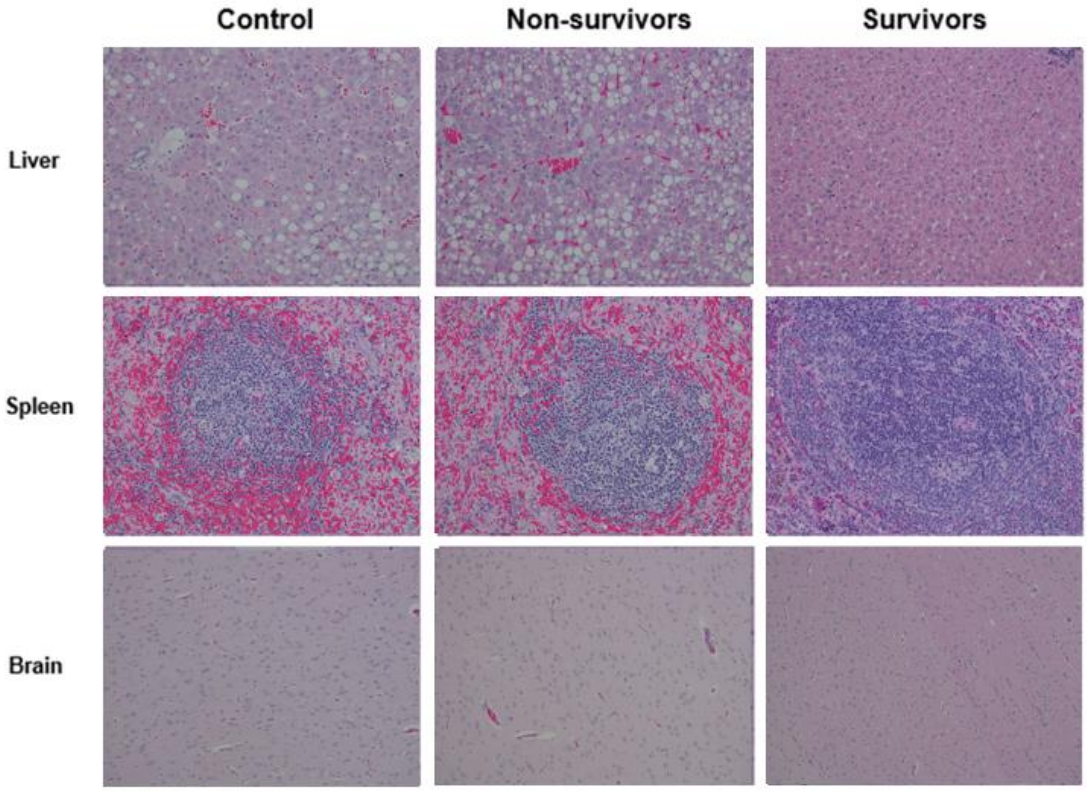
Control
Non-survivors
Survivors
Liver
Spleen
Brain

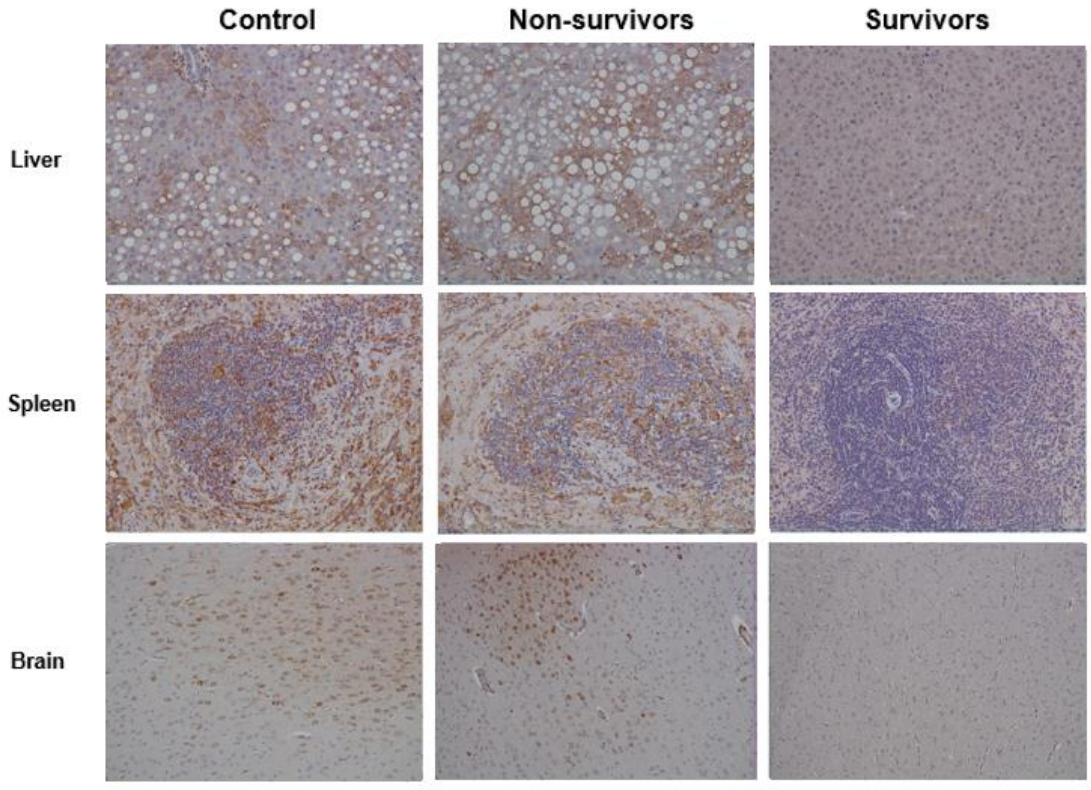
Control
Non-survivors
Survivors
Liver
Spleen
Brain

Figure 2-15. Histology and Immunohistochemistry from rVSVΔG-JUNVGP vaccinated animals – Experiment 3. Representative images of liver, spleen, and brain from control, non-surviving, and surviving animals. A, H&E: tissue stained with hematoxylin and eosin. Control and non-surviving animals have observable hepatocyte vacuolation (liver), germinal center degeneration characterized by lymphoid depletion and hemorrhage (spleen), and gliosis (brain). No significant lesions in liver, spleen, or brain of survivors. B, IHC: tissue stained with JUNV-specific polyclonal antibody. Control and non-surviving animals have observable immunolabeling of hepatocytes (liver), germinal centers (spleen), and neurons (brain). No detectable immunolabeling in the liver, spleen, or brain of survivors. Brain images are 10x and spleen/liver are 20x magnification

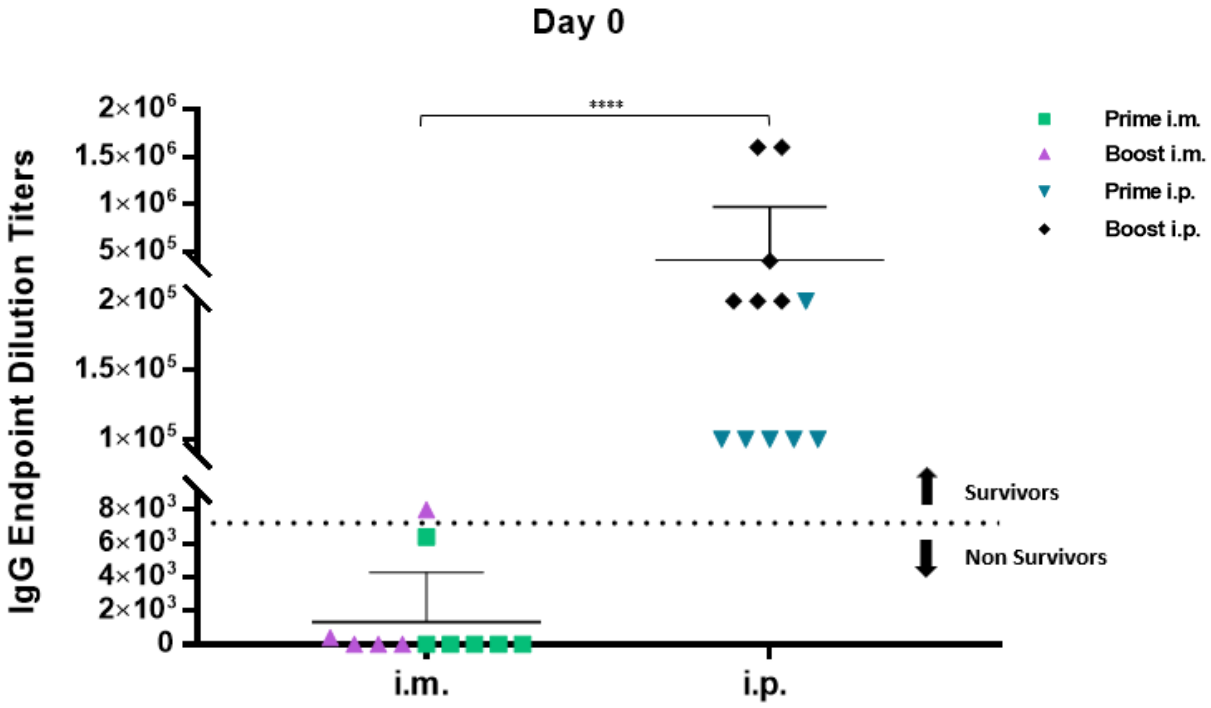

Figure 2-16. IgG antibody titers from i.m. versus i.p. vaccinated animals. IgG antibody reported as reciprocal endpoint dilution titers for each animal vaccinated with rVSVΔG-JUNVGP on day 0, comparing i.m. versus i.p. route of administration. Dotted line indicates IgG titer threshold for guinea pig survival: animals with a titer of 8000 and above survived, while animals with a titer of 6400 and below succumbed to JUNV challenge. Prime i.m. animals are represented in green, prime-boost i.m. animals in purple, prime i.p. animals in blue, and prime-boost i.p. animals in black.

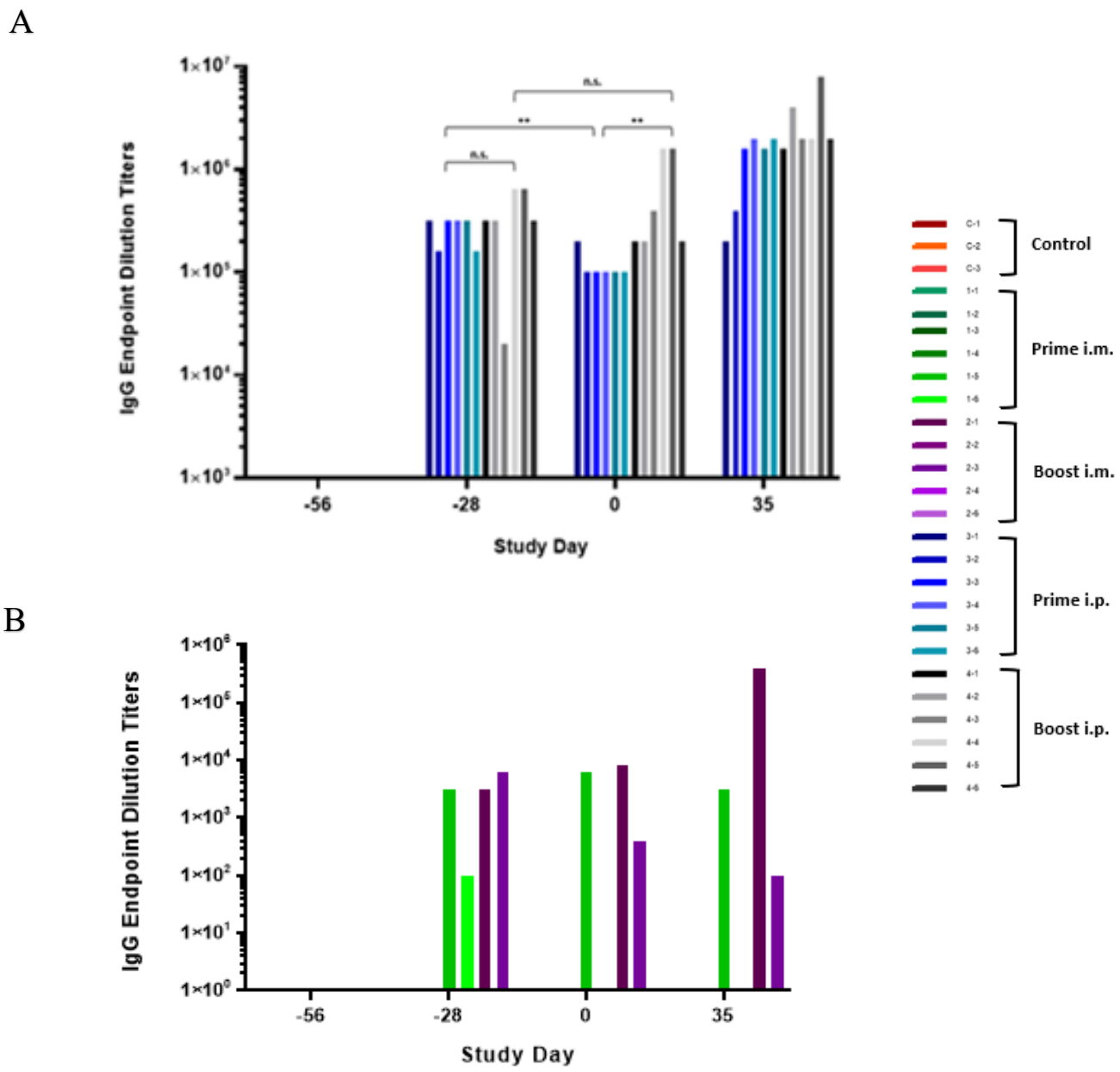

Figure 2-17. IgG antibody titers over time. A, JUNV GP-specific IgG reciprocal endpoint dilution titers for i.p. vaccinated animals on days -56, -28, 0, and 35. B, JUNV GP-specific IgG reciprocal endpoint dilution titers for i.m. vaccinated animals on days -56, -28, 0, and 35. Control animals are represented in red, prime i.m. animals in green, prime-boost i.m. animals in purple, prime i.p. animals in blue, and prime-boost i.p. animals in black/grey. All statistical notations correspond with the following p values: *p < 0.05, **p < 0.01, ***p < 0.001.

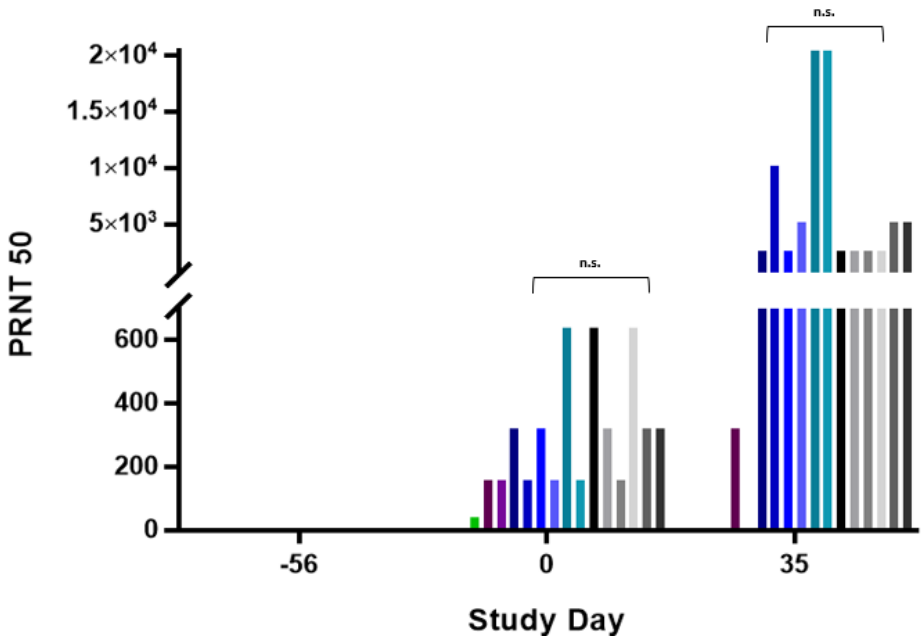

Figure 2-18. Antibody neutralization titers over time. Neutralization titers for vaccinated animals on days -56, 0, and 35. Control animals are represented in red, prime i.m. animals in green, prime-boost i.m. animals in purple, prime i.p. animals in blue, and prime-boost i.p. animals in black/grey. All statistical notations correspond with the following p values: *p < 0.05, **p < 0.01, ***p < 0.001.

of immune cells are inherently different in the peritoneal space where monocytes/macrophages can make up 90% of the leukocyte population and there is an abundance of mesenteric lymph nodes. In addition, some papers have suggested that the presence of B-1 cells ($CD4^+$ T cell-independent B cell), which are found almost exclusively in the peritoneal space, can affect downstream immune responses, including T-cell differentiation into proinflammatory Th17 cell subsets [139]. Additional, repeated studies would be needed to verify the results observed in Experiment 3 and to further elucidate route of vaccination differences for rVSVΔG-JUNVGP.

As mentioned, it was notable that animals 1-5 and 2-1 generated very similar IgG antibody titers but had different disease outcomes and we wondered what other immunologic factors may have played a role in this difference (Table 2-3). Specifically, we wondered whether differences in overall antibody quality or avidity may have played a role in their different survival outcomes. Notably, the surviving animal (2-1) was the recipient of a boost vaccination while the non-survivor (1-5) was not (Table 2-3). It has been shown that boost vaccinations serve to drive rapid affinity maturation in B-cells, increasing overall antibody avidity, and we therefore hypothesized that animal 2-1 may have had a higher overall antibody avidity profile on the day of challenge, contributing to its survival.

Prior to assessing antibody avidity from our guinea pig study, we wanted to determine whether we could correlate antibody quality with JUNV survival using the JUNV monoclonal antibodies discussed in Chapter 1. As previously mentioned, three JUNV monoclonal antibodies initially generated by Sanchez *et al.* (1989) were tested in a JUNV guinea pig model and determined to be protective; however, it was clear that antibody J199 protected the most effectively, followed by J200, and finally J202 (Table 2-2) [77, 90]. We performed an ELISA-based avidity assay of these antibodies which revealed that antibody J199 did, in fact, have the highest overall avidity of the three. Antibody/antigen dissociation for J199 could not be detected until exposure to 9M urea and 50% dissociation was not reached even using 11M urea (Figure 2-18). The antibody to protect guinea pigs most effectively after J199, antibody J200, was found to have the next highest antibody avidity as well, with dissociation first detected with exposure to 6M urea and 50% dissociation occurring with 11M urea. Lastly, J202 was the least protective *in vivo* and also had the lowest avidity of the three antibodies, with dissociation first detected at 4 M urea and 50% dissociation at 11M urea (Figure 2-18). Collectively, these data seem to support the idea that antibody quality may play an important role in protection against lethal JUNV infection.

Monoclonal Antibody	JUNV Target	Neutralizing	Epitope Specifity	Protective Efficacy In-vivo (guinea pig)
GB03-BE08 or J199	GP	Y	Unkown (G1- receptor binding domain hypothesized)	100% 2 days post-challenge (10mg) 100% 7 & 11 days post-challenge (10mg/dose)
GD01-AG02 or J200	GP	Y	G1- receptor binding domain	100% 2 days post-challenge (10mg) 67% 7 & 11 days post-challenge (10mg/dose)
QC03-BF11	GP	Y	G1- receptor binding domain	Unknown
OD01-AA09 or J202	GP	Y	G1- receptor binding domain	100% 2 days post-challenge (10mg) 17% 7 & 11 days post-challege (10mg/dose)
LD05-BF09	GP	N	Unknown	Unknown
MA03-BE06	NP	N	Unknown	Unknown

Table 2-2. Overview of JUNV monoclonal antibodies. Summary of a panel of six JUNV monoclonal antibodies first described by Sanchez *et al.* (1989). Each antibody is compared based on its JUNV protein/epitope specificity, neutralization ability, and demonstrated therapeutic efficacy *in vivo*.

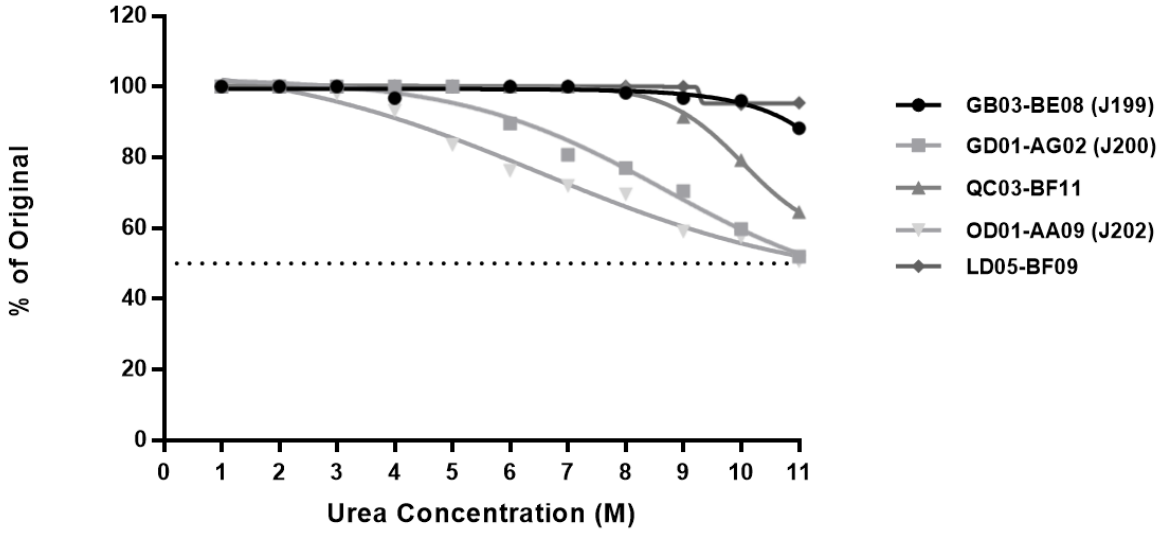

Figure 2-18. JUNV monoclonal antibody quality. Avidity of JUNV monoclonal antibodies detailed in Table 2-1. Data reported represent the dissociation of antibody/antigen binding with increasing concentrations of urea (1 M through 11 M).

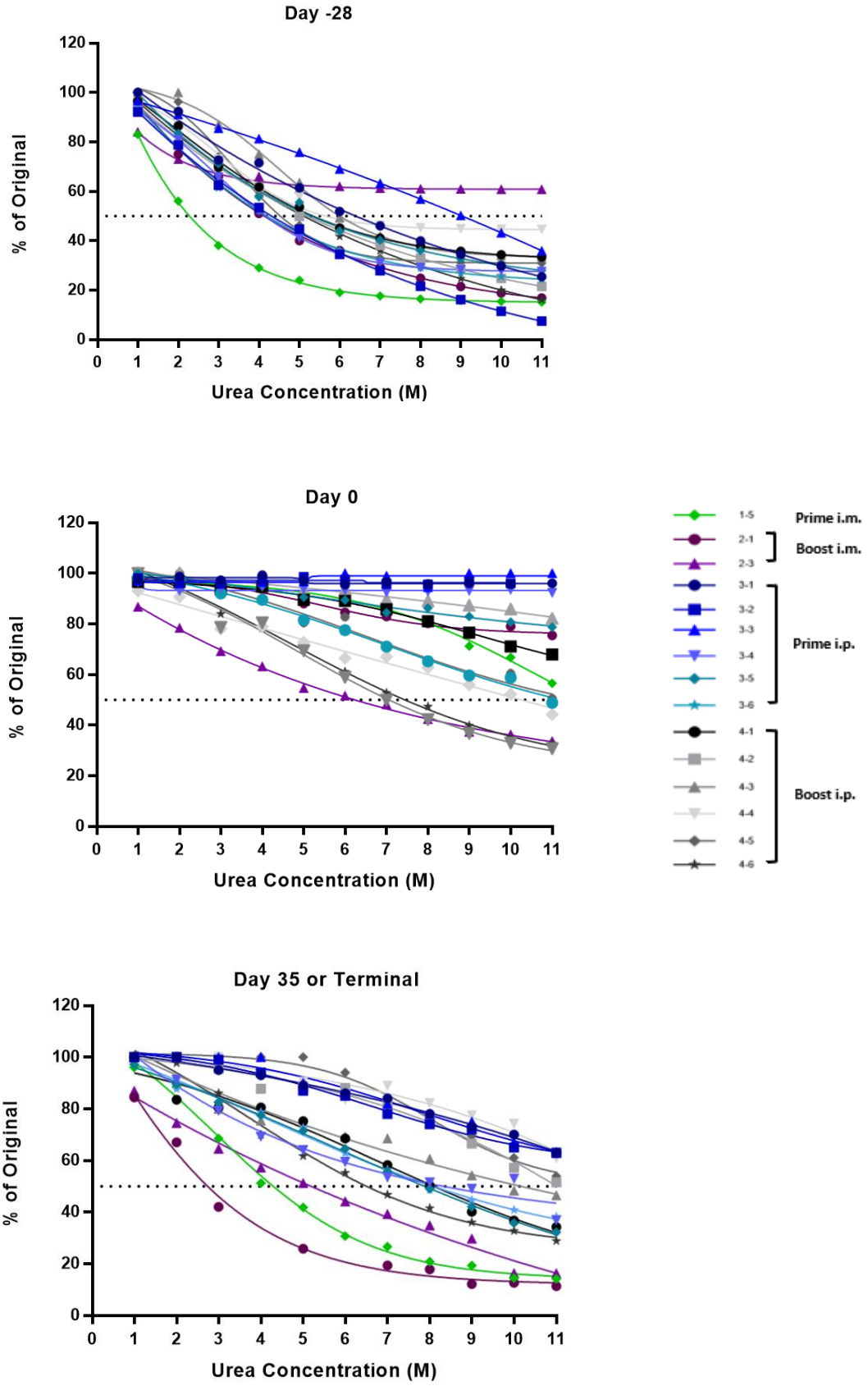
Day -28
% of Original
Urea Concentration (M)
Day 0
% of Original
Urea Concentration (M)
Day 35 or Terminal
% of Original
Urea Concentration (M)
1-5
2-1
2-3
3-1
3-2
3-3
3-4
3-5
3-6
4-1
4-2
4-3
4-4
4-5
4-6
Prime i.m.
Boost i.m.
Prime i.p.
Boost i.p.

Figure 2-19. IgG antibody quality. IgG antibody avidity on days -28, 0, and 35. Data reported represent the dissociation of antibody/antigen binding with increasing concentrations of urea (1 M through 11 M). Prime i.m. animals are represented in green, prime-boost i.m. animals in purple, prime i.p. animals in blue, and prime-boost i.p. animals in black.

Animal #	Survivor	Prime Vaccination	Boost Vaccination	JUNV-GP IgG Titer	AB Avidity	Neutralizing AB (PRNT 50)
1-5	N	X		6400	⬇	40
2-1	Y	X	X	8000	⬆	160

Table 2-3. Comparative antibody responses from rVSVΔG-JUNVGP vaccinated survivor versus non survivor. JUNV GP-specific IgG antibody titer, avidity and neutralizing antibody compared between guinea pig 1-5 (non-survivor) and 2-1 (survivor).

We moved on to assess IgG antibody quality/avidity from the guinea pigs in our study. We found that by day -28 all i.p. vaccinated animals had developed IgG antibodies with uniform avidity profiles, where 50% dissociation occurred with exposure to 4M - 6M urea except for a single outlier, animal 3-3 (9M urea) (Figure 2-19). Importantly, overall avidity was higher in these animals by day 0, suggesting ongoing B-cell affinity maturation over time (Figure 2-19).

Surprisingly, although overall avidity was higher on day 0, animals in the prime group were found to have significantly higher avidity on average than animals in the prime-boost group (Figure 2-19). While the scope of this work was not to investigate the mechanism behind this avidity difference, we would suggest that a secondary, boost vaccination serves to drive additional primary waves of immune activation while also driving affinity maturation in existing B-cell populations, the sum of which may have produced lower overall avidity in our prime-boost animals. As we have shown, overall

IgG titers were higher on day 0 in prime-boost i.p. vaccinated animals. It is possible the binding strength of high affinity antibodies in the population were diluted by the additional primary immune responses/activation induced by the boost. Interestingly, this phenomenon was also observed in the prime vaccine group after JUNV challenge; on day 35, the prime cohort had significantly higher IgG antibody titers but lower overall antibody avidity when compared with values from day 0. Ultimately, further studies are required to understand these avidity differences between the vaccine regimens.

In looking at antibody avidity from i.m. vaccinated animals, we found that on day -28 animal 2-1 had significantly higher overall avidity (50% dissociation at 4M) than animal 1-5 (50% dissociation at 2-3 M) (Figure 2-19). On day 0, the avidity profiles of both animals had increased and dissociation for both was first detectable at 2-3 M urea, however with increasing concentrations of urea, animal 2-1 had higher avidity (56% dissociation at 11M urea) than animal 1-5 (75 % dissociation at 11M urea) (Figure 2-19). Overall, in considering two animals with similar IgG titer but different survival outcomes, we found that the surviving animal (2-1) had a higher overall antibody avidity profile than the non-survivor (1-5) (Table 2-3). These data are not unexpected as animal 2-1 (survivor) received a boost vaccination which can serve to promote rapid affinity maturation in B-cell populations, increasing overall antibody avidity. Importantly, these data indicate that antibody quality may be important for JUNV protection and may contribute to protection from rVSVΔG-JUNV vaccination.

In addition to IgG titer and quality it was also important to assess the neutralizing antibody responses resulting from rVSVΔG-JUNVGP vaccination. All i.p. vaccinated animals developed detectable neutralizing antibodies by day 0 with $PRNT_{50}$ values ranging from 160-640 (reciprocal dilution) (Figure 2-18). Neutralization titers were found to be higher overall in the prime-boost versus prime i.p. vaccinated animals on day 0; however, this difference was not statistically significant (Figure 2-18). In terms of i.m. vaccinated animals, the survivor, animal 2-1 had a higher neutralization titer ($PRNT_{50}$ =

160) compared with the non-survivor, animal 1-5 ($PRNT_{50}$ = 40) (Table 2-3). These data indicate that IgG titer, quality, as well as neutralizing antibody titer may all play a role in rVSVΔG-JUNVGP-mediated protection.

CONCLUSIONS

Vaccine and therapeutic options are limited for the prevention and treatment of AHF making the development of countermeasures against JUNV an important biodefense priority. rVSV-based vaccines have demonstrated protective efficacy against hemorrhagic fever viruses in guinea pigs, hamsters, NHPs, and humans [109-112]. In this chapter I successfully recovered a rVSV vector expressing the JUNV GP and demonstrated that this construct could protect guinea pigs from lethal JUNV challenge.

It is important to note that in all *in vivo* experiments, rVSVΔG-JUNVGP-vaccinated surviving animals failed to develop signs of clinical disease post-challenge. Weight loss and elevated temperatures were detected in a single animal; however, no circulating systemic virus could be detected on day 7, 9, 14 or 35 in any vaccinated survivor. Additionally, no virus, viral antigen, or histopathologic changes were found in the liver, spleen, or brain of surviving animals. These findings regarding the brain are particularly important because rodent models of JUNV occasionally present with signs of late neurologic disease which is thought to be the result of viral recrudescence from persistence in the brain [42, 130]. This finding is also important because it indicates that rVSVΔG-JUNVGP circumvents the issues of neurotropism associated with Candid #1.

Further experiments will need to be performed to understand the vaccine correlates of protection, however, we found that all vaccinated surviving animals mounted high avidity, high titer IgG antibody responses and developed neutralizing antibodies by the day of challenge, all of which may contribute to protection. Importantly, all vaccinated surviving animals developed robust IgG titers after the initial prime vaccination and rarely

had a notable increase in IgG titer after boost. Additionally, antibody avidity was statistically lower in prime-boosted animals. Overall, these data indicate that a boost may not be necessary and support the idea of moving forward with rVSVΔG-JUNVGP as a single injection vaccine.

We also investigated several factors in order to understand their contribution to vaccine-induced protective immunity including route of vaccine administration, timing between vaccination and challenge, and heterologous JUNV challenge. The single factor which was associated with uniformly protective immune responses was increased timing (4 weeks) between vaccine prime, boost, and JUNV challenge doses. We found that 100% of i.p. vaccinated animals from Experiment 3 survived challenge 56 days post-vaccination, a phenomenon not observed when animals were challenged earlier, at 28 days post-vaccination (i.p.) (Experiments 1 & 2). Caution should be exercised with definitively correlating vaccine/challenge timing with protection, however. Uniformly high titer IgG antibodies were detected from all surviving animals in Experiment 3 by day -28 which was not observed in previous experiments. Whether these animals would have been protected if challenged on day -28 is unknown but should be investigated. Additional studies will be necessary to fully understand the role of timing between rVSVΔG-JUNVGP vaccine regimens /JUNV challenge and survival.

Here, we report for the first time, a VSV-based vaccine against JUNV which demonstrates 100% efficacy against lethal JUNV challenge in a guinea pig model. We have shown a single injection vaccine regimen is capable of inducing a robust and protective immune response, supporting the idea of advancing the development of rVSVΔG-JUNVGP as a potential biodefense vaccine.

Chapter 3: rVSVΔG-JUNVGP – A Screening Tool for JUNV Neutralizing Antibodies.

The development of technologies to rapidly detect and quantify JUNV neutralizing antibodies is important for a number of reasons. First, the detection of JUNV neutralizing antibodies from human serum is the primary and preferred method of serologic detection following acute JUNV infection [141]. Second, convalescent plasma from JUNV survivors, which is routinely used for the treatment of AHF, is administered on the basis of neutralizing antibody titer as this has been shown to correlate with protection [76]. Additionally, as discussed in Chapters 1 and 2, monoclonal antibody-based therapeutics have been explored for the treatment of AHF and several with known neutralization ability have demonstrated protective efficacy in a guinea pig model of lethal JUNV challenge [77, 90]. These data collectively provide merit to the pursuit of technologies/methodologies that can effectively detect and quantify JUNV neutralizing antibodies in the most accurate and efficient means possible.

There are currently a number of published methodologies for detecting and quantifying JUNV neutralizing antibodies; however, there are limitations associated with each method. PRNT assays utilizing wild type strains of JUNV require work in high containment (BSL-3/4), and while attenuated strains of JUNV do not, results from these assays require a 6-8 day waiting period. Rapid methods for the detection of JUNV neutralizing antibodies that do not require a high containment laboratory have been developed including a VSV pseudotyped virus system and a transcription-replication competent VLP system, however these methods require the need to purchase costly equipment in order to adequately generate data from their reporter signals (GFP or luciferase) (Table 3-1). In this chapter I will explore the idea that rVSVΔG-JUNVGP can overcome these limitations, detecting serum/plasma neutralizing antibodies and

monoclonal antibodies with the same sensitivity as currently available methods, but more rapidly and without the need for a high containment laboratory or extraneous equipment/supplies not currently used in conventional PRNT assays.

Argentina's Maiztegui Institute of Human Viral Diseases (INEVH), located in the JUNV endemic area, is the primary governmental agency responsible for JUNV diagnostic testing and could potentially benefit from the improvement of technologies for serological detection of JUNV neutralizing antibodies. Routine diagnosis of AHF in the endemic area typically begins with the clinical presentation of distinct symptoms including fever with the presence of oral petechia or lesions, gingival bleeding, and/or conjunctival congestion, with the distinct absence of respiratory involvement, all of which are typical during the first week of JUNV infection [38]. The presence of thrombocytopenia and leukopenia are considered hallmark hematologic findings that indicate JUNV infection should be considered in a differential diagnosis; however, along with the above described symptoms, can be consistent with the clinical presentation of several other endemic diseases including typhoid fever, leptospirosis, and hantaviruses [38].

Following a suspicion of AHF, several methods for direct detection and diagnosis of JUNV as the etiologic agent are available. Historically, virus amplification *in vitro* or *in vivo* from whole blood and subsequent IFA identification was the method of choice [142]. Vero cell monolayers were frequently used for virus amplification; however, Vero cell co-culture with peripheral blood mononuclear cells (PBMCs) or inoculation of suckling mice/guinea pigs enhances virus recovery [141]. Efforts to move away from these methods of virus detection have been made as these tests are time consuming; virus replication in Vero cells requires 5-7 days and amplification *in vivo* requires up to 20 days [143]. Additionally, JUNV amplification is currently required to be performed in the high containment biosafety level 3 (BSL-3) laboratory at INEVH which can also be cumbersome and time consuming. In order to facilitate more rapid diagnosis, a polymerase chain reaction (PCR)-based assay was developed and implemented for the detection of

JUNV RNA isolated from whole blood [143]. This assay is now used routinely at INEVH for detecting JUNV during the acute phase of infection and has been demonstrated to perform with 98% sensitivity, however, only performs with 76% specificity which means that false positives are an expected occurrence [144]. Accordingly, INEVH requires a secondary, serologic confirmatory test to establish a JUNV diagnosis.

Serologic diagnosis for JUNV infection was historically performed using complement fixation-based tests; however, in more recent years ELISA-based assays using whole virus lysates (strain XJ clone3) have been developed and implemented for use in the endemic area [133, 134]. Although the ELISA currently utilized at INEVH is highly sensitive (100%), issues have arisen with its use in the endemic area because overlap exists between JUNV and LCMV virus circulation [145]. There is little evidence in the literature to suggest that JUNV and LCMV are serologically cross-reactive *in vitro*, particularly because they are phylogenetically divergent. Despite this, evidence from the JUNV endemic area suggests that JUNV/LCMV co-infection or sequential infection does occur in human patients, which has complicated serologic diagnosis based on antibody titer alone [146].

A 1977 study from Barrera Oro *et al.* reviewed 3000 human cases of AHF and discovered that 6 patients had actually been infected with LCMV and had been misdiagnosed using an antibody-based assay [146]. Additionally, 150 out of the 3000 patients surveyed in the study showed serologic evidence of previous exposure to LCMV [146]. Interestingly, a follow-up *in vivo* experiment was then able to show that JUNV-infected guinea pig survivors subsequently infected with LCMV, developed a rise in antibody titer specific to both viruses [146, 147]. This is believed to be potentially due to detection of the NP protein which is the most conserved (61% sequence homology) and most abundant protein produced from arenavirus infection. These same studies elucidated the fact that although overall antibody titer increased to both viruses, neutralizing antibody titers to JUNV did not change in response to LCMV infection [146]. For this reason,

neutralization assays (PRNT) are the preferred method of serologic JUNV diagnosis due to their high specificity in targeting the viral GP protein (39% sequence homology amongst arenaviruses) (unpublished data, INEVH) [141]. In addition to being the preferred method of serologic diagnosis for JUNV infection, PRNT neutralization assays are also the preferred methodology for quantifying neutralizing antibodies in convalescent human donor plasma.

Traditional JUNV neutralization assays utilize either wild type or attenuated JUNV strains; INEVH specifically uses an attenuated XJ strain (XJ clone 3) and results take 6-8 days to be obtained. The development of a more rapid method for serologic diagnosis of JUNV infection would not necessarily affect the acute disease course in an individual patient, however, it could have important public-health related implications. More rapid confirmation of JUNV disease enables agencies such as INEVH to mobilize a more rapid public health response which includes timely follow-up of potentially infected or at-risk individuals during an outbreak, initiation of vaccination to at-risk individuals, and efforts to modulate rodent populations, particularly in urban areas where JUNV transmission has been increasing.

Efforts have already been made to develop rapid serologic assays for JUNV neutralizing antibody detection including a psuedotyped rVSVΔG-GFP system as well as a JUNV trVLP system which utilizes JUNV virus-like particles capable of replicating/transcribing a luciferase reporter [79, 132, 148] (Table 3-1). These methods, while capable of providing results quickly (24-48 hours), require expensive equipment in order to read out the relevant data accurately, *i.e.*, luciferase or GFP signal, that are not readily available at INEVH or other smaller laboratories in the endemic area (Table 3-1). Alternatively, a replication competent virus like rVSVΔG-JUNVGP can theoretically stand in as a surrogate for JUNV in traditional PRNT assays to detect JUNV neutralizing antibodies within 48 hours (5 days sooner than a traditional PRNT) while requiring no additional expense or equipment, *e.g.* plate readers, transfection reagents, materials for

plasmid propagation and purification. Additionally, maintaining working stocks of rVSVΔG-JUNVGP is convenient as the virus grows to high titers quickly and can be rapidly amplified in cell culture (Vero cells) using methods currently available at INEVH.

In addition to the potential benefit to INEVH, a method for JUNV neutralizing antibody detection that could be used outside of a high containment laboratory would be extremely helpful in facilitating research for JUNV monoclonal antibody therapies internationally. Currently, in the absence of a high containment BSL-4 lab, research on JUNV monoclonal antibody therapies is often conducted with attenuated strains of the virus, typically Candid #1. Attenuated JUNV strains such as Candid #1 are known to have GP-specific amino acid mutations and the effect of these mutations on the accuracy GP-specific monoclonal antibody screening is unknown [149, 150]. Instead, rVSVΔG-JUNVGP may be a good alternative for JUNV monoclonal antibody screening as it can be used in BSL-2 laboratories and expresses the glycoprotein of a wild type virulent JUNV strain which more accurately represents JUNV GP sequences circulating in nature [151, 152].

In this chapter I will explore the use of rVSVΔG-JUNVGP to accurately detect JUNV monoclonal antibodies as well as JUNV neutralizing antibodies from guinea pig plasma and human donor serum.

METHODS

Viruses and Cell lines

Vero 76 cells (American Type Culture Collection-ATCC) were maintained in Eagle's Minimum Essential Medium (EMEM) supplemented with 10% fetal bovine serum (FBS), 1% penicillin/streptomycin (P/S), and 1% GlutaMAX. JUNV strain Espindola (P3790), obtained from Dr. Thomas Ksiazek (UTMB), was passaged twice in Vero E6 cells and once in Vero 76 cells with prior passage history in mice (2x). JUNV attenuated vaccine

strain, Candid #1, was acquired from the UTMB Arbovirus Reference Collection with prior passage history in Vero (2x) and FRhL cells. All experiments conducted with JUNV were performed in biosafety level 4 (BSL-4) containment at the Galveston National Laboratory, UTMB.

Guinea Pig Plasma

Guinea pig plasma was obtained from (n = 25) animals vaccinated with rVSVΔG-JUNVGP via the methods described in Chapter 2.

Human Candid #1 Vaccinee Serum

This study was approved by the University of Texas Medical Branch (UTMB) Institutional Review Board (IRB#: 16-0196). We obtained written informed consent from 1 adult female participant who had been immunized with a single dose of live attenuated Candid #1 vaccine between 3 months to 8 years before blood donation. The donor was issued a unique study identifier and personnel processing any samples were blinded to any patient identifying information beyond the unique identifier. We separated donor serum or plasma from the donor blood samples and cryopreserved aliquots for subsequent analysis. This work also used de-identified, pooled normal human serum which met all the institutional IRB requirement for exempt classification for use in our studies.

JUNV Monoclonal Antibodies

A panel of six JUNV monoclonal antibodies, originally produced and characterized by Sanchez *et al.* (1989), were obtained from Biodefense and Emerging Infections Research Resources Repository (BEI Resources) [77]. Antibody GB03-BE08, also

identified as J199, was also obtained courtesy of Mapp Biopharmaceutical, Inc. GB03-BE08 was produced from mouse hybridoma while J199 was produced from transgenic *N. benthamiana* and contains an anti-human constant region; all neutralization data reported on these antibodies are cumulative and represent repeated testing with both GB03-BE08 and J199. Antibodies GD01-AG02, QC03-BF11, GB03-BF11, and OD01-AA09 are all neutralizing antibodies directed at G1 of the JUNV GP. Two control antibodies were utilized, MA03-BE06 which targets JUNV NP and LD05-BF09 which is a non-neutralizing antibody targeting the JUNV GP. See Chapter 2, Table 2-2 for detailed information regarding antibody epitope specificity and protective efficacy *in vivo*.

Neutralization Assays

Plaque reduction neutralization tests (PRNT) were performed to evaluate neutralizing antibody titers from human serum, guinea pig plasma, and JUNV monoclonal antibodies. Plasma or serum samples were first heat inactivated at 56ºC for 30 minutes and subsequently diluted two-fold (1:10 to 1:20480) in EMEM supplemented with 10% guinea pig complement (Rockland Immunochemicals Inc.) [19]. JUNV monoclonal antibodies were diluted 10-fold (10 – 0.00001 μg/ml) in EMEM. Plasma/serum and monoclonal antibody dilutions were then incubated 1:1 with 100 PFU of JUNV Espindola, Candid #1, or rVSVΔG-JUNVGP for 1 hour at 37ºC. Plasma/serum/monoclonal antibody and virus dilutions were plated in duplicate (200μl) on Vero 76 cell monolayers with 0.8% agarose overlay. All plates were stained with 5% neutral red and plaques were counted to determine the plaque reduction (PRNT value) for each dilution. Plasma samples were normalized to baseline plasma from each guinea pig and human donor serum was normalized to uninfected (normal) pooled human serum. JUNV Espindola plates were stained on day 5 PI and plaques counted on day 6 PI. Candid #1 plates were stained day 6 PI and plaques

counted on day 7 PI. rVSVΔG-JUNVGP plates were stained 24 hours PI and plaques were quantified 48- and 72-hours PI.

Statistical Analyses

GraphPad Prism 7.03 was utilized to generate dose-response curves based on PRNT values for each animal or human donor. Unpaired t-test was used to compare PRNT50 values obtained utilizing JUNV Espindola versus rVSVΔG-JUNVGP for each guinea pig. Statistical notations correspond with the following p values: *p < 0.05, **p < 0.01, ***p < 0.001, ****p<0.0001.

RESULTS AND DISCUSSION

Monoclonal Antibody Screening

In order to evaluate the ability of rVSVΔG-JUNVGP to accurately serve as a surrogate for identifying JUNV neutralizing antibodies, I conducted a series of PRNT assays using a panel of 6 neutralizing antibodies previously described (Table 2-2) [77, 79, 90]. A series of 10-fold dilutions were made for each antibody and then incubated with either JUNV Espindola, Candid #1, or rVSVΔG-JUNVGP. JUNV Espindola and rVSVΔG-JUNVGP yielded virtually identical PRNT values and dose-response curves for all 6 antibodies (Figure 3-1). Interestingly Candid #1 yielded similar PRNT values and dose-response curves to both JUNV Espindola and rVSVΔG-JUNVGP in only 4 out of 6 antibodies tested (Figure 3-1). Control antibodies LD05-BF09 and MA03-BE06 failed to neutralize any of the 3 viruses tested, as expected; one is a non-neutralizing JUNV GP-specific antibody and the other is a NP-specific antibody.

The fact that Candid #1 failed to adequately generate neutralization results consistent with wild type JUNV Espindola (or rVSVΔG-JUNVGP) for 2 out of 6 antibodies (Figure 3-1). Importantly, these two antibodies, J199 and J200, performed the best *in vivo* at protecting guinea pigs from JUNV challenge [90]. This is a significant finding because it is important that the tools utilized for monoclonal antibody detection in the lab accurately reflect the neutralization activities against wild type viruses circulating in nature. The results regarding Candid #1 are not entirely surprising as this virus has 8 amino acid differences in the GPC gene compared with JUNV Espindola, 4 of which are within the G1 protein which is an important target of JUNV neutralizing antibodies [149, 150]. Phylogenetic studies of JUNV GPC diversity in the field show the vast majority of viral isolates cluster with JUNV strain Espindola rather than Candid #1. These data collectively suggest that rVSVΔG-JUNVGP more accurately recapitulates the ability of antibodies to neutralize wild type JUNV Espindola.

Method/System of Detection	Biosafety Level	Time-to-Results	Data Readout	Specialized Equipment Necessary?	References
PRNT - Wild Type JUNV	BSL-4 BSL-3 (Argentina, INEVH)	6-7 Days	Enumeration of plaque reduction	N	Sanchez *et al.* 1989, Kenyon *et al.* 1990
PRNT - Attenuated JUNV (Candid #1, XJ Clone 3)	BSL-2	6-8 Days	Enumeration of plaque reduction	N	Enria *et al.* 1984, Barrera Oro *et al.* 1990
VSV pseudotyped virus system (rVSVΔG-GFP)	BSL-2	24 hours	GFP reporter signal	Y	Whitt 2010, Iha 2013, Brouillette *et al.* 2017
JUNV transcription-replication competent virus-like particle (trVLP) system	BSL-2	48 hours	Luciferase reporter signal	Y	Dunham *et al.* 2018, Leske *et al.* 2019
PRNT - rVSVΔG-JUNVGP	BSL-2	48 hours	Enumeration of plaque reduction	N	Sorvillo *et al.* Unpublished Data

Table 3-1. Comparative Methods for the Detection of JUNV Neutralizing Antibodies. A summary of published methodologies for the detection of JUNV neutralizing antibodies are listed. All methods are compared to one another on the basis of required biosafety containment, timeline for acquisition of results, type of data output, and whether the method requires specialized equipment (*i.e.* quantitative luminescence or fluorescence).

Comparative Neutralization Titers - Guinea Pig Plasma and Human Serum

In order to assess whether rVSVΔG-JUNVGP can accurately detect neutralizing antibody titers from plasma/serum, I utilized guinea pig plasma from animals vaccinated with rVSVΔG-JUNVGP (Chapter 2) as well as serum from a single human Candid #1 vaccinee. Twenty-five guinea pig samples were evaluated via PRNT assay to determine $PRNT_{50}$ values using either JUNV Espindola or rVSVΔG-JUNVGP (Figure 3-3A/B). No statistically significant differences were found comparing the $PRNT_{50}$ values that were generated using the two viruses (Figure 3-3A). Additionally, the correlation coefficient of the derived values was calculated and indicates a strong positive correlation ($r = 0.8527$) between values generated from JUNV Espindola and rVSVΔG-JUNVGP (Figure 3-3B). Eighteen of the guinea pig plasma samples were also used to generate dose-response curves for a more thorough comparison of additional PRNT values generated by the two separate viruses (Figure 3-2, Appendix A-2). Again, there were no significant differences detected between dose-response curves generated from wild type JUNV Espindola and rVSVΔG-JUNVGP (Figure 3-2, Appendix A-2). These data, similar to the JUNV monoclonal antibody data, indicate that rVSVΔG-JUNVGP can be used in place of wild type JUNV for serologic detection of neutralizing activity. It was also important; however, to demonstrate these results could be verified for accuracy in human samples. I was able to acquire a single sample of serum from a human Candid #1 vaccinee in order to evaluate the potential of this data to be extrapolated to use in human samples. I conducted PRNT assays and generated dose-response curves comparing the neutralization titer values

obtained from wild type JUNV Espindola versus rVSVΔG-JUNVGP and was able to confirm that, in this particular human sample, the viruses yielded very similar results with no statistically significant difference.

These results overall are significant because rVSVΔG-JUNV was able to detect and provide accurate results about neutralization titer in guinea pig plasma and human serum, and, these results were obtained 5 days sooner than the results from a traditional JUNV PRNT assay.

CONCLUSIONS

In this chapter I evaluated the potential of rVSVΔG-JUNVGP to serve as a surrogate for JUNV in conventional PRNT assays for the detection of JUNV neutralizing antibodies. The use of this construct for neutralizing antibody detection could be beneficial for multiple reasons. We know that neutralizing antibody detection via PRNT is the preferred method for JUNV serologic confirmatory diagnostic testing in the endemic area. rVSVΔG-JUNVGP has the potential to deliver these confirmatory results within 48 hours, 5 days earlier than traditional PRNT assays, which may have important public health implications. A more rapid serologic confirmation of AHF cases has the potential to mobilize a more rapid response from public health agencies like INEVH, enabling them to track down other potentially exposed or at-risk persons for vaccination or treatment in a timely manner. PRNT assays utilizing rVSVΔG-JUNVGP would not only be more rapid, but also convenient, as they would not require the addition of equipment or reagents not already available or in use at INEVH. Lastly, rVSVΔG-JUNVGP does not require handling in a high containment BSL-4 laboratory which could enable more widespread research into JUNV monoclonal antibody therapies.

I was able to show that rVSVΔG-JUNVGP detects monoclonal antibodies *in vitro* as accurately as wild type JUNV Espindola and more accurately than the attenuated JUNV

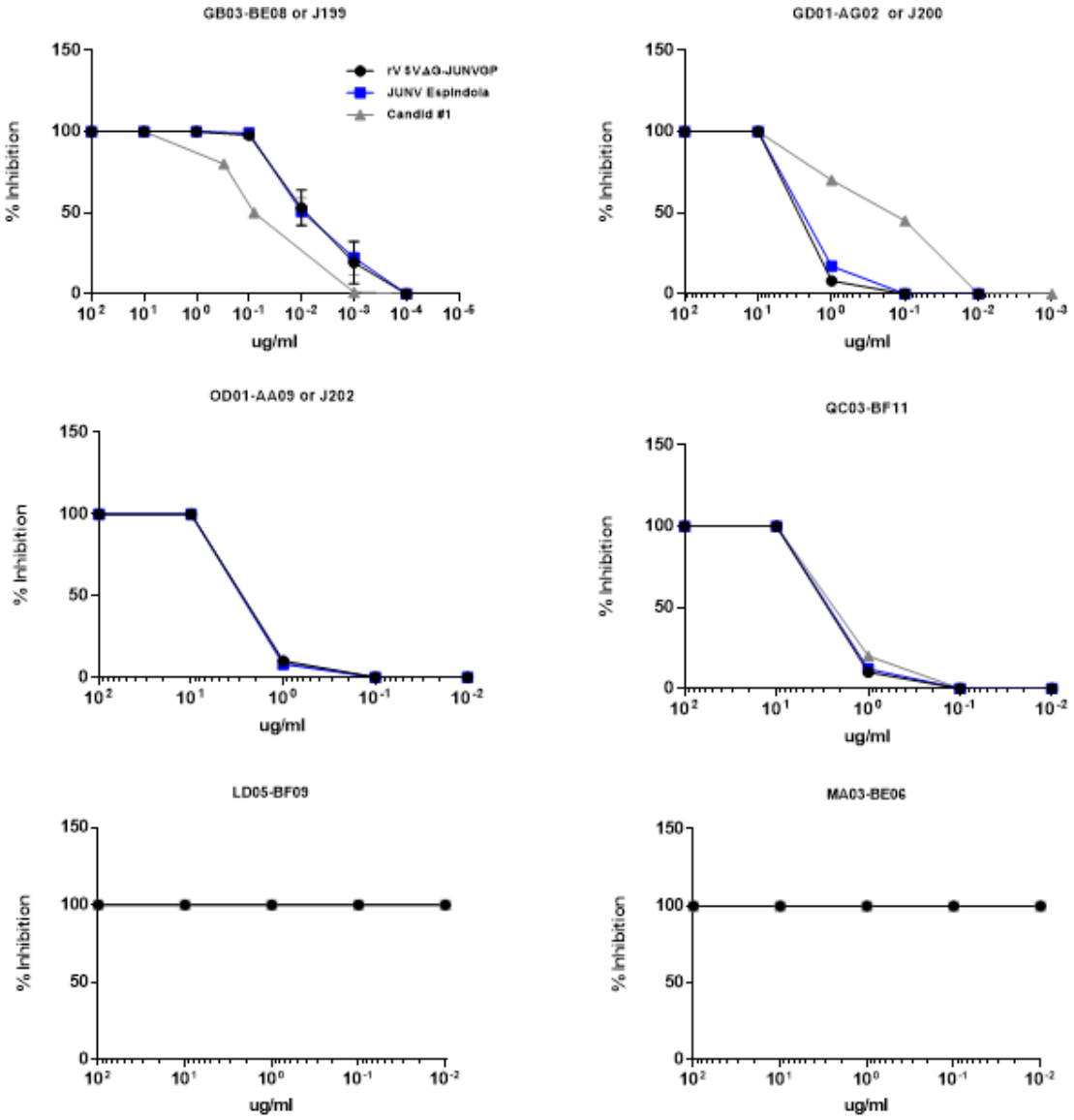

Figure 3-1. JUNV Monoclonal Antibody PRNT Assays. Six JUNV monoclonal antibodies were evaluated for their ability to neutralize/inhibit infectious JUNV (PFUs) diluted tenfold concentrations (10– 0.00001 µg/ml). Antibodies were compared in their ability to neutralize JUNV Espindola, Candid #1, and rVSVΔG-JUNVGP viruses. Antibodies GB03-BE08, OD01-AA09, GD01-AG02, and QC03-BF11 are known neutralizing antibodies. Antibodies LD05-BF09 and MA03-BE06 are non-neutralizing antibodies targeting the JUNV GP and JUNV NP, respectively. GraphPad Prism 7.03 was utilized to generate dose-response curves.

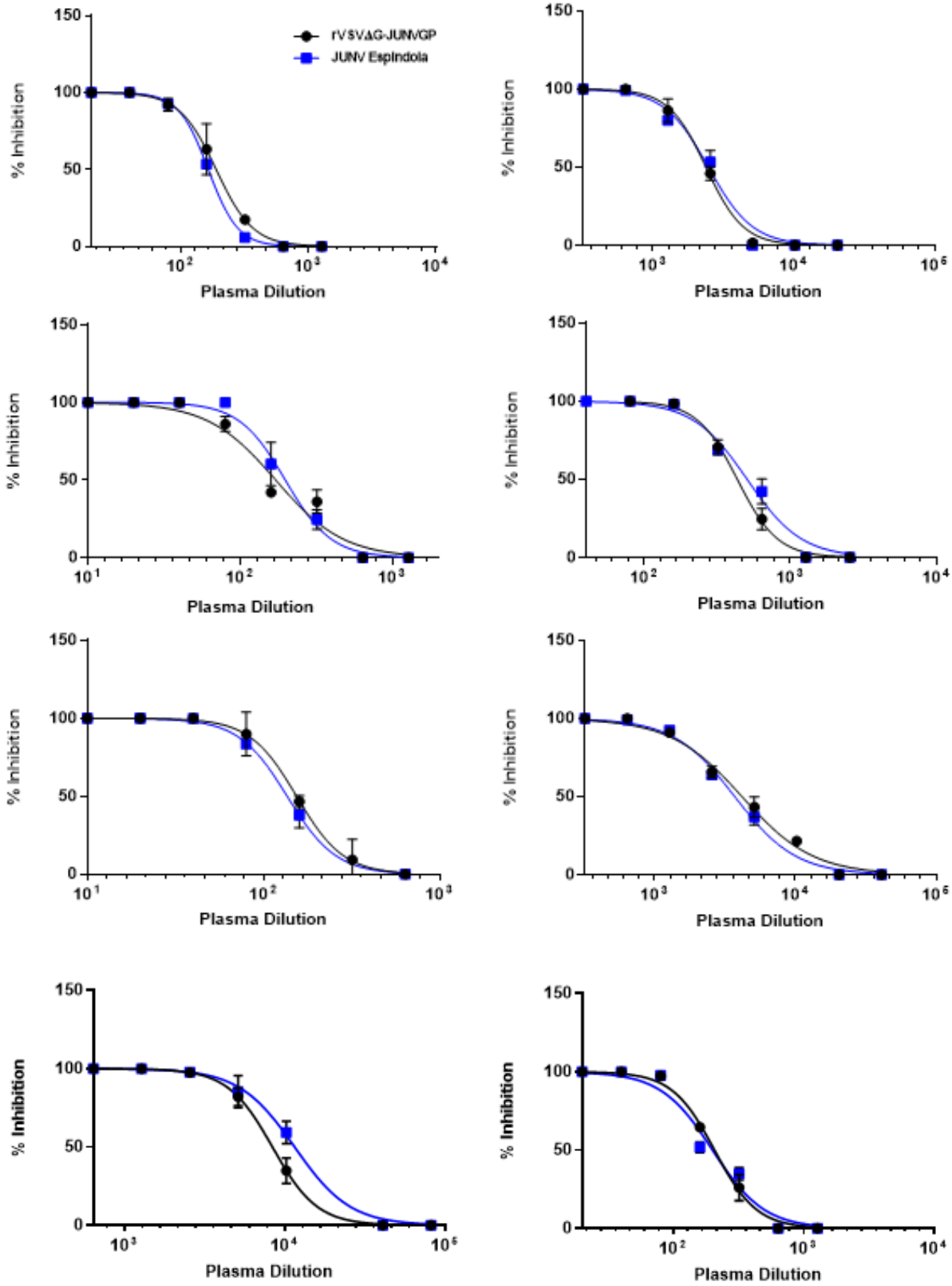
rVSVΔG-JUNVGP
JUNV Espindola
% Inhibition
Plasma Dilution

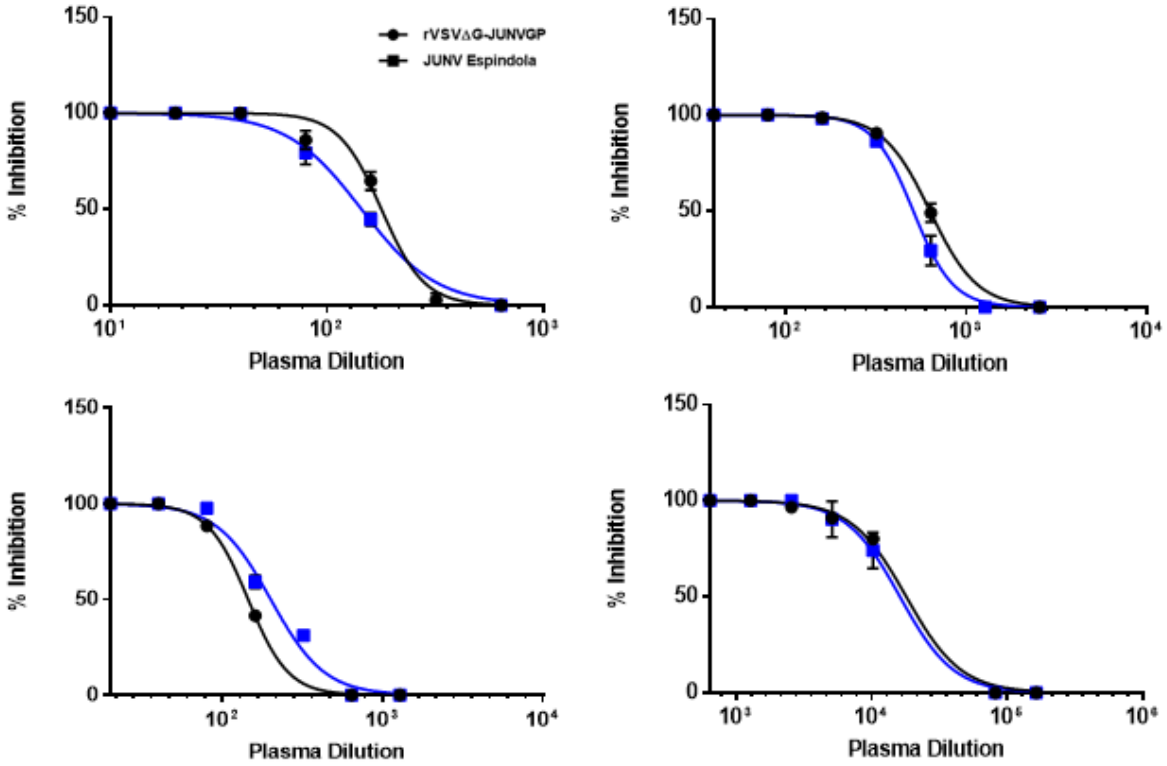

Figure 3-2. Detection of JUNV neutralizing antibodies from rVSVΔG-JUNVGP vaccinated guinea pig plasma. Eighteen guinea pig plasma samples were evaluated for their ability to neutralize either JUNV Espindola or rVSVΔG-JUNVGP. GraphPad Prism 7.03 was utilized to generate dose-response curves. Each graph depicts data from a single animal/plasma sample. See Appendix A-2 for additional graphs/data.

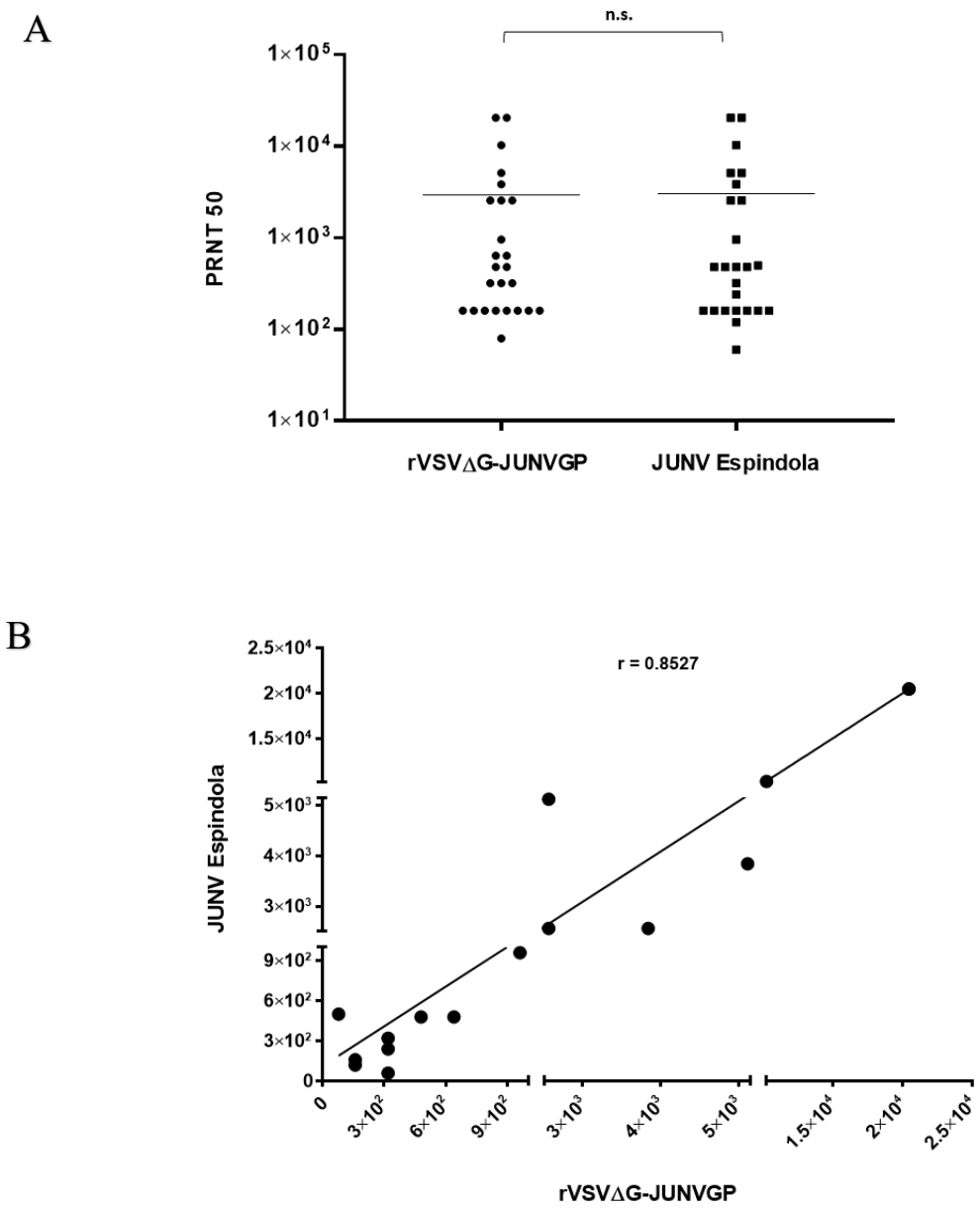

Figure 3-3. JUNV Espindola versus rVSVΔG-JUNVGP: detection of JUNV neutralizing antibodies from rVSVΔG-JUNVGP vaccinated guinea pig plasma. Twenty-five guinea pig plasma samples were evaluated for their ability to neutralize either JUNV Espindola or rVSVΔG-JUNVGP. A, $PRNT_{50}$ values derived from each virus are reported. B, Correlation of values derived from JUNV Espindola versus rVSVΔG-JUNVGP (correlation coefficient (r) = 0.8527). Statistical notations correspond with the following p values: *$p < 0.05$, **$p < 0.01$, ***$p < 0.001$.

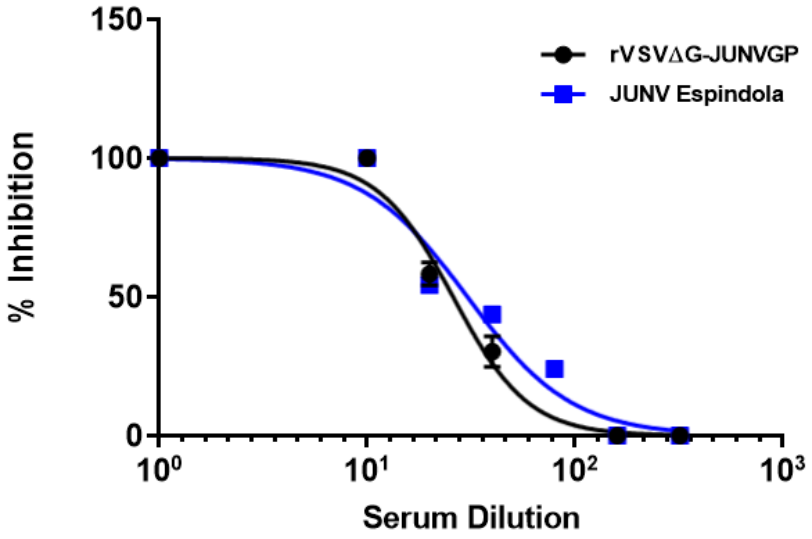

Figure 3-4. Detection of JUNV neutralizing antibodies in human serum from a Candid #1 vaccinee. A single serum sample obtained from a human Candid #1 vaccinee was evaluated for its ability to neutralize either JUNV Espindola or rVSVΔG-JUNVGP. GraphPad Prism 7.03 was utilized to generate the dose-response curve. Approved by the UTMB Institutional Review Board (IRB#: 16-0196).

strain Candid #1. It is important to remember that rVSVΔG-JUNVGP, by design, has the same GP as JUNV Espindola so accuracy in the detection of neutralizing antibodies between the two viruses could be expected. We might be cautious to assume that this similarity can be broadly applied to all wild type JUNV isolates and further data will need to be obtained to understand this more clearly. It is clear; however that Candid #1 has a number of specific GP mutations which are not necessarily found in wild type viruses. In fact, based on phylogenetic data, Candid #1 generally does not accurately represent wild type virus genetic sequences, suggesting that rVSVΔG-JUNVGP may be a better choice for JUNV neutralizing antibody detection [151, 152]. Further studies would need to be performed using other strains of JUNV for confirmation.

In this chapter I was also able to show that rVSVΔG-JUNVGP detects neutralizing antibodies in guinea pig plasma and human serum with the same accuracy as wild type JUNV Espindola, but can generate these results 5 days more quickly than traditional methodologies. Taken together, the findings in this chapter indicate that rVSVΔG-JUNVGP can detect serum/plasma neutralizing antibodies and monoclonal antibodies with the same sensitivity as currently available methods, but more rapidly and without the need for a high containment laboratory or extraneous equipment/supplies not currently used in conventional PRNT assays. Ultimately this tool would need to be thoroughly evaluated in the endemic area side-by-side with current methodologies for serologic JUNV detection (PRNT using strain XJ Clone 33) in order to assess its sensitivity and specificity. The data in this chapter, however, have demonstrated that rVSVΔG-JUNVGP has merit for further evaluation and development, and may eventually serve as a useful replacement for standard serologic detection methods in the JUNV endemic area.

Chapter 4: Chimeric Arenavirus Glycoproteins Toward A Cross-Protective Arenavirus Vaccine

As discussed in Chapter 1, arenaviruses have widespread impact on global public health. The vast majority of arenaviral infections are the result of LASV infection with an estimated incidence exceeding 300,000 cases and 5,000 deaths per year [153]. JUNV also has a significant public health impact with an annual incidence reaching 300 - 1000 cases despite widespread administration of a live-attenuated vaccine [33]. The incidence of other disease-causing arenaviruses is more sporadic. MACV, the causative agent of Bolivian hemorrhagic fever, has caused 6 documented outbreaks since its discovery in 1959, causing over 1000 cumulative cases with a mortality rate of approximately 25% [154]. GTOV, or Venezuelan hemorrhagic fever, was first documented in 1989 causing two notable outbreaks with an incidence of 104 and 20 cases each and a mortality rate also around 25% [3, 4]. As important as these viruses are from a public health standpoint, these diseases are also very significant from a biosecurity perspective. The pathogenic arenaviruses listed above are all considered NIAID category A priority pathogens because they are easily transmitted via aerosol and cause significant hemorrhagic and/or neurologic symptoms with accompanying mortality rates as high as 30%.

rVSV-based vaccines have demonstrated protective efficacy against many different hemorrhagic fever viruses including EBOV, MARV, Crimean-Congo hemorrhagic fever, Andes virus, and LASV [109, 112, 113, 116]. I have now been able to demonstrate that a rVSV-based vaccine against JUNV demonstrates protective efficacy as well (Chapter 2). With the development of so many rVSV-based vaccines, some with overlapping endemic areas (*e.g.,* LASV and EBOV) it raises questions about the ability of multiple, sequential rVSV vaccinations to induce protective immune responses. This is particularly relevant in areas of overlapping endemicity but also in the case of military personnel and/or

international health care workers who may come into contact with multiple virulent pathogens and would benefit from multiple rVSV vaccinations. A study by Marzi *et al.* (2015) demonstrated that sequential vaccination with two different rVSV vaccines (LASV and EBOV) 90 days apart could induce protective responses to both viruses [155]; however, testing of more than two rVSV vaccines has not been attempted. This issue may be particularly relevant when considering rVSV vaccines targeting South American hemorrhagic fever viruses like the New World arenaviruses. In recent years new transmission scenarios for JUNV have emerged, revealing at-risk populations of migrant farm workers who travel and work in the endemic areas of multiple arenaviruses and who could benefit substantially from arenavirus cross-protection [13].

For the biodefense and public health purposes described above, the development of a cross protective arenavirus vaccine may be important. While multi-valent rVSV vaccines have been described, containing multiple open reading frames that can encode multiple antigens, there are some limitations to this approach for a cross-protective vaccine [110]. Specifically, VSV undergoes polar transcription creating inherent differences in antigen expression levels which may affect downstream protective immune responses against certain antigens. An alternative strategy is the development of chimeric proteins which can simultaneously express protective epitopes from multiple pathogens. In fact, some groundwork has already been laid for the development of chimeric arenavirus glycoproteins. Albarino *et al.* (2010) attempted to generate a recombinant Candid #1 virus that expresses chimeric JUNV/LASV GPCs. The study effectively showed that in order to ensure proper cellular processing and subsequent functionality of a LASV/JUNV chimeric GP, the SSP and G2 transmembrane domain (C terminus) must be homologous [156]. Martin *et al.* developed chimeric arenavirus G1 proteins in order to investigate New World arenavirus (Clade B) tropism [157]. In their study they determined that the arenavirus G1 could be divided into 5 segments separated by 4 conserved cysteine amino acid residues which are essential for maintaining important disulfide bonds in the mature GP (Figure 4-

1) [157]. They evaluated whether swaps of nucleotide sequences could be made between the 5 segments, substituting arenavirus sequences from JUNV, *Tacaribe mammarenavirus* (TCRV), GTOV, and *Amapari mammarenavirus* (AMAV). The study discovered that properly processed and functional GPs could be generated from swaps of the segments as long as the cysteine residues remained conserved [157]. This same strategy was also used by Brouillette *et al.* (2017) to evaluate GP receptor binding site cross-reactivity between JUNV and MACV where functional chimeric MACV/JUNV GPs were generated. [79]

Using the above-mentioned studies as a guide, and with the ultimate objective of developing antigens for use in a cross-protective arenavirus vaccine, I designed a panel of chimeric arenavirus GPC sequences (Figure 4-1). I chose to include known immunogenic epitopes from four important arenaviruses, all of which have small animal (guinea pig models) established for ease of screening downstream: JUNV, MACV, LASV, and GTOV [42, 89, 158-160]. In this chapter I will detail the *in silico* design of each chimeric GPC and subsequent studies to evaluate whether these recombinant proteins are functional to ultimately determine which may be the best candidates for vaccine development.

METHODS

Cell lines

Baby hamster kidney cells (BHK) cells (Michael Whitt, University of Tennessee Health Science Center) were maintained in Dulbecco's Modified Eagle's Medium (DMEM) supplemented with 5% FBS, 1% P/S, and 1% GlutaMAX.

Chimeric Arenavirus GPC Design and Cloning

Chimeric arenavirus GPC sequences were designed *in silico* using SnapGene 4.1.9 software. Each gene sequence was designed to be flanked by Mlu1 and Nhe1 restriction sites ensuring it would be compatible for cloning into a pCAGGS-G-NJ expression plasmid (obtained courtesy of Dr. Michael Whitt, University of Tennessee Health Science Center). Chimeric arenavirus GPC genes were generated and obtained from GenScript.

Immunofluorescence Assay

BHK cells were transfected with pCAGGS expression vectors containing each of the 7 chimeric GPCs. Transfections were performed using Lipofectamine 2000 reagent (Invitrogen). 24 hours post-transfection cell monolayers were fixed with 4% paraformaldehyde for 10 minutes, followed by PBS-Glycine (0.1M) rinse. The JUNV GP monoclonal antibody J199 was used as a 1^0 antibody (Mapp Biopharmaceutical, Inc.), diluted 1:5000 and incubated overnight at 4^0 C. Rinses were performed with PBS-tween80 (0.05%). Anti-human IgG Alexa Flour 488 was used as a 2^0 antibody and was diluted 1:5000 and incubated for 1 hour.

Generation of rVSVΔG-GFP Pseudotypes

VSV pseudotypes were generated based on the published methods by Whitt (2010) [161]. Briefly, BHK cells were transfected as described above with each of the 7 pCAGGS-ChimericGPC plasmids and, after 24-hour incubation, cells were infected with rVSVΔG-GFP virus (MOI of 5). Supernatants were harvested and clarified via centrifugation 24-hours PI. In order to assay for pseudotype functionality, BHK cells were transfected with each pCAGGS-ChimericGPC plasmid and, 24 hours later, infected with the matching pseudotyped rVSVΔG-GFP virus. GFP expression was assessed via fluorescent microscopy to determine pseudotype functionality.

RESULTS AND DISCUSSION

Chimeric Arenavirus GPC Design and Cloning

I generated a panel of 7 chimeric glycoproteins designed to contain epitopes from both New and Old World arenaviruses including: LASV, JUNV, MACV, and GTOV. Studies have shown neutralizing LASV antibodies target different regions of the arenavirus GP than do those of New World arenaviruses. As previously described, antibody responses to the receptor binding domain within G1 are known to be important for New World arenavirus neutralization and protection [79, 81, 82]. In contrast, a recently characterized LASV neutralizing antibody was discovered to depend on binding to the G2 subunit. Studies have also demonstrated that antibodies directed exclusively against the LASV G1 do not effectively neutralize the virus [162, 163]. Evidence also suggests that G2 of the mature arenavirus GP generates the most cross-protective antibody responses (non-neutralizing) between arenaviruses [164, 165]. As a result, I designed the majority of chimeric GPCs to contain the LASV sequence in the G2 position and used G1 for insertion of New World arenavirus epitopes.

I designed a panel of 7 chimeric GPC sequences which are detailed in Figure 4-1. G1 can be divided into 5 segments around 4 conserved cysteine residues. We know that JUNV protective antibodies bind directly to epitopes around the receptor binding domain and as a result I designed all but one chimeric GPC to contain the JUNV sequence in segment 2 of G1. Data from Brouillette *et al.* (2017) looked at identifying MACV epitopes within G1 by generating JUNV/MACV G1 chimeras and found that the presence of the MACV sequence in segment 4 of G1 was important for the generation of a functional protein. The study also suggested that the MACV sequence from segment 4 creates a loop structure over the receptor binding domain in the mature protein. This loop is hypothesized to occlude antibodies that have not been specifically generated to MACV (*i.e.,* JUNV

antibodies). By including this sequence in the chimeric GPCs I could theoretically ensure that any subsequent antibody responses generated would be able to effectively navigate binding around this extra loop structure in response to MACV challenge. As a result, I designed many of the chimeric GPCs to encode MACV in position 4 of G1 [79]. Data regarding protective epitopes for GTOV is scarce. I was able to identify a T-cell epitope published in the literature that exists in segment 3 of G1, unfortunately I do not have any data regarding the protective responses generated by this epitope [166]. Nonetheless these data provided some framework for the placement of GTOV sequences within G1.

During the design of chimeric GPC sequences, I was concurrently exploring the idea that amino acid 116 of the JUNV GP may have an important role to play in protection during vaccination (see Chapter 2, Experiment 2). JUNV strain Romero and strain Espindola GPC sequences contain a single amino acid difference, residue 116 (Romero 116E and Espindola 116A). As previously mentioned, I designed nearly all chimeric GPCs to maintain a JUNV-specific sequence in segment 2 of G1 which also contains amino acid 116. As a result, for each chimeric GPC sequence designed, I created two versions that were identical except for amino acid 116 (116A or 116E).

Detecting Chimeric Arenavirus GP Cell Surface Expression

In order to evaluate whether chimeric GPC genes could be adequately processed and expressed as mature GP's on the surface of cells I transfected BHK cells with pCAGGS expression vectors encoding each chimeric GPC. I subsequently performed an immunofluorescence assay using the JUNV monoclonal antibody J199. There is evidence that J199 binds to the receptor binding domain of G1 which is located in segment 2. As described, I designed all but one chimeric GPC to contain the JUNV sequence in segment 2 of G1, indicating that J199 could theoretically bind all but one chimeric GP (chGP1). Immunofluorescence assays resulted in the detection of fluorescent signal comparable in

intensity to a positive control (JUNV Romero GP) from two chimeric glycoproteins: chGP2 and chGP3 (Figure 4-2). These particular GPs are chimeras of JUNV and LASV only, encoding JUNV in subunit G1 and LASV in G2, and differ in only a single amino acid (116A or 116E). These data indicate that chGP2 and chGP3 underwent effective cellular processing and were capable of being expressed from the plasma membrane of cells. All other chimeric GPCs gave no signal over the mock-transfected control. It is important to note that even though J199 targets the JUNV sequence in segment 2/subunit G1, this does not mean that the necessary epitope was maintained in the structure of mature chimeric GPs. While J199 immunostaining could not be detected from 5 chimeric GPCs, this does not indicate that these GPs were unable to be expressed on the plasma membrane. I moved on to a series of experiments designed to evaluate with more certainty whether the GPCs were, not only expressed on the cell surface, but also functional in their ability to be packaged onto a VSV virion and subsequently undergo cellular entry.

Detecting Chimeric Arenavirus Functionality

In order to assess the expression and functionality of each chimeric GP we created rVSVΔG-GFP virus pseudotypes. BHK cells were transfected with pCAGGS expression vectors of each chimeric GPC. Cells were then infected with the matching pseudotyped rVSVΔG-GFP virus. Observable GFP expression was an indication that the designated GPC was adequately processed, expressed from the plasma membrane, packaged into the rVSVΔG-GFP virion, and capable of cellular entry. Wild type VSV-G and JUNV Romero GP were utilized as positive controls. As expected GFP expression from BHK cells was intensely observable after infection with wild type VSV-G psudotyped virus (Figure 4-3). GFP expression was less pronounced but nonetheless detectable after infection with JUNV Romero GP pseudotyped virus (Figure 4-3). Surprisingly, all chimeric GP virus pseudotypes generated observable GFP expression matching the JUNV Romero GP

positive control which was substantially greater than the background autofluorescence observed in mock infected cells (Figure 4-3). This finding indicates that all 7 chimeric arenavirus glycoproteins may effectively be expressed from the plasma membrane, incorporated into VSV virions, and may be functionally capable of cellular entry.

CONCLUSIONS

Several pathogenic arenaviruses are considered significant from both public health and biosecurity perspectives including LASV, JUNV, GTOV. These viruses are considered NIAID category A priority pathogens because they are easily transmitted via aerosol and cause significant hemorrhagic and/or neurologic symptoms with accompanying mortality rates as high as 30%.

The development of a cross-protective arenavirus vaccine to generate protection from these pathogens simultaneously could be important for several reasons. First, military personnel and/or international health care workers who may come into contact with multiple pathogenic arenaviruses through their work would benefit from a cross-protective vaccine. Additionally, migrant farm workers in South America have recently been identified as an at-risk population due to their travel and work in the endemic areas of multiple arenaviruses could benefit substantially from arenavirus cross-protection.

In this chapter, I designed a panel of chimeric arenavirus GPC genes that could potentially be used in a rVSV-based cross-protective arenavirus vaccine. Through a pseudotyped rVSVΔG-GFP virus system, I was able to demonstrate that all chimeric GPCs were adequately processed intracellularly, expressed from the plasma membrane, packaged into the rVSVΔG-GFP virion, and capable of cellular entry. These findings indicate that all 7 chimeric GPs may be good candidates to move forward into a rVSV vaccine vector for evaluation of protective efficacy *in vivo*.

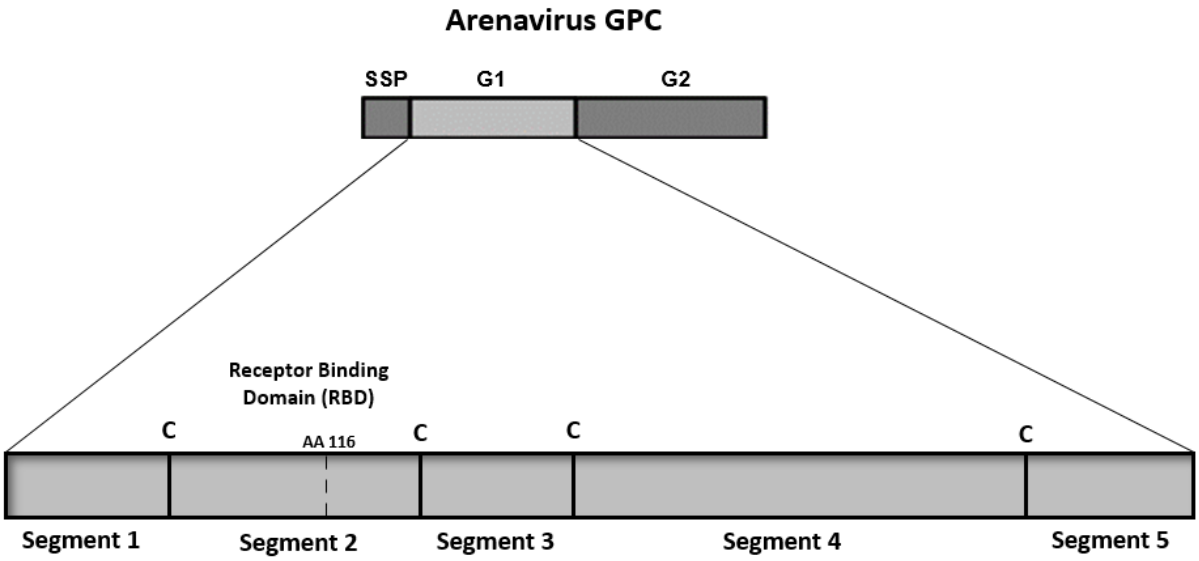
Arenavirus GPC
SSP
G1
G2
Receptor Binding
Domain (RBD)
C
AA 116
C
C
C
Segment 1
Segment 2
Segment 3
Segment 4
Segment 5

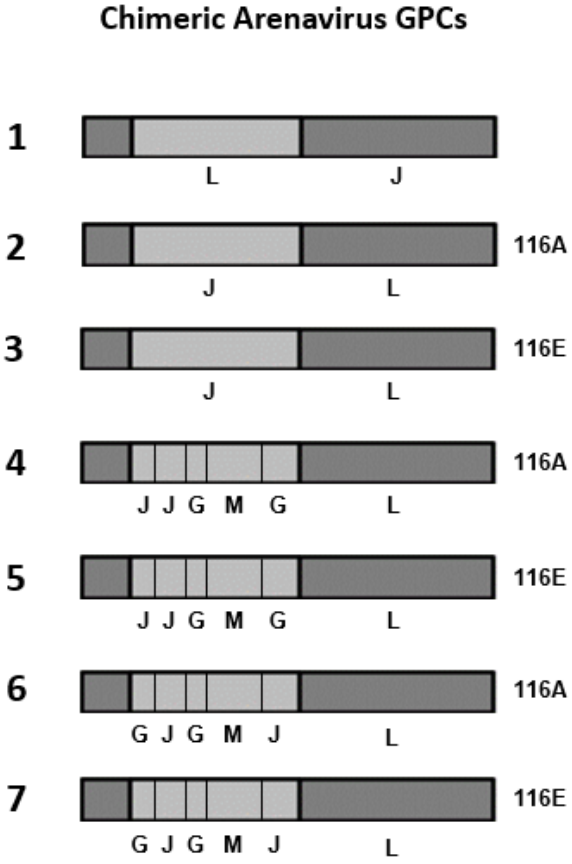
Chimeric Arenavirus GPCs
1
L
J
2
116A
J
L
3
116E
J
L
4
116A
J J G M G
L
5
116E
J J G M G
L
6
116A
G J G M J
L
7
116E
G J G M J
L

Figure 4-1. Chimeric arenavirus GPC sequences. Representative image of the arenavirus GPC composed of SSP, G1, and G2 segment. G1 can be further divided into 5 segments divided by 4 conserved cystine amino acid residues. Amino acid residue 116 is highlighted because it is the single amino acid difference between JUNV strains Romero (E) and Espindola (A) GPC sequences. The design of seven chimeric arenavirus GPC sequences are depicted: L (LASV), J (JUNV), M (MACV), G (GTOV).

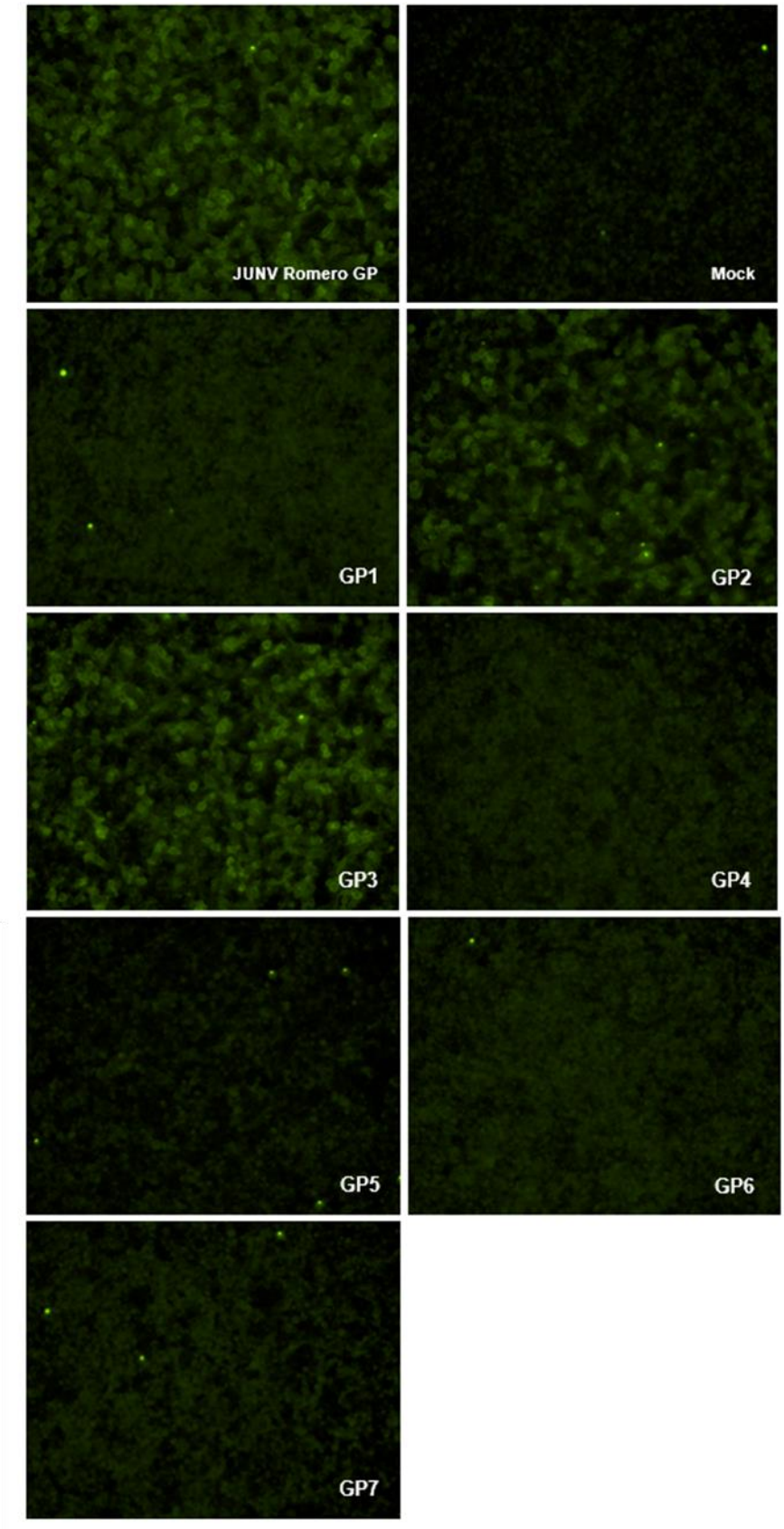
JUNV Romero GP
Mock
GP1
GP2
GP3
GP4
GP5
GP6
GP7

Figure 4-2. Immunofluorescent detection of chimeric arenavirus glycoproteins. BHK cells were transfected with pCAGGS expression vectors containing each chimeric GPC sequence. Chimeric GP cell surface expression was evaluated via JUNV monoclonal antibody (J199) immunostaining. Positive signal (Alexa Flour 488, green) can be seen from JUNV Romero GP (positive control), GP2, and GP3 transfected cells. Mock infected cells were treated with lipofectamine alone.

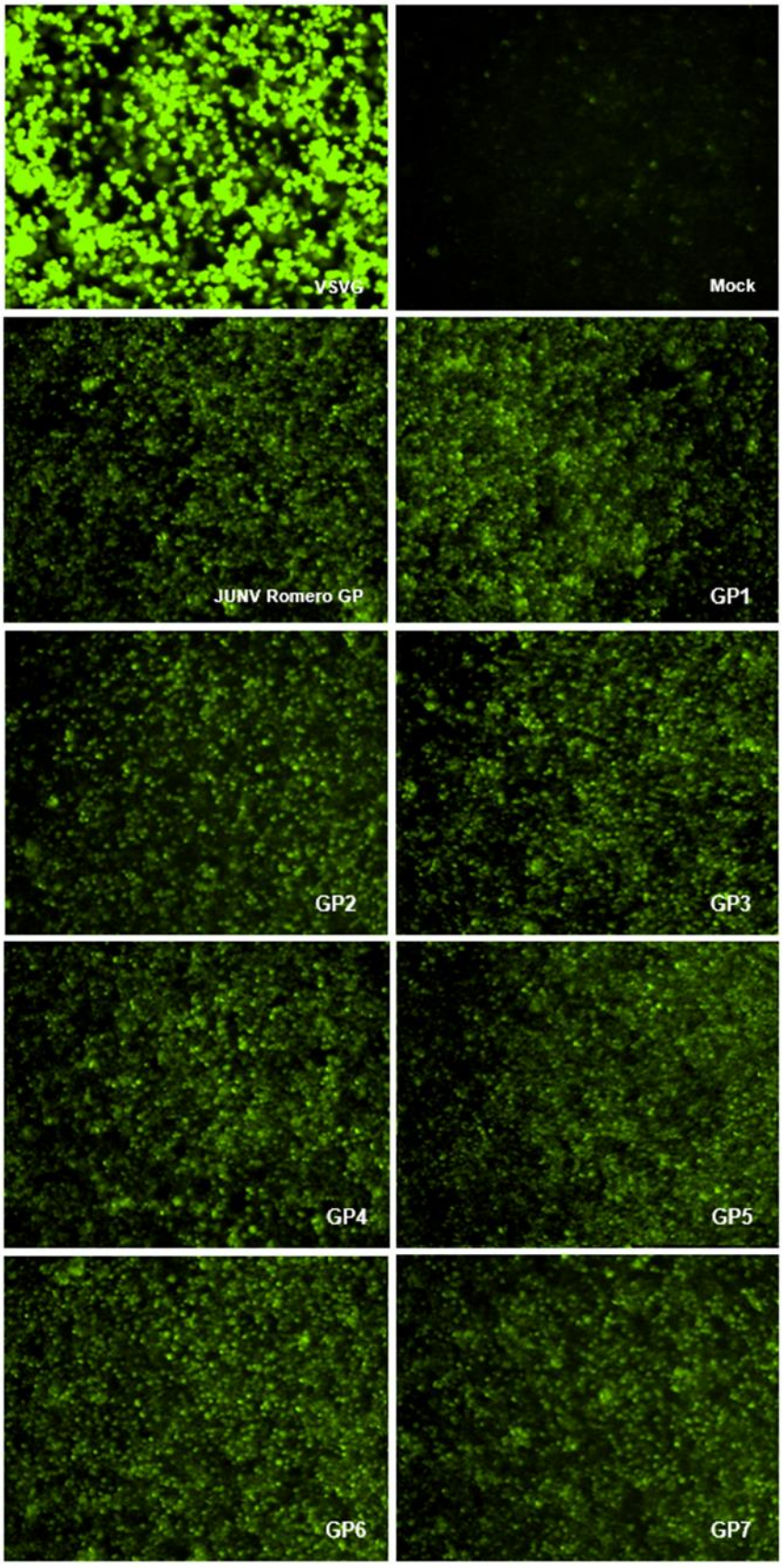
VSVG
Mock
JUNV Romero GP
GP1
GP2
GP3
GP4
GP5
GP6
GP7

Figure 4-3. rVSVΔG-GFP pseudotypes. Attempts were made to pseudotype rVSVΔG-GFP viruses with each chimeric GP in order to assess for GP functionality (Whitt, 2010). BHK cells were transfected with pCAGGS expression vectors of each chimeric GPC. Cells were then infected with the matching psudotyped virus. GFP expression is an indication that the designated GPC was adequately processed, expressed from the plasma membrane, packaged into the rVSVΔG-GFP virion, and capable of cellular entry. Wild type VSV-G and JUNV Romero GP were utilized as positive controls.

Chapter 5: Discussion

No one can foretell the future, but one thing is clear: The emergence and reemergence of deadly pathogens predicted in the 1992 NASEM report has come to fruition and will continue into the future, only more rapidly and with a bigger impact. As clearly demonstrated by arenaviruses, we will continue to see expanding zoonotic transmission of disease as human populations continue to expand into previously uninhabited areas of the world. We will also continue to see expanding pathogenic threats to biosafety and biosecurity. As our world becomes more connected, we will also continue to see the spread of pathogens into new cities, countries, and communities via our global infrastructure. In response, the advancement of research on emerging pathogens will be essential to combatting the next major public health or biodefense threat.

The work presented in this dissertation addressed a need for the development of countermeasures against an important group of emerging pathogens: arenaviruses. This group of viruses are particularly significant because they cause severe disease with high mortality rates and are considered biodefense priority pathogens as they are easily transmitted via aerosol. FDA approved vaccines and therapeutics are limited for the prevention and treatment of arenaviruses; therefore, the development of novel countermeasures and diagnostic capabilities is an important research objective. My project centered around the development of a recombinant vesicular stomatitis virus expressing the JUNV glycoprotein (rVSVΔG-JUVGP) which, as I was able to show, can be utilized in multiple ways to address the threats associated with JUNV. My project also looked at developing chimeric antigens that could be used for generating arenavirus cross-protection.

The first major objective of this dissertation was to develop rVSVΔG-JUVGP as a vaccine against lethal JUNV challenge. Although a live-attenuated vaccine, Candid #1, is currently utilized effectively to prevent JUNV disease in the endemic area, this vaccine was evaluated and denied approval by the FDA due to issues of attenuation instability and

neurotropism. I wanted to generate a vaccine alternative which might overcome these hurdles to FDA approval, and which could be used as a potential biodefense vaccine. I was able to show that in a guinea pig model of lethal JUNV infection, rVSVΔG-JUVGP provided 100% protection using only a single vaccine injection. In addition to assessing survival outcomes, I was able to demonstrate that the vaccine protected against systemic viral dissemination in surviving animals. I began to investigate the correlates of vaccine protection, where I was able to identify the presence of high titer IgG antibody in surviving animals along with the presence of neutralizing antibodies, suggesting these may both play a role in protection. Additional studies to evaluate correlates of vaccine protection will be important moving forward, specifically ones which attempt to confirm the importance of antibodies in protection. Studies in NHP models will also be important for determining the role of cell-mediated immunity in protection. Through this work I was also able to demonstrate the potential importance of antibody avidity in JUNV protection, a finding that could help to inform research on JUNV monoclonal antibody-based therapeutics. With the long-term objective of advancing rVSVΔG-JUNVGP as a candidate vaccine for possible FDA licensure, it will be essential to evaluate its safety and efficacy in an NHP model of JUNV infection in the future.

The second objective of my dissertation was to use rVSVΔG-JUNVGP to address a public health need in the JUNV endemic area, *i.e.* rapid serologic detection of JUNV neutralizing antibodies. On a personal note, I had the great fortune and opportunity to visit INEVH during the course of my graduate studies and my second dissertation objective was a direct inspiration from discussions and interactions with people on the ground, combatting JUNV infection in real-time, at INEVH. I was able to show that rVSVΔG-JUVGP could be used for accurate and rapid detection of JUNV neutralizing antibodies in both guinea pig plasma and human Candid #1 vaccinee serum. Importantly, rVSVΔG-JUVGP generated results 5 days sooner than the traditional PRNT assays utilized by INEVH, and although this difference would not affect the outcome of an individual acute

human case, it has larger public health implications, *i.e.*, a more rapid confirmation of JUNV exposures can generate a more rapid response in order to contact other at-risk persons for monitoring and/or vaccination. Overall, I have been able to show that this tool merits further evaluation for use in JUNV serologic detection and diagnosis. Future studies will be essential in order to evaluate its potential for use within the endemic area and to specifically examine its ability to screen for neutralizing antibodies generated by a wide variety of wild type JUNV stains. Studies would also need to be performed to ensure that the assay performs with the same sensitivity and specificity as current methods in the endemic area. Ultimately, with advancement through additional research, I envision this tool being employed as a replacement for current methods to provide more rapid serologic confirmation of JUNV infection in the endemic area.

The last aim of this dissertation explored the beginning stages of developing chimeric arenavirus glycoproteins for future use as antigens in a cross-protective arenavirus vaccine. As our world continues to become more interconnected it will be essential to generate vaccines which can protect people from multiple pathogens simultaneously. I was able to generate a panel of 7 chimeric GPs with epitopes to four highly pathogenic arenaviruses, and demonstrate that they were all functional, indicating that they may be promising antigens for use in a rVSV-based cross-protective arenavirus vaccine. Further studies would need to be performed to evaluate the ability of the selected epitopes to generate protective immune responses against each arenavirus. Evaluating the ability of polyclonal arenavirus antibody to neutralize rVSV-chimeric GP pesudotypes may be an important next step, where the pseudotypes cross-neutralized most effectively by each set of virus-specific antibodies would be advanced and cloned into the rVSV system. These constructs would then be evaluated in a small animal model to assess their protective efficacy against lethal challenge with each arenavirus. Ultimately, long-term success would be defined as developing one or more chimeric antigen into a cross-protective arenavirus vaccine candidate for evaluation in an NHP model.

As our world continues to evolve in the direction of advancing technology, human expansion, and climate change, so must our response to the emerging infectious diseases that will undoubtedly impact our world in the coming decades. The tools that I have developed here move the field forward in terms of arenavirus and JUNV-specific countermeasures that can be used from a biodefense and public health standpoint.

Appendix A Supplemental Data

CHAPTER 2 SUPPLEMENTAL DATA

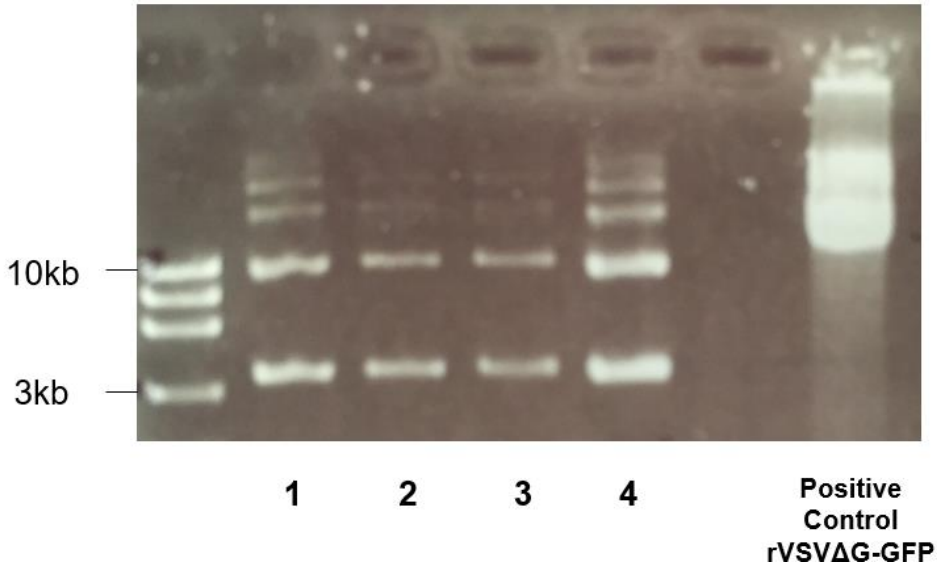

Appendix A-1. Truncated rVSVΔG-JUNVGPC plasmid DNA isolated from *E. coli* C600 bacteria. rVSVΔG vector and JUNV GPC insert fragments were ligated and transformed into *E. coli* strain C600 bacteria. PCR screening of bacterial colonies for the expected rVSVΔG-JUNVGPC plasmid yielded negative results. The DNA isolated from PCR-negative bacterial colonies was evaluated using 0.8% agarose gel stained with ethidium bromide (10mg/ml). Lanes 1-4 represent separate bacterial colonies. A rVSVΔG-GFP plasmid was run as a positive control for size comparison and shows that the recovered plasmid DNA is a smaller (possibly truncated rVSVΔG-JUNVGPC) plasmid.

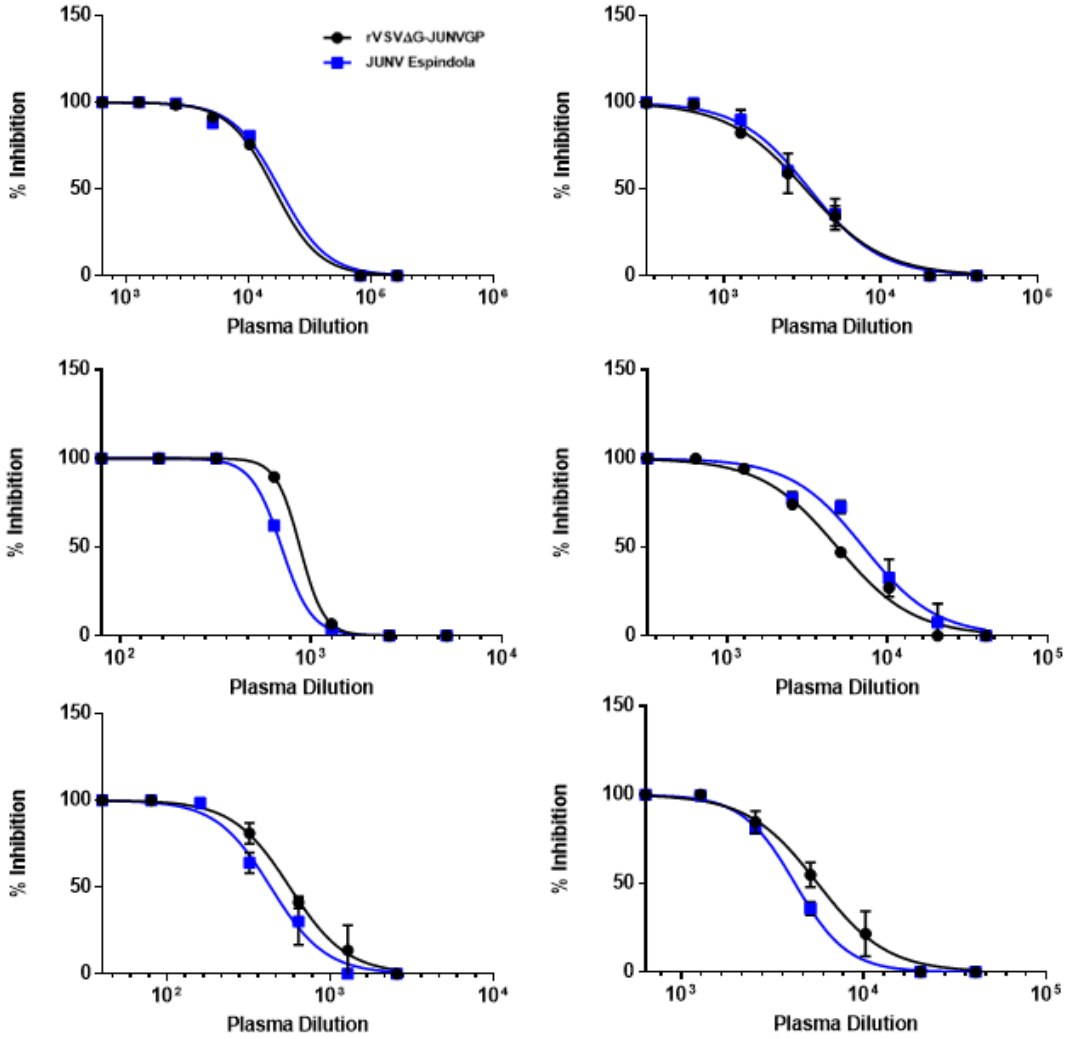

Appendix A-2. Detection of JUNV neutralizing antibodies from rVSVΔG-JUNVGP vaccinated guinea pig plasma. Eighteen guinea pig plasma samples were evaluated for their ability to neutralize either JUNV Espindola or rVSVΔG-JUNVGP. GraphPad Prism 7.03 was utilized to generate dose-response curves. Each graph depicts data from a single animal/plasma sample. See Figure 3-2 for additional graphs/data.

References

1. Le Duc JW, Sorvillo TE. A Quarter Century of Emerging Infectious Diseases - Where Have We Been and Where Are We Going? Acta Med Acad **2018**; 47:117-30.

2. Health CoEMTt. Emerging Infections: Microbial Threats to Health in the United States. United States: National Academies Press, **1992**.

3. Salas R, de Manzione N, Tesh RB, et al. Venezuelan haemorrhagic fever. Lancet **1991**; 338:1033-6.

4. Tesh RB, Jahrling PB, Salas R, Shope RE. Description of Guanarito virus (Arenaviridae: Arenavirus), the etiologic agent of Venezuelan hemorrhagic fever. Am J Trop Med Hyg **1994**; 50:452-9.

5. Organization PAHOWH. Epidemiological Alert: Hemorrhagic fever due to Arenavirus in Bolivia. Washington D.C.: PAHO / WHO, **2019**.

6. Chevalier MS, Chung W, Smith J, et al. Ebola virus disease cluster in the United States--Dallas County, Texas, 2014. MMWR Morb Mortal Wkly Rep **2014**; 63:1087-8.

7. Amorosa V, MacNeil A, McConnell R, et al. Imported Lassa fever, Pennsylvania, USA, 2010. Emerg Infect Dis **2010**; 16:1598-600.

8. Holmes GP, McCormick JB, Trock SC, et al. Lassa fever in the United States. Investigation of a case and new guidelines for management. N Engl J Med **1990**; 323:1120-3.

9. Kofman A, Choi MJ, Rollin PE. Lassa Fever in Travelers from West Africa, 1969-2016. Emerg Infect Dis **2019**; 25:245-8.

10. Ufberg JW, Karras DJ. Update on emerging infections: news from the Centers for Disease Control and Prevention. Imported Lassa fever--New Jersey, 2004. Ann Emerg Med **2005**; 45:323-6.

11. Blaine JW. Establishing a national biological laboratory safety and security monitoring program. Biosecur Bioterror **2012**; 10:396-400.

12. Ambrosio A, Saavedra M, Mariani M, Gamboa G, Maiza A. Argentine hemorrhagic fever vaccines. Hum Vaccin **2011**; 7:694-700.

13. Briggiler A, Sinchi A, Coronel F, et al. [New transmission scenarios of the Argentine hemorrhagic fever since the introduction of the live attenuated junin virus vaccine (Candid #1): an experience in migrant workers]. Rev Peru Med Exp Salud Publica **2015**; 32:165-71.

14. Maes P, Alkhovsky SV, Bào Y, et al. Taxonomy of the family Arenaviridae and the order Bunyavirales: update 2018. Arch Virol **2018**; 163:2295-310.

15. Wolff H, Lange JV, Webb PA. Interrelationships among arenaviruses measured by indirect immunofluorescence. Intervirology **1978**; 9:344-50.

16. Briese T, Paweska JT, McMullan LK, et al. Genetic detection and characterization of Lujo virus, a new hemorrhagic fever-associated arenavirus from southern Africa. PLoS Pathog **2009**; 5:e1000455.

17. Oldstone MB, Ahmed R, Byrne J, Buchmeier MJ, Riviere Y, Southern P. Virus and immune responses: lymphocytic choriomeningitis virus as a prototype model of viral pathogenesis. Br Med Bull **1985**; 41:70-4.

18. Hallam SJ, Koma T, Maruyama J, Paessler S. Review of. Front Microbiol **2018**; 9:1751.

19. Bruns M, Martínez Peralta L, Lehmann-Grube F. Lymphocytic choriomeningitis virus. III. Structural proteins of the virion. J Gen Virol **1983**; 64 Pt 3:599-611.

20. Southern PJ, Singh MK, Riviere Y, Jacoby DR, Buchmeier MJ, Oldstone MB. Molecular characterization of the genomic S RNA segment from lymphocytic choriomeningitis virus. Virology **1987**; 157:145-55.

21. Auperin DD, Romanowski V, Galinski M, Bishop DH. Sequencing studies of pichinde arenavirus S RNA indicate a novel coding strategy, an ambisense viral S RNA. J Virol **1984**; 52:897-904.

22. Rojek JM, Sanchez AB, Nguyen NT, de la Torre JC, Kunz S. Different mechanisms of cell entry by human-pathogenic Old World and New World arenaviruses. J Virol **2008**; 82:7677-87.

23. Eschli B, Quirin K, Wepf A, Weber J, Zinkernagel R, Hengartner H. Identification of an N-terminal trimeric coiled-coil core within arenavirus glycoprotein 2 permits assignment to class I viral fusion proteins. J Virol **2006**; 80:5897-907.

24. York J, Nunberg JH. Role of the stable signal peptide of Junín arenavirus envelope glycoprotein in pH-dependent membrane fusion. J Virol **2006**; 80:7775-80.

25. Cao W, Henry MD, Borrow P, et al. Identification of alpha-dystroglycan as a receptor for lymphocytic choriomeningitis virus and Lassa fever virus. Science **1998**; 282:2079-81.

26. Radoshitzky SR, Abraham J, Spiropoulou CF, et al. Transferrin receptor 1 is a cellular receptor for New World haemorrhagic fever arenaviruses. Nature **2007**; 446:92-6.

27. Fuller-Pace FV, Southern PJ. Temporal analysis of transcription and replication during acute infection with lymphocytic choriomeningitis virus. Virology **1988**; 162:260-3.

28. Pinschewer DD, Perez M, de la Torre JC. Role of the virus nucleoprotein in the regulation of lymphocytic choriomeningitis virus transcription and RNA replication. J Virol **2003**; 77:3882-7.

29. Lenz O, ter Meulen J, Klenk HD, Seidah NG, Garten W. The Lassa virus glycoprotein precursor GP-C is proteolytically processed by subtilase SKI-1/S1P. Proc Natl Acad Sci U S A **2001**; 98:12701-5.

30. Cordo SM, Valko A, Martinez GM, Candurra NA. Membrane localization of Junín virus glycoproteins requires cholesterol and cholesterol rich membranes. Biochem Biophys Res Commun **2013**; 430:912-7.

31. Wilda M, Lopez N, Casabona JC, Franze-Fernandez MT. Mapping of the tacaribe arenavirus Z-protein binding sites on the L protein identified both amino acids within the putative polymerase domain and a region at the N terminus of L that are critically involved in binding. J Virol **2008**; 82:11454-60.

32. Enria DA, Barrera Oro JG. Junin virus vaccines. Curr Top Microbiol Immunol **2002**; 263:239-61.

33. Enria DA, Briggiler AM, Sánchez Z. Treatment of Argentine hemorrhagic fever. Antiviral Res **2008**; 78:132-9.

34. Maiztegui J, Feuillade M, Briggiler A. Progressive extension of the endemic area and changing incidence of Argentine Hemorrhagic Fever. Med Microbiol Immunol **1986**; 175:149-52.

35. Arribalzaga RA. Una nueva enfermedad epide´mica a germen desconocido: hipertermia nefroto´xica, leucope´nica y enantematica. . Vol. 27: Dia. Med., **1955**:1204-10.

36. Parodi AS, Greenway DJ, Rugiero HR, et al. Sobre la etiologıca del brote epidemico en Junın. Vol. 30: Dia Med, **1958**:2300-2.

37. Weissenbacher MC, Sabattini MS, Avila MM, et al. Junin virus activity in two rural populations of the Argentine hemorrhagic fever (AHF) endemic area. J Med Virol **1983**; 12:273-80.

38. Enria DA, Briggiler AM, Feuillade MR. An overview of the epidemiological, ecological, and preventive hallmarks of Argentine haemorrhagic fever (Junin virus). Bull Inst Pasteur **1998**; 96:103-14.

39. Mills JN, Ellis BA, McKee KT, et al. A longitudinal study of Junin virus activity in the rodent reservoir of Argentine hemorrhagic fever. Am J Trop Med Hyg **1992**; 47:749-63.

40. Mills JN, Ellis BA, Childs JE, et al. Prevalence of infection with Junin virus in rodent populations in the epidemic area of Argentine hemorrhagic fever. Am J Trop Med Hyg **1994**; 51:554-62.

41. Castillo E, Priotto J, Ambrosio AM, et al. Commensal and wild rodents in an urban area of Argentina. International Biodeterioration & Biodegredation **2003**; 52:135-41.

42. Kenyon RH, Green DE, Maiztegui JI, Peters CJ. Viral strain dependent differences in experimental Argentine hemorrhagic fever (Junin virus) infection of guinea pigs. Intervirology **1988**; 29:133-43.

43. Kenyon RH, McKee KT, Maiztegui JI, Green DE, Peters CJ. Heterogeneity of Junin virus strains. Med Microbiol Immunol **1986**; 175:169-72.

44. McKee KT, Mahlandt BG, Maiztegui JI, Green DE, Peters CJ. Virus-specific factors in experimental Argentine hemorrhagic fever in rhesus macaques. J Med Virol **1987**; 22:99-111.

45. González PH, Cossio PM, Arana R, Maiztegui JI, Laguens RP. Lymphatic tissue in Argentine hemorrhagic fever. Pathologic features. Arch Pathol Lab Med **1980**; 104:250-4.

46. Elsner B, Schwarz E, Mando OG, Maiztegui J, Vilches A. Pathology of 12 fatal cases of Argentine hemorrhagic fever. Am J Trop Med Hyg **1973**; 22:229-36.

47. Peters CJ, Liu CT, Anderson GW, Morrill JC, Jahrling PB. Pathogenesis of viral hemorrhagic fevers: Rift Valley fever and Lassa fever contrasted. Rev Infect Dis **1989**; 11 Suppl 4:S743-9.

48. Sundberg E, Hultdin J, Nilsson S, Ahlm C. Evidence of disseminated intravascular coagulation in a hemorrhagic fever with renal syndrome-scoring models and severe illness. PLoS One **2011**; 6:e21134.

49. Geisbert TW, Young HA, Jahrling PB, Davis KJ, Kagan E, Hensley LE. Mechanisms underlying coagulation abnormalities in ebola hemorrhagic fever: overexpression of tissue factor in primate monocytes/macrophages is a key event. J Infect Dis **2003**; 188:1618-29.

50. Levi M, Toh CH, Thachil J, Watson HG. Guidelines for the diagnosis and management of disseminated intravascular coagulation. British Committee for Standards in Haematology. Br J Haematol **2009**; 145:24-33.

51. Molinas FC, de Bracco MM, Maiztegui JI. Hemostasis and the complement system in Argentine hemorrhagic fever. Rev Infect Dis **1989**; 11 Suppl 4:S762-70.

52. Heller MV, Marta RF, Sturk A, et al. Early markers of blood coagulation and fibrinolysis activation in Argentine hemorrhagic fever. Thromb Haemost **1995**; 73:368-73.

53. Marta RF, Enria D, Molinas FC. Relationship between hematopoietic growth factors levels and hematological parameters in Argentine hemorrhagic fever. Am J Hematol **2000**; 64:1-6.

54. Gomez RM, Pozner RG, Lazzari MA, et al. Endothelial cell function alteration after Junin virus infection. Thromb Haemost **2003**; 90:326-33.

55. Andrews BS, Theofilopoulos AN, Peters CJ, Loskutoff DJ, Brandt WE, Dixon FJ. Replication of dengue and junin viruses in cultured rabbit and human endothelial cells. Infect Immun **1978**; 20:776-81.

56. Clark PR, Manes TD, Pober JS, Kluger MS. Increased ICAM-1 expression causes endothelial cell leakiness, cytoskeletal reorganization and junctional alterations. J Invest Dermatol **2007**; 127:762-74.

57. Durán WN, Breslin JW, Sánchez FA. The NO cascade, eNOS location, and microvascular permeability. Cardiovasc Res **2010**; 87:254-61.

58. Lander HM, Grant AM, Albrecht T, Hill T, Peters CJ. Endothelial cell permeability and adherens junction disruption induced by junín virus infection. Am J Trop Med Hyg **2014**; 90:993-1002.

59. Maruo N, Morita I, Shirao M, Murota S. IL-6 increases endothelial permeability in vitro. Endocrinology **1992**; 131:710-4.

60. Lee YR, Liu MT, Lei HY, et al. MCP-1, a highly expressed chemokine in dengue haemorrhagic fever/dengue shock syndrome patients, may cause permeability change, possibly through reduced tight junctions of vascular endothelium cells. J Gen Virol **2006**; 87:3623-30.

61. Angulo J, Martínez-Valdebenito C, Marco C, et al. Serum levels of interleukin-6 are linked to the severity of the disease caused by Andes Virus. PLoS Negl Trop Dis **2017**; 11:e0005757.

62. Masood KI, Jamil B, Rahim M, Islam M, Farhan M, Hasan Z. Role of TNF α, IL-6 and CXCL10 in Dengue disease severity. Iran J Microbiol **2018**; 10:202-7.

63. Fan L, Briese T, Lipkin WI. Z proteins of New World arenaviruses bind RIG-I and interfere with type I interferon induction. J Virol **2010**; 84:1785-91.

64. Martínez-Sobrido L, Giannakas P, Cubitt B, García-Sastre A, de la Torre JC. Differential inhibition of type I interferon induction by arenavirus nucleoproteins. J Virol **2007**; 81:12696-703.

65. Levis SC, Saavedra MC, Ceccoli C, et al. Endogenous interferon in Argentine hemorrhagic fever. J Infect Dis **1984**; 149:428-33.

66. Levis SC, Saavedra MC, Ceccoli C, et al. Correlation between endogenous interferon and the clinical evolution of patients with Argentine hemorrhagic fever. J Interferon Res **1985**; 5:383-9.

67. Marta RF, Montero VS, Hack CE, Sturk A, Maiztegui JI, Molinas FC. Proinflammatory cytokines and elastase-alpha-1-antitrypsin in Argentine hemorrhagic fever. Am J Trop Med Hyg **1999**; 60:85-9.

68. Groseth A, Hoenen T, Weber M, et al. Tacaribe virus but not junin virus infection induces cytokine release from primary human monocytes and macrophages. PLoS Negl Trop Dis **2011**; 5:e1137.

69. Huang C, Kolokoltsova OA, Yun NE, et al. Highly Pathogenic New World and Old World Human Arenaviruses Induce Distinct Interferon Responses in Human Cells. J Virol **2015**; 89:7079-88.

70. Negrotto S, Mena HA, Ure AE, et al. Human Plasmacytoid Dendritic Cells Elicited Different Responses after Infection with Pathogenic and Nonpathogenic Junin Virus Strains. J Virol **2015**; 89:7409-13.

71. Huang C, Kolokoltsova OA, Yun NE, et al. Junín virus infection activates the type I interferon pathway in a RIG-I-dependent manner. PLoS Negl Trop Dis **2012**; 6:e1659.

72. Moreno H, Möller R, Fedeli C, Gerold G, Kunz S. Comparison of the Innate Immune Responses to Pathogenic and Nonpathogenic Clade B New World Arenaviruses. J Virol **2019**; 93.

73. Flatz L, Rieger T, Merkler D, et al. T cell-dependence of Lassa fever pathogenesis. PLoS Pathog **2010**; 6:e1000836.

74. Enria DA, Maiztegui JI. Antiviral treatment of Argentine hemorrhagic fever. Antiviral Res **1994**; 23:23-31.

75. Maiztegui JI, Fernandez NJ, de Damilano AJ. Efficacy of immune plasma in treatment of Argentine haemorrhagic fever and association between treatment and a late neurological syndrome. Lancet **1979**; 2:1216-7.

76. Enria DA, Briggiler AM, Fernandez NJ, Levis SC, Maiztegui JI. Importance of dose of neutralising antibodies in treatment of Argentine haemorrhagic fever with immune plasma. Lancet **1984**; 2:255-6.

77. Sanchez A, Pifat DY, Kenyon RH, Peters CJ, McCormick JB, Kiley MP. Junin virus monoclonal antibodies: characterization and cross-reactivity with other arenaviruses. J Gen Virol **1989**; 70 (Pt 5):1125-32.

78. Golden JW, Maes P, Kwilas SA, Ballantyne J, Hooper JW. Glycoprotein-Specific Antibodies Produced by DNA Vaccination Protect Guinea Pigs from Lethal Argentine and Venezuelan Hemorrhagic Fever. J Virol **2016**; 90:3515-29.

79. Brouillette RB, Phillips EK, Ayithan N, Maury W. Differences in Glycoprotein Complex Receptor Binding Site Accessibility Prompt Poor Cross-Reactivity of Neutralizing Antibodies between Closely Related Arenaviruses. J Virol **2017**; 91.

80. Mahmutovic S, Clark L, Levis SC, et al. Molecular Basis for Antibody-Mediated Neutralization of New World Hemorrhagic Fever Mammarenaviruses. Cell Host Microbe **2015**; 18:705-13.

81. Clark LE, Mahmutovic S, Raymond DD, et al. Vaccine-elicited receptor-binding site antibodies neutralize two New World hemorrhagic fever arenaviruses. Nat Commun **2018**; 9:1884.

82. Zeltina A, Krumm SA, Sahin M, et al. Convergent immunological solutions to Argentine hemorrhagic fever virus neutralization. Proc Natl Acad Sci U S A **2017**; 114:7031-6.

83. Linero F, Sepúlveda C, Christopoulou I, Hulpiau P, Scolaro L, Saelens X. Neutralization of Junín virus by single domain antibodies targeted against the nucleoprotein. Sci Rep **2018**; 8:11451.

84. Kenyon RH, Condie RM, Jahrling PB, Peters CJ. Protection of guinea pigs against experimental Argentine hemorrhagic fever by purified human IgG: importance of elimination of infected cells. Microb Pathog **1990**; 9:219-26.

85. del Carmen Saavedra M, Sottosanti JM, Riera L, Ambrosio AM. IgG subclasses in human immune response to wild and attenuated (vaccine) Junin virus infection. J Med Virol **2003**; 69:447-50.

86. Weissenbacher MC, de Guerrero LB, Boxaca MC. Experimental biology and pathogenesis of Junin virus infection in animals and man. Bull World Health Organ **1975**; 52:507-15.

87. Campetella OE, Galassi NV, Sanjuan N, Barrios HA. Susceptible adult murine model for Junin virus. J Med Virol **1988**; 26:443-51.

88. Giovanniello OA, Nejamkis MR, Galassi NV, Nota NR. Immunosuppression in experimental Junin virus infection of mice. Intervirology **1980**; 13:122-5.

89. Yun NE, Linde NS, Dziuba N, et al. Pathogenesis of XJ and Romero strains of Junin virus in two strains of guinea pigs. Am J Trop Med Hyg **2008**; 79:275-82.

90. Zeitlin L, Geisbert JB, Deer DJ, et al. Monoclonal antibody therapy for Junin virus infection. Proc Natl Acad Sci U S A **2016**; 113:4458-63.

91. Emonet SF, Seregin AV, Yun NE, et al. Rescue from cloned cDNAs and in vivo characterization of recombinant pathogenic Romero and live-attenuated Candid #1 strains of Junin virus, the causative agent of Argentine hemorrhagic fever disease. J Virol **2011**; 85:1473-83.

92. McKee KT, Oro JG, Kuehne AI, Spisso JA, Mahlandt BG. Candid No. 1 Argentine hemorrhagic fever vaccine protects against lethal Junin virus challenge in rhesus macaques. Intervirology **1992**; 34:154-63.

93. Avila MM, Samoilovich SR, Laguens RP, Merani MS, Weissenbacher MC. Protection of Junín virus-infected marmosets by passive administration of immune serum: association with late neurologic signs. J Med Virol **1987**; 21:67-74.

94. Samoilovich SR, Calello MA, Laguens RP, Weissenbacher MC. Long-term protection against Argentine hemorrhagic fever in Tacaribe virus infected marmosets: virologic and histopathologic findings. J Med Virol **1988**; 24:229-36.

95. Weissenbacher MC, Calello MA, Colillas OJ, Rondinone SN, Frigerio MJ. Argentine hemorrhagic fever: a primate model. Intervirology **1979**; 11:363-5.

96. Weissenbacher MC, Coto CE, Calello MA, Rondinone SN, Damonte EB, Frigerio MJ. Cross-protection in nonhuman primates against Argentine hemorrhagic fever. Infect Immun **1982**; 35:425-30.

97. González PH, Laguens RP, Frigerio MJ, Calello MA, Weissenbacher MC. Junin virus infection of Callithrix jacchus: pathologic features. Am J Trop Med Hyg **1983**; 32:417-23.

98. Green DE, Mahlandt BG, McKee KT. Experimental Argentine hemorrhagic fever in rhesus macaques: virus-specific variations in pathology. J Med Virol **1987**; 22:113-33.

99. McKee KT, Mahlandt BG, Maiztegui JI, Eddy GA, Peters CJ. Experimental Argentine hemorrhagic fever in rhesus macaques: viral strain-dependent clinical response. J Infect Dis **1985**; 152:218-21.

100. Kenyon RH, McKee KT, Zack PM, et al. Aerosol infection of rhesus macaques with Junin virus. Intervirology **1992**; 33:23-31.

101. Daddario-DiCaprio KM, Geisbert TW, Ströher U, et al. Postexposure protection against Marburg haemorrhagic fever with recombinant vesicular stomatitis virus vectors in non-human primates: an efficacy assessment. Lancet **2006**; 367:1399-404.

102. McKee KT, Oro JG, Kuehne AI, Spisso JA, Mahlandt BG. Safety and immunogenicity of a live-attenuated Junin (Argentine hemorrhagic fever) vaccine in rhesus macaques. Am J Trop Med Hyg **1993**; 48:403-11.

103. Weissenbacher MC, Calello MA, Merani MS, McCormick JB, Rodriguez M. Therapeutic effect of the antiviral agent ribavirin in Junín virus infection of primates. J Med Virol **1986**; 20:261-7.

104. Enria DA, Briggiler AM, Levis S, Vallejos D, Maiztegui JI, Canonico PG. Tolerance and antiviral effect of ribavirin in patients with Argentine hemorrhagic fever. Antiviral Res **1987**; 7:353-9.

105. McKee KT, Huggins JW, Trahan CJ, Mahlandt BG. Ribavirin prophylaxis and therapy for experimental argentine hemorrhagic fever. Antimicrob Agents Chemother **1988**; 32:1304-9.

106. Gowen BB, Juelich TL, Sefing EJ, et al. Favipiravir (T-705) inhibits Junín virus infection and reduces mortality in a guinea pig model of Argentine hemorrhagic fever. PLoS Negl Trop Dis **2013**; 7:e2614.

107. Artuso MC, Ellenberg PC, Scolaro LA, Damonte EB, García CC. Inhibition of Junín virus replication by small interfering RNAs. Antiviral Res **2009**; 84:31-7.

108. Albariño CG, Bird BH, Chakrabarti AK, et al. The major determinant of attenuation in mice of the Candid1 vaccine for Argentine hemorrhagic fever is located in the G2 glycoprotein transmembrane domain. J Virol **2011**; 85:10404-8.

109. Rodriguez SE, Cross RW, Fenton KA, Bente DA, Mire CE, Geisbert TW. Vesicular Stomatitis Virus-Based Vaccine Protects Mice against Crimean-Congo Hemorrhagic Fever. Sci Rep **2019**; 9:7755.

110. Mire CE, Geisbert JB, Versteeg KM, et al. A Single-Vector, Single-Injection Trivalent Filovirus Vaccine: Proof of Concept Study in Outbred Guinea Pigs. J Infect Dis **2015**; 212 Suppl 2:S384-8.

111. Henao-Restrepo AM, Camacho A, Longini IM, et al. Efficacy and effectiveness of an rVSV-vectored vaccine in preventing Ebola virus disease: final results from the Guinea ring vaccination, open-label, cluster-randomised trial (Ebola Ça Suffit!). Lancet **2017**; 389:505-18.

112. Brown KS, Safronetz D, Marzi A, Ebihara H, Feldmann H. Vesicular stomatitis virus-based vaccine protects hamsters against lethal challenge with Andes virus. J Virol **2011**; 85:12781-91.

113. Geisbert TW, Jones S, Fritz EA, et al. Development of a new vaccine for the prevention of Lassa fever. PLoS Med **2005**; 2:e183.

114. Stein DR, Warner BM, Soule G, et al. A recombinant vesicular stomatitis-based Lassa fever vaccine elicits rapid and long-term protection from lethal Lassa virus infection in guinea pigs. NPJ Vaccines **2019**; 4:8.

115. BRANDLY CA, HANSON RP. Epizootiology of vesicular stomatitis. Am J Public Health Nations Health **1957**; 47:205-9.

116. Geisbert TW, Feldmann H. Recombinant vesicular stomatitis virus-based vaccines against Ebola and Marburg virus infections. J Infect Dis **2011**; 204 Suppl 3:S1075-81.

117. Hanson RP, Estupiñan J, Castañeda J. Vesicular stomatitis in the Americas. Bull Off Int Epizoot **1968**; 70:37-47.

118. Geisbert TW, Hensley LE, Geisbert JB, et al. Postexposure treatment of Marburg virus infection. Emerg Infect Dis **2010**; 16:1119-22.

119. Geisbert TW, Daddario-DiCaprio KM, Williams KJ, et al. Recombinant vesicular stomatitis virus vector mediates postexposure protection against Sudan Ebola hemorrhagic fever in nonhuman primates. J Virol **2008**; 82:5664-8.

120. Geisbert TW, Daddario-Dicaprio KM, Lewis MG, et al. Vesicular stomatitis virus-based ebola vaccine is well-tolerated and protects immunocompromised nonhuman primates. PLoS Pathog **2008**; 4:e1000225.

121. Lévy Y, Lane C, Piot P, et al. Prevention of Ebola virus disease through vaccination: where we are in 2018. Lancet **2018**; 392:787-90.

122. Mire CE, Geisbert JB, Agans KN, et al. Durability of a vesicular stomatitis virus-based marburg virus vaccine in nonhuman primates. PLoS One **2014**; 9:e94355.

123. Wong G, Audet J, Fernando L, et al. Immunization with vesicular stomatitis virus vaccine expressing the Ebola glycoprotein provides sustained long-term protection in rodents. Vaccine **2014**; 32:5722-9.

124. Huttner A, Agnandji ST, Combescure C, et al. Determinants of antibody persistence across doses and continents after single-dose rVSV-ZEBOV vaccination for Ebola virus disease: an observational cohort study. Lancet Infect Dis **2018**; 18:738-48.

125. Huttner A, Siegrist CA. Durability of single-dose rVSV-ZEBOV vaccine responses: what do we know? Expert Rev Vaccines **2018**; 17:1105-10.

126. Schnell MJ, Buonocore L, Kretzschmar E, Johnson E, Rose JK. Foreign glycoproteins expressed from recombinant vesicular stomatitis viruses are incorporated efficiently into virus particles. Proc Natl Acad Sci U S A **1996**; 93:11359-65.

127. Lawson ND, Stillman EA, Whitt MA, Rose JK. Recombinant vesicular stomatitis viruses from DNA. Proc Natl Acad Sci U S A **1995**; 92:4477-81.

128. Barrera Oro JG, McKee KT, Spisso J, Mahlandt BG, Maiztegui JI. A refined complement-enhanced neutralization test for detecting antibodies to Junin virus. J Virol Methods **1990**; 29:71-80.

129. Aguilera A, Gómez-González B. Genome instability: a mechanistic view of its causes and consequences. Nat Rev Genet **2008**; 9:204-17.

130. Weissenbacher MC, Lascano EF, Avila MM, Berría MI. Chronic neurologic disease in Junín virus-infected rats. J Med Virol **1986**; 20:57-65.

131. Marzi A, Engelmann F, Feldmann F, et al. Antibodies are necessary for rVSV/ZEBOV-GP-mediated protection against lethal Ebola virus challenge in nonhuman primates. Proc Natl Acad Sci U S A **2013**; 110:1893-8.

132. Leske A, Waßmann I, Schnepel K, et al. Assessing cross-reactivity of Junín virus-directed neutralizing antibodies. Antiviral Res **2019**; 163:106-16.

133. García Franco S, Ambrosio AM, Feuillade MR, Maiztegui JI. Evaluation of an enzyme-linked immunosorbent assay for quantitation of antibodies to Junin virus in human sera. J Virol Methods **1988**; 19:299-305.

134. Riera LM, Feuillade MR, Saavedra MC, Ambrosio AM. Evaluation of an enzyme immunosorbent assay for the diagnosis of Argentine haemorrhagic fever. Acta Virol **1997**; 41:305-10.

135. Turner PV, Brabb T, Pekow C, Vasbinder MA. Administration of substances to laboratory animals: routes of administration and factors to consider. J Am Assoc Lab Anim Sci **2011**; 50:600-13.

136. Siegrist C. Vaccine Immunology. In: **Stanley A. Plotkin WAOaPAOt**, ed. Vaccines. 6th ed: Elsevier Inc., **2013**:14-32.

137. Weissenbacher MC, Coto CE, Calello MA. Cross-protection between Tacaribe complex viruses. Presence of neutralizing antibodies against Junin virus (Argentine hemorrhagic fever) in guinea pigs infected with Tacaribe virus. Intervirology **1975**; 6:42-9.

138. López N, Scolaro L, Rossi C, et al. Homologous and heterologous glycoproteins induce protection against Junin virus challenge in guinea pigs. J Gen Virol **2000**; 81:1273-81.

139. Gautam A, Park BK, Kim TH, et al. Peritoneal Cells Mediate Immune Responses and Cross-Protection Against Influenza A Virus. Front Immunol **2019**; 10:1160.

140. DeMeio JL. Effect of the route of inoculation on antibody formation in guinea pigs immunized with parinfluenza virus vaccines. Appl Microbiol **1968**; 16:1207-10.

141. Charrel RN, de Lamballerie X. Arenaviruses other than Lassa virus. Antiviral Res **2003**; 57:89-100.

142. Lascano EF, Berria MI, Candurra NA. Diagnosis of Junin virus in cell cultures by immunoperoxidase staining. Arch Virol **1981**; 70:79-82.

143. Lozano ME, Ghiringhelli PD, Romanowski V, Grau O. A simple nucleic acid amplification assay for the rapid detection of Junín virus in whole blood samples. Virus Res **1993**; 27:37-53.

144. Lozano ME, Enría D, Maiztegui JI, Grau O, Romanowski V. Rapid diagnosis of Argentine hemorrhagic fever by reverse transcriptase PCR-based assay. J Clin Microbiol **1995**; 33:1327-32.

145. Ambrosio AM, Feuillade MR, Gamboa GS, Maiztegui JI. Prevalence of lymphocytic choriomeningitis virus infection in a human population of Argentina. Am J Trop Med Hyg **1994**; 50:381-6.

146. Barrera Oro JG, Greza ME, Zannoli VH, Garcia CA. Anticuerpos contra virus Junin y LCM en casos presuntivos de Fiebre hemorrhagica Argentina. Vol. 37. Buenos Aires: Medicina, **1977**:69-77.

147. Barrera Oro JG, al. e. Evidencias serologicas preliminares de la actividad de un "arenavirus" relacionado con el de la coriomeningitis linfocitica (LCM) en presuntos enfermos de Fiebre hemorrhagica Argentina (FHA). Rev Asoc Argent Microbiol **1970**; 2:185.

148. Iha K. Pseudotyped vesicular stomatitis virus for analysis of entry of arenaviruses and its application to serodiagnosis of Argentine hemorrhagic fever. PhD Dissertation. Tokyo, Japan: University of Tokyo, **2013**.

149. Seregin AV, Yun NE, Miller M, et al. The glycoprotein precursor gene of Junin virus determines the virulence of the Romero strain and the attenuation of the Candid #1 strain in a representative animal model of Argentine hemorrhagic fever. J Virol **2015**; 89:5949-56.

150. Stephan BI, Lozano ME, Goñi SE. Watching every step of the way: junín virus attenuation markers in the vaccine lineage. Curr Genomics **2013**; 14:415-24.

151. García JB, Morzunov SP, Levis S, et al. Genetic diversity of the Junin virus in Argentina: geographic and temporal patterns. Virology **2000**; 272:127-36.

152. Goñi SE, Stephan BI, Iserte JA, Contigiani MS, Lozano ME, Tenorio A. Viral diversity of Junín virus field strains. Virus Res **2011**; 160:150-8.

153. Olschläger S, Flatz L. Vaccination strategies against highly pathogenic arenaviruses: the next steps toward clinical trials. PLoS Pathog **2013**; 9:e1003212.

154. Patterson M, Grant A, Paessler S. Epidemiology and pathogenesis of Bolivian hemorrhagic fever. Curr Opin Virol **2014**; 5:82-90.

155. Marzi A, Feldmann F, Geisbert TW, Feldmann H, Safronetz D. Vesicular stomatitis virus-based vaccines against Lassa and Ebola viruses. Emerg Infect Dis **2015**; 21:305-7.

156. Albariño CG, Bird BH, Chakrabarti AK, et al. Reverse genetics generation of chimeric infectious Junin/Lassa virus is dependent on interaction of homologous glycoprotein stable signal peptide and G2 cytoplasmic domains. J Virol **2011**; 85:112-22.

157. Martin VK, Droniou-Bonzom ME, Reignier T, Oldenburg JE, Cox AU, Cannon PM. Investigation of clade B New World arenavirus tropism by using chimeric GP1 proteins. J Virol **2010**; 84:1176-82.

158. Bell TM, Bunton TE, Shaia CI, et al. Pathogenesis of Bolivian Hemorrhagic Fever in Guinea Pigs. Vet Pathol **2016**; 53:190-9.

159. Hall WC, Geisbert TW, Huggins JW, Jahrling PB. Experimental infection of guinea pigs with Venezuelan hemorrhagic fever virus (Guanarito): a model of human disease. Am J Trop Med Hyg **1996**; 55:81-8.

160. Jahrling PB. Protection of Lassa virus-infected guinea pigs with Lassa-immune plasma of guinea pig, primate, and human origin. J Med Virol **1983**; 12:93-102.

161. Whitt MA. Generation of VSV pseudotypes using recombinant ΔG-VSV for studies on virus entry, identification of entry inhibitors, and immune responses to vaccines. J Virol Methods **2010**; 169:365-74.

162. Borenstein-Katz A, Shulman A, Hamawi H, Leitner O, Diskin R. Differential Antibody-Based Immune Response against Isolated GP1 Receptor-Binding Domains from Lassa and Junín Viruses. J Virol **2019**; 93.

163. Hastie KM, Zandonatti MA, Kleinfelter LM, et al. Structural basis for antibody-mediated neutralization of Lassa virus. Science **2017**; 356:923-8.

164. Amanat F, Duehr J, Oestereich L, Hastie KM, Ollmann Saphire E, Krammer F. Antibodies to the Glycoprotein GP2 Subunit Cross-React between Old and New World Arenaviruses. mSphere **2018**; 3.

165. Ruo SL, Mitchell SW, Kiley MP, Roumillat LF, Fisher-Hoch SP, McCormick JB. Antigenic relatedness between arenaviruses defined at the epitope level by monoclonal antibodies. J Gen Virol **1991**; 72 (Pt 3):549-55.

166. Kotturi MF, Botten J, Maybeno M, et al. Polyfunctional CD4+ T cell responses to a set of pathogenic arenaviruses provide broad population coverage. Immunome Res **2010**; 6:4.

.

Vita

Teresa Eirena Sorvillo was born on February 10th, 1985 to Francis (Frank) J. Sorvillo and Jeanne M. Favreau-Sorvillo in Anaheim, California. She attended Cornelia Connelly High School in Anaheim, California, graduating in May 2003. She pursued her love for science by majoring in biology at Loyola Marymount University. During her undergraduate years she was also able to explore a passion for public health by conducting undergraduate research through the University of California Los Angeles (UCLA) School of Public Health investigating the emerging raccoon roundworm, *Baylisascaris procyonis*. This research resulted in multiple presentations at undergraduate research conferences as well as two peer-reviewed publications. After receiving her Bachelor of Science degree in 2007, Teresa began working for the San Gabriel Valley Mosquito and Vector Control District in West Covina, California where she worked for 5 years conducting public health surveillance for arboviral and zoonotic diseases including West Nile and Sin Nombre viruses, work which she had the opportunity to present at state and national conferences, as well as publish in a third peer-reviewed article. Teresa began a Doctor of Philosophy (PhD) program in the Microbiology and Immunology Department at the University of Texas Medical Branch (UTMB) in August of 2013. She joined the lab of Dr. Thomas Geisbert and has focused her training on high containment (BSL-4) virology at the Galveston National Laboratory. Her dissertation work investigated the use of a recombinant vesicular stomatitis virus expressing the Junin virus glycoprotein for the development of countermeasures against highly pathogenic arenaviruses.

EDUCATION:

08/2013 to 12/2019 **Doctor of Philosophy, Microbiology and Immunology**
The University of Texas Medical Branch, Galveston, TX

08/2003-12/2007 **Bachelor of Science in Biology**
Loyola Marymount University, Los Angeles, CA

CERTIFICATIONS:

2015 to present **Biosafety Level 4**, University of Texas Medical Branch

2014 to present **Biosafety Level 3**, University of Texas Medical Branch

2018 to present **Nonhuman Primate Training**, University of Texas Medical Branch

2017 to present **Animal Biosafety Level 2**, University of Texas Medical Branch

2009 to 2013 **Mosquito Biology & Control**, California Dept of Public Health

2009 to 2013 **Vertebrate Vector Control**, California Dept of Public Health

2009 to 2013 **Terrestrial Invertebrate Vector Control**, California Dept of Public Health

PROFESSIONAL EXPERIENCE:

Professional Experience:

08/2013 to present **Graduate Research Assistant**, Department of Microbiology & Immunology, University of Texas Medical Branch, Galveston, TX. Mentor: Thomas Geisbert, PhD

Projects:

1. Development of vesicular stomatitis virus-based vaccine against Junin virus (rVSVΔG-JUNVGP).
2. rVSVΔG-JUNVGP for Serological Detection of Junin Virus-Specific Neutralizing Antibodies.
3. Development of chimeric arenavirus glycoproteins for a cross-protective arenavirus vaccine.
4. Investigating liver tropism of Ebola Makona virus.

09/2010-08/2013 **Vector Ecologist**, San Gabriel Valley Mosquito and Vector Control District, West Covina, CA. Mentor: Kenn Fujioka, PhD.

Projects:

1. Direct West Nile virus surveillance for San Gabriel Valley, CA.

2. Direct surveillance and control efforts related to invasive *Aedes albopictus* mosquito population.

05/2008-09/2010 **Assistant Vector Ecologist**, San Gabriel Valley Mosquito and Vector Control District, West Covina, CA. Mentor: Kenn Fujioka, PhD.

Projects:

1. Conduct surveillance for vector-borne diseases in the San Gabriel Valley, CA with a primary focus on West Nile virus. Secondary pathogens include, among others, Sin Nombre virus and *B. burgdorferi*.

2. Conduct trials to evaluate pesticide resistance in local *Culex quinquefasciatus* mosquito populations.

05/2006-05/2007 **Intern**, Department of Epidemiology, UCLA School of Public Health, Los Angeles, CA. Mentors: Shira Shafir, PhD; Lawrence Ash, PhD.

Project:

Conduct research to determine the parameters of viability of the infectious stage of the raccoon roundworm *Baylisascaris procyonis*, an emerging zoonotic infection.

HONORS AND AWARDS

12/2017 Sealy Center for Vaccine Development Award, University of Texas Medical Branch.

04/2017 Travel award - International Institute of Field Epidemiology Course, University of Texas Medical Branch.

2007 1st Place Poster Presentation Award, West Coast Biological Sciences Undergraduate Research Conference, Loyola Marymount University.

BIBLIOGRAPHY:

Publications

Sorvillo TE, Cross RW, Fenton KA, Mire CE, Geisbert TW. Single Dose rVSVΔG-JUNVGP Vaccine Protects Guinea Pigs Against Lethal Junin Virus Challenge. Submitted to: npj Vaccines. 2019 Oct.

LeDuc JW, **Sorvillo T**. A quarter century of emerging infectious diseases - where have we been and where are we going? Acta Med Acad. 2018 May;47(1):117-130.

Zhong D, Lo E, Hu R, Metzger ME, Cummings R, Bonizzoni M, Fujioka KK, **Sorvillo TE**, Kluh S, Healy SP, Fredregill C, Kramer VL, Chen X, Yan G. Genetic analysis of invasive Aedes albopictus populations in Los Angeles County, California and its potential public health impact. PLoS One. 2013 Jul 5;8(7):e68586.

Shafir SC, Sorvillo FJ, **Sorvillo T**, Eberhard ML. Viability of Baylisascaris procyonis Eggs. Emerg Infect Dis. 2011 Jul;17(7):1293-5.

Shafir SC, Wang W, Sorvillo FJ, Wise ME, Moore L, **Sorvillo T**, Eberhard ML. Thermal death point of Baylisascaris procyonis eggs. Emerg Infect Dis. 2007 Jan;13(1):172-3.

Oral presentations

Sorvillo T. Arenavirus vaccine and therapeutic development at the Galveston National Laboratory, University of Texas Medical Branch. Invited presentation: The Institute of Human Viral Diseases "J. Maiztegui". 2018 October 29; Pergamino, Argentina.

Sorvillo T, Middleton K, Sorvillo B, Tanaka M, Fujioka K. Surveillance and control of Aedes albopictus in the San Gabriel Valley, Los Angeles County, CA. Presented at: 79th Annual Meeting of the American Mosquito Control Association. 2013 Feb 24-28; Atlantic City, NJ.

Sorvillo T, Middleton K, Sorvillo B, Tanaka M, Fujioka K. Addressing a new infestation of Aedes albopictus in the San Gabriel Valley, Los Angeles County. Presented at: 81st Annual Conference of the Mosquito and Vector Control Association of California. 2013 Feb 1-3; Sacramento, CA.

Sorvillo T, Middleton K, Brisco A, Cook M, Fujioka K. A New Invasion by Aedes albopictus in the San Gabriel Valley, Los Angeles County, California. Presented at: 78th Annual Meeting of the American Mosquito Control Association. 2012 Feb 26-Mar 1; Austin, TX.

Poster presentations

Sorvillo T, Deer DJ, Fenton KA, Geisbert JB, Mire CE, Geisbert TW. A recombinant vesicular stomatitis virus expressing the Junin virus glycoprotein protects guinea pigs from lethal Junin virus challenge. Poster Presented at: The Institute for Human Infections and Immunity McLaughlin Colloquium, University of Texas Medical Branch. 2018 Mar 30; Galveston, TX.

Sorvillo T, Mire CE, Fenton KA, Agans KN, Geisbert JB, Geisbert TW. Liver tropism of Ebola Makona virus. Poster Presented at: The Institute for Human Infections and Immunity McLaughlin Colloquium, University of Texas Medical Branch. 2017 Mar 31; Galveston, TX.

Sorvillo T, Mire CE, Fenton KA, Agans KN, Geisbert JB, Geisbert TW. Liver tropism of Ebola Makona virus. Poster Presented at: Hemorrhagic Fever Viruses Keystone Symposium. 2016 Dec 4-8; Santa Fe, NM.

Sorvillo T, Kibbie J. Determination of parameters of viability of Baylisascaris procyonis. Poster Presented at: 32nd West Coast Biological Sciences Undergraduate Research Conference. 2007 Apr 28; Los Angeles, CA.

Sorvillo T, Kibbie J. Determination of the thermal death point of Baylisascaris procyonis larvae. Poster Presented at: Southern California Conference for Undergraduate Research. 2006; Costa Mesa, CA